



**DEPARTAMENTO DE CIÊNCIAS DA VIDA**

**FACULDADE DE CIÊNCIAS E TECNOLOGIA**

**UNIVERSIDADE DE COIMBRA**

# **Mechanisms of Hexavalent Chromium Carcinogenicity: Effects on the Stress Response and on the Genomic Stability of the BEAS-2B Cell Line**

**Patrícia Alexandra Lona Abreu**

---

**2016**





**DEPARTAMENTO DE CIÊNCIAS DA VIDA**

**FACULDADE DE CIÊNCIAS E TECNOLOGIA**

**UNIVERSIDADE DE COIMBRA**

# **Mechanisms of Hexavalent Chromium Carcinogenicity: Effects on the Stress Response and on the Genomic Stability of the BEAS-2B Cell Line**

Dissertação apresentada à Universidade de Coimbra para cumprimento dos requisitos necessários à obtenção do grau de Mestre em Bioquímica, realizada sob a orientação científica da Professora Doutora Ana Margarida Urbano (Universidade de Coimbra).

**Patrícia Alexandra Lona Abreu**

---

2016



The work presented in this dissertation was developed at the Química-Física Molecular research unit, with funding from FCT (grant UID/MULTI/00070/2013, to Química-Física Molecular research unit) and CIMAGO (grant 16/12, to Professor Ana Margarida Urbano).





**À memória de minha avó Dulce**

---



**“What we know is a drop, what we don't know is an ocean.”**

Sir Isaac Newton

---



## Agradecimentos

Chegado o final desta etapa do meu percurso académico, quero expressar os meus sinceros agradecimentos a todos os que, de forma direta ou indireta, contribuíram para a concretização desta dissertação.

À Professora Doutora Ana Margarida Urbano, orientadora desta dissertação, por me ter recebido no seu laboratório e por desde muito cedo ter acreditado em mim. Por ter continuado sempre a confiar em mim e a incentivar-me a fazer mais e melhor. Por tudo o que me ensinou e que fez de mim não só uma melhor cientista, mas também uma melhor pessoa. Por todo o acompanhamento, atenção e disponibilidade, sem os quais nada disto teria sido possível.

À Professora Doutora Isabel Carreira, por ter aceitado colaborar neste projeto, por toda a disponibilidade para delinear e discutir o mesmo e por tão bem me ter recebido no seu laboratório. À Professora Doutora Joana Melo, pela disponibilidade para participar em todas as reuniões relacionadas com este projeto e pelas valiosas sugestões científicas. Dentro da equipa do Laboratório de Citogenética e Genómica da Faculdade de Medicina da Universidade de Coimbra, deixo também o meu especial agradecimento às técnicas superiores Cláudia Pais e Patrícia Machado, pela preparação das placas metafásicas, e Alexandra Mascarenhas, pelos conhecimentos que me transmitiu, por me ter introduzido à construção e análise de cariótipos, pela preciosa ajuda durante todo o projeto e pela disponibilidade para rever e corrigir o trabalho realizado.

Ao Professor Doutor Paulo Oliveira, pela oportunidade que me deu de enriquecer este trabalho com a realização das experiências de RT-qPCR e pela simpatia com que me recebeu no seu laboratório. À Doutora Teresa Cunha-Oliveira pelos conhecimentos que me transmitiu sobre a técnica de RT-qPCR, por toda a ajuda na planificação e realização das experiências, pelo rigor científico, pela paciência para esclarecer as minhas intermináveis dúvidas e pela sua amabilidade e boa disposição.

Ao Professor Doutor Ângelo Tomé pela sua disponibilidade e pelo auxílio prestado nas determinações dos níveis intracelulares de nucleótidos de adenina.

A todos os elementos da Unidade de Química-Física Molecular pela simpatia e boa disposição que tornaram os longos dias no laboratório muito mais agradáveis.

À Daniela Ferreira por ser uma excelente companheira de laboratório e uma amiga ainda melhor, por todas as horas passadas na sala de cultura, por todo o auxílio e

disponibilidade, por estar sempre presente nos bons e maus momentos. Esta não foi uma caminhada fácil, mas sem ti teria sido muito mais difícil.

Aos meus amigos, pelo apoio constante e ajuda, por me conseguirem sempre animar e colocar um sorriso na cara, por todos os momentos fantásticos que passámos juntos.

Ao meu avô por me ter dado a oportunidade de continuar o meu percurso académico, o que me permitirá certamente construir um futuro melhor, pelo interesse e preocupação com o meu trabalho, e sobretudo pelo apoio e carinho constantes. Espero, sinceramente, que a concretização deste trabalho te deixe orgulhoso.

Aos meus pais e à irmã pelo amor incondicional, por terem estado sempre comigo nesta longa caminhada, pela paciência que tiveram comigo nos momentos mais difíceis, por acreditarem em mim e nunca me deixarem desistir. Devo-vos tudo aquilo que sou e conquistei e não tenho palavras suficientes para vos agradecer.

## Index

<b>Abbreviations and Symbols</b> .....	v
<b>Abstract</b> .....	ix
<b>Sumário</b> .....	xi
<b>1. Introduction</b> .....	1
1.1. Hexavalent chromium: a lung carcinogen .....	3
1.1.1. Chromium: general aspects.....	4
1.1.2. Intracellular metabolism of Cr(VI) .....	5
1.1.3. Molecular basis of Cr(VI)-induced carcinogenesis.....	7
1.1.4. Importance of the model system in the study of Cr(VI)-induced carcinogenesis .....	10
1.1.4.1. The BEAS-2B cell line as a model system for human bronchial epithelium .....	12
1.2. The importance of the stress response in biological systems.....	14
1.2.1. The involvement of the stress response in carcinogenesis .....	15
1.2.1.1. Hsp90.....	16
1.2.1.2. Hsp70.....	19
1.2.1.3. HSF1 .....	21
1.2.2. Hsps and HSF1 inhibitors as anticancer agents: a new therapeutic approach .....	25
1.2.3. Heavy metals and the stress response .....	27
1.2.3.1. The case of Cr(VI).....	28
1.3. Genomic instability and cancer .....	31
1.3.1. The role of genomic instability in Cr(VI)-induced carcinogenesis.....	35
1.4. Objectives.....	38

<b>2. Materials and Methods</b> .....	39
2.1. General materials .....	41
2.2. Biological material .....	43
2.3. Equipment .....	44
2.4. Culture of BEAS-2B cells.....	46
2.4.1. Solutions commonly used in the culture of BEAS-2B cells.....	46
2.4.2. Cell culture routine.....	48
2.4.3. Culture initiation .....	50
2.4.4. Cryopreservation of cells.....	50
2.5. Cell counting by the Trypan Blue exclusion method .....	52
2.6. Morphological studies.....	53
2.7. Quantification of L-glutamine and ammonia in the culture medium.....	53
2.8. Determination of doubling times.....	55
2.9. Cytogenetic analysis .....	56
2.10. Cellular treatment with Cr(VI).....	57
2.11. Cytotoxicity assays .....	58
2.12. Heat shock assays .....	58
2.13. Quantification of intracellular adenine nucleotide levels .....	59
2.14. Total protein quantification.....	61
2.15. Quantification of individual protein levels .....	62
2.16. Quantification of individual mRNA levels .....	66
2.17. Statistical analysis.....	72
<b>3. Results and Discussion</b> .....	73
3.1. Impact of culturing conditions and culture age on the growth characteristics and genomic stability of the BEAS-2B cell line.....	75
3.1.1. Assessment of the culturing conditions adopted in our laboratory .....	75

3.1.2. Impact of culturing conditions on the growth characteristics of the BEAS-2B cell line .....	78
3.1.3. Impact of culture age on the growth characteristics and genomic stability of the BEAS-2B cell line.....	83
3.2. Effects of a short-term exposure to Cr(VI) on the stress response of BEAS-2B cells .....	90
3.2.1. Establishment of the exposure regimen to Cr(VI) and to heat shock .....	90
3.2.2. Effects of Cr(VI) on the proliferation of BEAS-2B cells subjected to an acute heat shock.....	92
3.2.3. Effects of an acute heat shock on the energy status of BEAS-2B cells pre-incubated with Cr(VI).....	93
3.2.4. Effects of Cr(VI) on the expression of key components of the stress response .....	96
3.2.5. Effects of Cr(VI) on the mRNA levels of components of cancer-associated pathways related to the stress response.....	100
3.3. Effects of a long-term exposure to Cr(VI) on the genomic stability and morphology of BEAS-2B cells .....	103
<b>4. Conclusions and Future Perspectives .....</b>	<b>109</b>
<b>References .....</b>	<b>115</b>
<b>Appendices .....</b>	<b>135</b>
A.1. Evaluation of RNA integrity .....	137
A.2. Evaluation of the specificity of RT-qPCR reactions .....	138



## Abbreviations and Symbols

### Abbreviations

<b>Ad-12</b>	Adenovirus 12
<b>ADP</b>	Adenosine diphosphate
<b>AMP</b>	Adenosine monophosphate
<b>Asc</b>	Ascorbate
<b>ATCC</b>	American Type Culture Collection
<b>ATM</b>	Ataxia telangiectasia mutated
<b>ATP</b>	Adenosine triphosphate
<b>ATR</b>	ATM-Rad3-related
<b>BRCA</b>	Breast cancer susceptibility
<b>BSA</b>	Bovine serum albumin
<b>CIN</b>	Chromosomal instability
<b>Cq</b>	Quantification cycle
<b>Cr(III)</b>	Trivalent chromium
<b>Cr(IV)</b>	Tetravalent chromium
<b>Cr(V)</b>	Pentavalent chromium
<b>Cr(VI)</b>	Hexavalent chromium
<b>Cys</b>	Cysteine
<b>DMSO</b>	Dimethyl sulfoxide
<b>DSB</b>	Double-strand break
<b>ECACC</b>	European Collection of Cell Cultures
<b>ECM</b>	Extracellular matrix
<b>ELISA</b>	Enzyme-linked immunosorbent assay
<b>ER</b>	Endoplasmic reticulum
<b>FBS</b>	Fetal bovine serum
<b>FNT(-) CS</b>	Fibronectin-free coating solution
<b>FNT(+ ) CS</b>	Fibronectin-containing coating solution
<b>GIDH</b>	Gultamate dehydrogenase
<b>GRP</b>	Glucose-regulated protein
<b>GSH</b>	Glutathione

<b>HBSS</b>	Hank's balanced salt solution
<b>HER</b>	Human epidermal growth factor 2
<b>HIF-1<math>\alpha</math></b>	Hypoxia-inducible factor 1-alpha
<b>HR</b>	Homologous repair
<b>HRP</b>	Horseradish peroxidase
<b>HSE</b>	Heat shock element
<b>HSF</b>	Heat shock factor
<b>Hsp</b>	Heat shock protein
<b>LT</b>	Large T antigen
<b>MMP</b>	Matrix metalloproteinase
<b>MMR</b>	Mismatch repair
<b>mono</b>	Monosomy
<b>mRNA</b>	Messenger RNA
<b>MSI</b>	Microsatellite instability
<b>NHBE</b>	Normal human bronchial epithelial
<b>NHEJ</b>	Non-homologous end-joining
<b>NSCLC</b>	Non-small cell lung carcinoma
<b>PBS</b>	Phosphate-buffered saline
<b>PCA</b>	Perchloric acid
<b>ROS</b>	Reactive oxygen species
<b>RP-HPLC</b>	Reverse-phase high performance liquid chromatography
<b>RQI</b>	RNA quality indicator
<b>rRNA</b>	Ribosomal RNA
<b>RT-qPCR</b>	Quantitative reverse-transcription polymerase chain reaction
<b>SEM</b>	Standard error of the mean
<b>SQ</b>	Starting quantity
<b>SSB</b>	Single-strand break
<b>SV40</b>	Simian virus 40
<b>TBE</b>	Tris-Borate-EDTA
<b>TMB</b>	3,3',5,5'-Tetramethylbenzidine
<b>TRAP1</b>	TNF receptor-associated protein 1
<b>tri</b>	Trisomy
<b><math>\gamma</math>-H2AX</b>	Gamma-H2AX

## **Symbols**

<b>#</b>	Passage number
<b><math>\Delta A</math></b>	Change in absorbance
<b>add</b>	Additional material of unknown origin
<b>der</b>	Derivative chromosome
<b>i</b>	Isochromosome
<b>p</b>	Short arm of chromosome
<b>q</b>	Long arm of chromosome



## Abstract

Hexavalent chromium [Cr(VI)] has long been recognized as an occupational lung carcinogen. However, despite several studies, the molecular basis of Cr(VI)-induced carcinogenesis remains essentially elusive. This elusiveness can be, at least partially, attributed to the use, in many of those studies, of experimental models and exposure regimens that are of questionable biological relevance.

Activation of the stress response and genomic instability have been proposed to have important roles in cancer development and progression, but little is known about the role they might play in Cr(VI)-induced carcinogenesis. To gain some insight on this topic, the effects of a short-term exposure to Cr(VI) on the stress response and of a long-term exposure on genomic stability were investigated in the present study.

To address the question of biological relevance, the BEAS-2B cell line, a cellular model representative of the human bronchial epithelium, which is the main target of Cr(VI) carcinogenicity *in vivo*, was used. Initially, the impact of the culturing conditions and the culture age on the growth characteristics and genomic stability of this cell line was evaluated. All modifications of the culturing conditions tested in this study, as well as the culture age, induced some alterations to the morphology and growth pattern of BEAS-2B cells. The culture age also had a significant impact on the chromosomal complement of these cells.

A short-term exposure of BEAS-2B cells to Cr(VI) conferred a certain resistance against the inhibitory effect on proliferation produced by an acute heat shock. This resistance cannot be explained by alterations in the cellular energy status, nor, apparently, through elevated protein levels of key components of the stress response. In fact, the impact of Cr(VI) on the intracellular levels of the heat shock proteins 90 $\alpha$  (Hsp90 $\alpha$ ) and 72 (Hsp72) and of the heat shock factor 1 (HSF1) was evaluated and the only significant effect observed was a decrease in the levels of Hsp90 $\alpha$ . At the mRNA level, Cr(VI) caused a decrease in the levels of *HSPA1A*, which encodes Hsp72. In addition, the impact of Cr(VI) on the mRNA levels of some components of cancer-associated pathways also related to the stress response was investigated and alterations were observed in the levels of *ATM* and *ATR*, which encode important components of the DNA damage response. The mRNA levels of *ATM* were decreased, while those of *ATR* were increased.

A long-term exposure to Cr(VI), for over eight months, did not induced genomic instability nor morphological alterations, suggesting that no neoplastic transformation occurred.

**Keywords:** Hexavalent chromium; Lung cancer; BEAS-2B cell line; Stress response; Genomic stability.

## Sumário

O crómio hexavalente [Cr(VI)] foi há muito reconhecido como agente cancerígeno pulmonar. Contudo, apesar dos diversos estudos já realizados, ainda muito pouco se sabe sobre a base molecular da carcinogénese induzida pelo Cr(VI). Isto deve-se, em parte, ao facto de muitos desses estudos terem usado modelos experimentais e regimes de exposição cuja relevância biológica é questionável.

A ativação da resposta ao stress e a instabilidade genómica parecem ter importantes papéis no desenvolvimento e progressão do cancro, mas pouco se sabe o sobre o papel que poderão ter no contexto da carcinogénese induzida pelo Cr(VI). Para tentar obter alguma informação sobre este assunto, neste estudo foram investigados os efeitos de uma exposição de curta duração a Cr(VI) na resposta ao stress e os de uma exposição de longa duração na estabilidade genómica.

Tendo em consideração a questão da relevância biológica, usou-se nesta investigação a linha celular BEAS-2B, um modelo representativo do epitélio brônquico humano, que é o principal alvo da ação carcinogénica do Cr(VI) *in vivo*. Inicialmente, o impacto das condições e idade da cultura na morfologia, padrão de crescimento e estabilidade genómica desta linha celular foi avaliado. Todas as alterações às condições de cultura testadas neste estudo, bem como a idade da cultura, induziram algumas alterações na morfologia e padrão de crescimento das células BEAS-2B. A idade da cultura teve também um impacto significativo no complemento cromossómico destas células.

Uma exposição de curta duração de células BEAS-2B a Cr(VI) conferiu uma certa resistência à inibição da proliferação causada por um choque térmico de curta duração. Esta resistência não pode ser explicada por alterações no estado energético celular, nem, aparentemente, por um aumento nos níveis de alguns componentes-chave da resposta ao stress. De facto, o impacto do Cr(VI) nos níveis intracelulares das proteínas do choque térmico 90 $\alpha$  (Hsp90 $\alpha$ ) e 72 (Hsp72) e do factor de choque térmico 1 (HSF1) foi avaliado e o único efeito significativo observado foi uma diminuição nos níveis da Hsp90 $\alpha$ . Em termos de níveis de mRNA, o Cr(VI) causou uma diminuição dos níveis de *HSPA1A*, que codifica a Hsp72. Além disto, o impacto do Cr(VI) nos níveis de mRNA de alguns elementos associados com a carcinogénese e também relacionados com a resposta ao stress foi investigado e observaram-se alterações nos níveis de *ATM* e *ATR*, que codificam

componentes envolvidos nos mecanismos de resposta a danos no DNA. Os níveis de mRNA de *ATM* sofreram uma diminuição, enquanto os de *ATR* aumentaram.

Uma exposição de longa duração, durante mais de oito meses, a Cr(VI) não induziu instabilidade genómica nem alterações morfológicas, o que sugere que não ocorreu transformação neoplásica.

**Palavras-chave:** Crómio hexavalente; Cancro do pulmão; Linha celular BEAS-2B; Resposta ao stress; Estabilidade genómica.

# **1. Introduction**

---



## 1.1. Hexavalent chromium: a lung carcinogen

For many years, hexavalent chromium [Cr(VI)] compounds (chromates) have been extensively used in the chemical, metallurgical and refractory industries [1]. Over the years, it has also been noticed that these compounds constitute a significant health hazard, in particular to the skin and respiratory tract. Since 1890, when the first case of a carcinoma detected in a chromate worker was reported [2], suspicions arose that chromates could be carcinogenic to humans. In the decades that followed, several investigations, including *in vitro*, *in vivo* and epidemiologic studies, were undertaken and clearly showed a correlation between occupational exposure to Cr(VI) and increased incidence of lung cancer [3]. Based on these studies, the major international agencies, such as the National Toxicology Program (NTP) and the International Agency for Research on Cancer (IARC), classified Cr(VI) as a human lung carcinogen [4, 5]. More recently, some suspicions arose that chromates could also be associated with cancers in the central nervous system and the gastrointestinal tract, but the data collected were not conclusive [4, 6]. It is important to note that, currently, the environmental exposure to this carcinogen is increasing, due to a widespread contamination with Cr(VI), which is the result of industrial waste disposal, fossil fuel combustion, stainless steel production and, possibly, tobacco smoke [7].

Understanding the mechanisms of Cr(VI)-induced damage and its carcinogenic action has been the goal of many investigators throughout the years and it is essential for the development of better preventive strategies and more effective therapeutics. The few studies where lung cancer samples from chromate workers were analysed have suggested that Cr(VI)-induced lung carcinomas might have some interesting specificities that distinguish them from other lung cancers, namely those associated with tobacco smoking habits [7]. The distinguish features observed were: a low incidence of *TP53* mutations which, when observed, had a different pattern from that commonly found in lung cancers [8]; an infrequent activation of *RAS* oncogenes [9]; reduced expression and aberrant methylation of p16<sup>INK4a</sup> [10]; and frequent microsatellite instability (MSI) [11, 12]. Notwithstanding, the molecular mechanisms underlying these features are still poorly understood.

### 1.1.1. Chromium: general aspects

Chromium is one of the most abundant elements in the Earth's crust. This element is extremely versatile, occurring naturally in several oxidation states (-II to +VI). Chromium's potential began to be explored shortly after its discovery in the 18th century, by Vauquelin, and, currently, chromium compounds have a wide range of applications, such as stainless steel production, tanning, wood preservation and corrosion inhibition [1].

Chromium's most stable and biologically relevant valence states are the trivalent [Cr(III)] and hexavalent states [3, 13]. Cr(III) complexes are characterized by an octahedral geometry, positive charge and, generally, kinetical inertia [14]. Due to these properties, Cr(III) complexes are not able to use the transporters present on the cellular membrane and, thus, cannot easily cross it. This behavior may explain why Cr(III) presents low toxicity to cells and organisms, despite the fact that it shows great capacity to react with proteins, nucleic acids and other biomolecules in studies performed in acellular systems [7]. Extracellularly, Cr(III) has been proposed to have a role in insulin metabolism, leading some authors to consider it an essential trace element [4]. As for Cr(VI), in aqueous solution, it forms essentially tetrahedral complexes, existing, depending on the pH, predominantly as the oxyanions chromate  $[(CrO_4)^{2-}]$  (pH > 6) or dichromate  $[(CrO_7)^{2-}]$  (pH between 2 and 6) [14]. The tetrahedral structure of chromate, the major Cr(VI) complex at physiological pH, closely resembles those of phosphates and sulfates [14, 15]. Therefore, chromate can be non-specifically transported by anionic channels, entering the cells, where it will exert its genotoxic, clastogenic and cytotoxic effects.

Fortunately, there are some mammalian defense mechanisms that will inactivate a significant fraction of Cr(VI) before it enters the cells. The inactivation results from the extracellular reduction of Cr(VI) to Cr(III) by whole blood, lung epithelial fluid, alveolar macrophages and peripheral parenchyma cells [16, 17]. However, when the exposure is very prolonged and/or the doses are very high, these mechanisms cannot completely avoid the entry of the compound into the cells. Bypass of detoxification mechanisms is a major concern when the inhalation of chromates in particulate forms occurs. The particles are retained in the bifurcations of the tracheobronchial tree and their solubilization leads to the release of chromate oxyanions in the close vicinity of epithelial cells. Some of the released chromate will be actively transported into the cells before reduction can occur,

and, in this situation, Cr(VI) will exert its carcinogenic effects. This is the main reason why most lung tumors associated with Cr(VI)-exposure appear in the bifurcations of the lung [18, 19].

### 1.1.2. Intracellular metabolism of Cr(VI)

*In vitro* studies have shown that Cr(VI) has a reduced capacity of interacting with biomolecules and, thus, it exhibits little relevant biological activity. Notwithstanding, Cr(VI) is a strong oxidizing agent [14] and, once inside the cells, which constitute a reductive environment, it suffers a rapid and stepwise reduction to Cr(III), which triggers the subsequent genotoxic, mutagenic and clastogenic effects, among others involved in Cr(VI)-induced cellular malignization (Figure 1.1). In addition, during the reduction process, several other harmful species are generated. Among these are the pentavalent [Cr(V)] and tetravalent [Cr(IV)] chromium reduction intermediates, reductant-specific thiyls and carbon-based radicals, as well as reactive oxygen species (ROS) [14, 20].

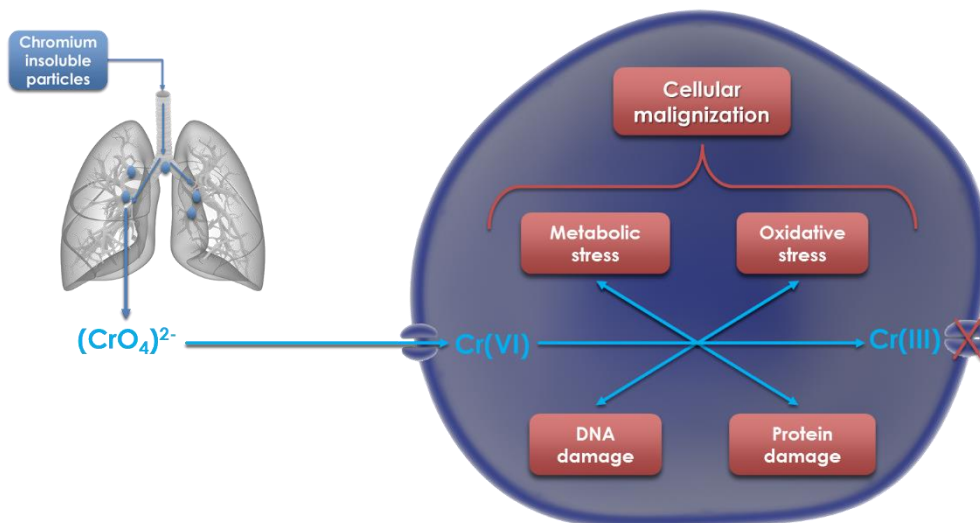


**Figure 1.1 | Schematic representation of some of the mechanisms likely involved in Cr(VI)-induced cellular malignization.** Chromium insoluble particles accumulate in the tracheobronchial bifurcations, from where soluble Cr(VI), in the form of chromate  $[(CrO_4)^{2-}]$ , is slowly released. A significant portion of the chromate released will be extracellularly reduced, but some can be actively transported into the cells. Once inside the cells, Cr(VI) will be quickly reduced, generating Cr(III) and several other reactive species. These species cause a plethora of alterations in the cell, leading to cellular malignization.

A significant number of cellular components, such as ascorbate (Asc), reduced glutathione (GSH), cysteine (Cys), hydrogen peroxide (H<sub>2</sub>O<sub>2</sub>), nicotinamide coenzymes (NADH and NADPH), flavoenzymes and also some redox proteins (hemoglobin, cytochrome P450 and complex I of the electron transport chain (ETC)), have the potential to reduce Cr(VI) [7, 21]. However, it is possible that not all of these components have a relevant contribution to the overall Cr(VI) reduction. For instance, since Cr(VI) partitions poorly to the mitochondria, the contribution of complex I may not be significant [16].

Currently, it is considered that the intracellular reduction of Cr(VI) is essentially a non-enzymatic process, involving Asc, GSH and Cys (Figure 1.2). Asc is seen as the primary reducer, due to its high intracellular concentration (in the millimolar range) and faster reduction kinetics. On the other hand, Cys, which has a lower intracellular concentration and is a slower reducer, might only have a biologically relevant role in Cr(VI) reduction when there is a depletion of the other two reducers [7, 16].

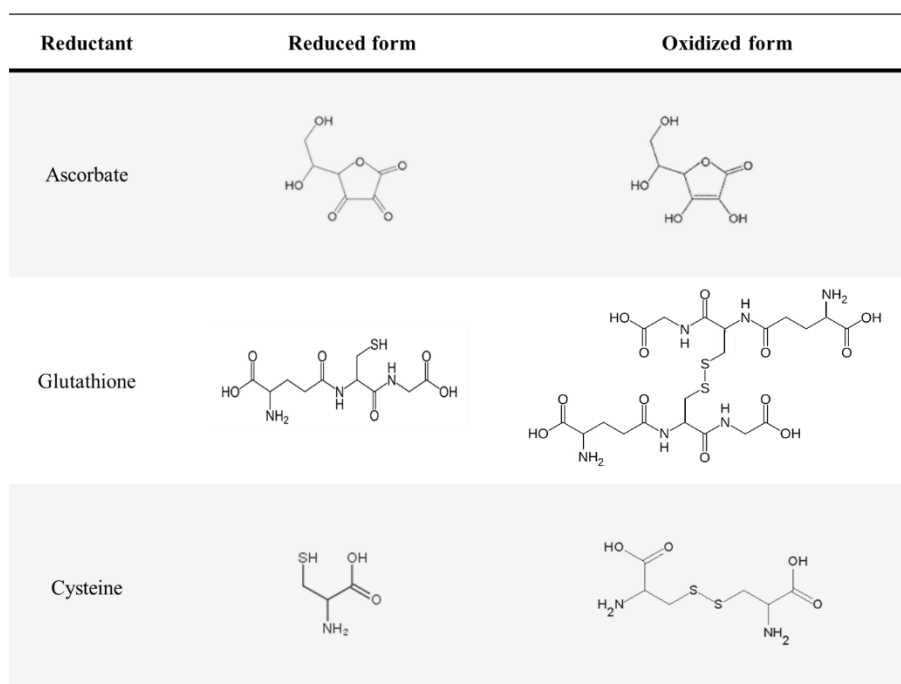


**Figure 1.2 | Chemical structures of reduced and oxidized forms of the three major Cr(VI)-reducing agents.** Intracellularly, Cr(VI) suffers a quick reduction to Cr(III). Currently, it is considered that this process is essentially non-enzymatic, involving ascorbate, glutathione and cysteine.

Two mechanisms have been proposed for the intracellular Cr(VI) reduction. One occurs at relatively low levels of Asc and consists in a series of one-electron transfers, leading to the sequential generation of Cr(V), Cr(IV) and Cr(III) [22]. On the contrary,

when the amount of Asc is not limiting, it acts essentially as a two-electron donor and Cr(VI) is directly reduced to Cr(IV), followed by a one electron reduction to Cr(III) [23, 24]. These two pathways are also possible when either GSH or Cys are the reducers. It is important to note that, *in vivo*, the predominance of one of the pathways depends not only on the proportion of reducer to Cr(VI), but also on additional factors, like the presence of other oxidants and of catalytic metals, such as Fe [16]. As previously mentioned, during these reduction reactions several other reactive species are also generated. For instance, the concomitant oxidation of the reducing agents leads to the formation of reductant-specific thiyls and carbon-based radicals, and ROS were shown to be generated when Cr(VI) reduction occurs in the presence of H<sub>2</sub>O<sub>2</sub> or lipid peroxides [16].

### **1.1.3. Molecular basis of Cr(VI)-induced carcinogenesis**

One of the major goals of the scientists studying the neoplastic transformation induced by Cr(VI) is to identify and understand the molecular basis of this process. This is, indeed, the greatest challenge of oncobiology in general, as it is very difficult to distinguish between the initiating events of carcinogenesis and the ones that are a consequence of that process. Notwithstanding, it has already been possible to identify a characteristic set of traits acquired by all cells that undergo neoplastic transformation – the hallmarks of cancer. The first six hallmarks were defined, in 2000, by Hanahan and Weinberg [25]. In 2011, the same investigators expanded the set, which now includes two emerging hallmarks [26] (Figure 1.3). The investigators have also identified tumour-promoting inflammation and genomic instability and mutation as two enabling characteristics, i.e. features of cancer cells that facilitate the acquisition of the core and emerging hallmarks [26].

Since the hallmarks of cancer are, by definition, shared by all cells that underwent neoplastic transformation, it is not surprising that many studies reported that cells exposed to Cr(VI) present several of those capacities, namely resistance to cell death [27-29], ability to sustain proliferative signaling [29-33], activation of invasion and metastasis [29, 34], induction of angiogenesis [35] and deregulation of cellular energetics [36], as well as the above-mentioned enabling characteristics [7, 30, 31, 37]. Nonetheless, it has been difficult to clearly define the molecular mechanisms underlying the acquisition of these capacities.

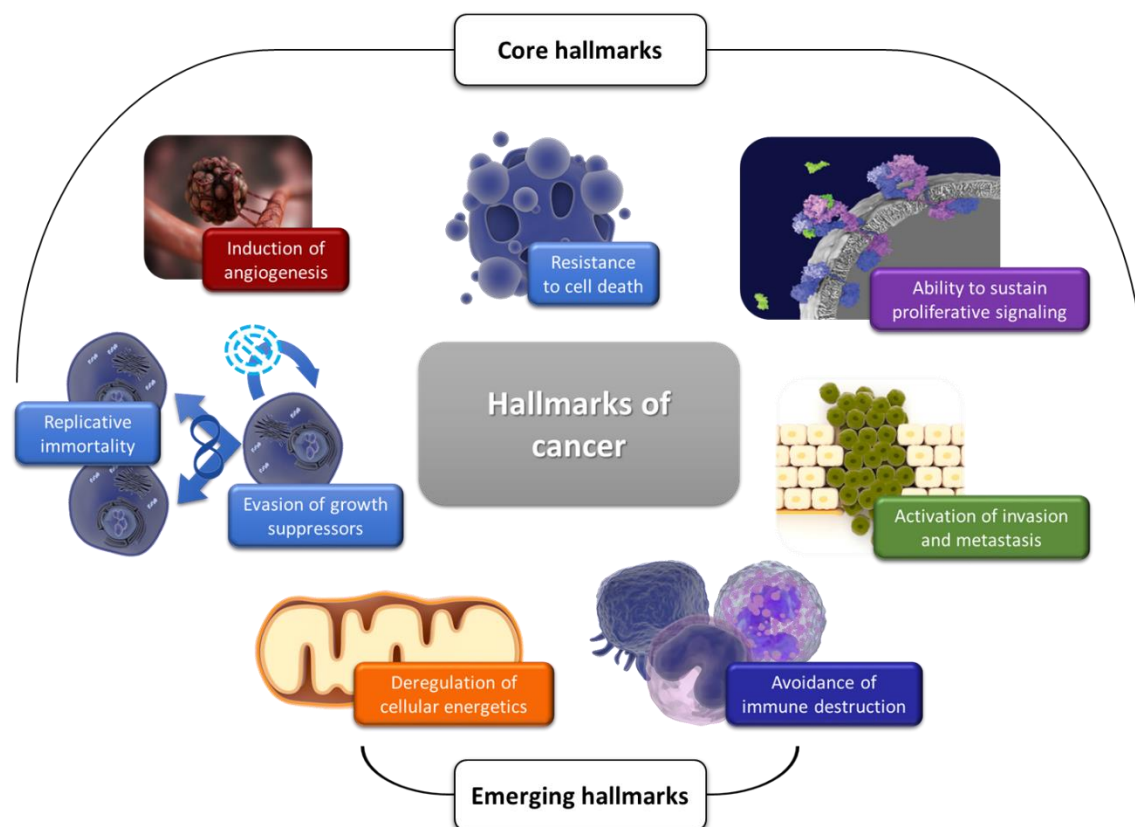


**Figure 1.3 | The hallmarks of cancer.** The investigators Hanahan and Weinberg identified a characteristic set of traits that are acquired by all cells that undergo neoplastic transformation, the so-called hallmarks of cancer. This set, which is schematically represented in this figure, includes six core hallmarks (resistance to cell death, ability to sustain proliferative signaling, activation of invasion and metastasis, evasion of growth suppressors, replicative immortality and induction of angiogenesis) and two emerging hallmarks (avoidance of immune destruction and deregulation of cellular energetics). Adapted from [26].

Concerning the enabling characteristics, it has been known since the early 1980s that Cr(VI)-exposed cells exhibited genomic instability and mutability [16]. Since cancer has long been seen essentially as a genetic disease, much effort has been put into the investigation of the mutagenic and genotoxic effects of carcinogenic agents, and Cr(VI) has been no exception.

As mentioned before, *in vitro* studies clearly showed that Cr(VI) itself is unable to interact with nucleic acids, but most of the species generated during its reduction, specially Cr(III), can bind to these biomolecules [20]. Cr(III) has great capacity to coordinate with DNA and form Cr(III)-DNA adducts. These Cr(III)-DNA adducts are generally in the form of ternary complexes, since Cr(III) tends to establish coordinate bonds with its intracellular reducers. Other types of DNA lesions, such as DNA-protein crosslinks, DNA inter/intrastrand crosslinks, single and double-strand breaks (SSBs and

DSBs, respectively), oxidized bases and abasic sites, have also been observed in Cr(VI)-exposed cells [38]. This capacity of Cr(VI) to generate DNA strand breaks is directly associated with its clastogenic action, i.e. its capacity to induce chromosomal abnormalities [16]. In fact, there are numerous studies reporting both structural and numerical chromosomal alterations in cells exposed to Cr(VI) [37, 39]. Unfortunately, these studies did not identify the specific chromosomes affected, precluding a better understanding of the role that these chromosomal alterations might have in the development of Cr(VI)-induced carcinogenesis, namely through the activation of oncogenes and/or inhibition of tumour suppressor genes.

The Cr(VI)-induced genotoxic effects might result not only from the well-established mutagenic capacity of Cr(III)-DNA adducts [38], but also from oxidative damage associated with Cr(VI) exposure. This latter can be induced by direct electron abstraction by Cr(V), Cr(IV) and other reactive species formed during the reduction of Cr(VI), such as Cr(V)-peroxo-intermediates or ROS [16]. Increased ROS levels upon Cr(VI) exposure have been frequently reported [36] and, not surprisingly, considering the widely recognized capacity of these species to modulate signalling pathways, pointed as possible modulators of some cellular responses induced by Cr(VI), including p53-dependent cell cycle arrest, apoptosis, activation of NF- $\kappa$ B and expression of metabolic enzymes [40, 41]. In support to this hypothesis, it was reported that the presence of peroxidases and other ROS scavengers can have protective effects against Cr(VI)-induced damage [42].

It is of interest to note the capacity of Cr(VI) to alter the expression of metabolic enzymes, since the deregulation of cellular energetics was, as previously mentioned, proposed as one of the emerging hallmarks of cancer, and the metabolic reprogramming of cancer cells is now a hot topic in research and a feature extensively explored in novel targeted anticancer therapies [43]. The impact of Cr(VI)-exposure on the bioenergetic phenotype begun to be studied in the 1980s and the data now available on the impact of Cr(VI) on bioenergetics has been recently reviewed by our group [36]. The information gathered so far suggests that cells exposed to Cr(VI) are under metabolic stress and undergo a metabolic shift towards a more fermentative metabolism. The increased dependence of cancer cells on lactic acid fermentation for energy production compared to that of the normal cells from which they derive, was first observed and proposed as a driving force of carcinogenesis by Otto Warburg, in the 1920s [44]. In cells exposed to Cr(VI), an increase in glucose consumption and in lactate production, and a decrease in

oxygen consumption have been frequently observed. These alterations also translate into decreased levels of adenosine triphosphate (ATP) and a decreased energy charge<sup>1</sup> [36, 45].

As previously discussed, metabolic stress is not the only type of stress that Cr(VI)-exposed cells face, and oxidative stress is also frequently observed. It could be expected that these and other stresses are partially responsible for the cytotoxic effects of Cr(VI), i.e. its capacity to cause a dose-dependent induction of cell death. Interestingly, our group has repeatedly observed that BEAS-2B cells that resist to low concentrations of Cr(VI) (0.1 to 1  $\mu$ M) exhibit increased proliferation rates [46-48]. In light of these observations, it is tempting to speculate that the aforementioned stresses may lead to an activation of the stress response in the exposed cells, which might involve increased levels of key components of this response. Since the stress response is the ubiquitous response of cells to stress and essential to maintain cellular homeostasis [49] (section 1.2), its activation would protect Cr(VI)-exposed cells not only from the stresses induced by Cr(VI) itself, but also from further stresses, such as those encountered during neoplastic transformation, thus explaining their increased resistance to cell death. To gain insight into the mechanisms involved this resistance, it would be interesting to investigate the impact of exposure to Cr(VI) on the stress response.

#### **1.1.4. Importance of the model system in the study of Cr(VI)-induced carcinogenesis**

Choosing an appropriate model is an essential step in every scientific investigation. The model used conditions not only the type of studies that one can perform, but also the conclusions and extrapolations that can be safely done. Several parameters have to be taken into account when choosing the model system that will be used, namely the biological relevance and adequacy of the model to the objectives of the study and to its duration, but also more practical aspects, such as the cost, the availability and the ethical issues associated with the model under consideration.

There are several obstacles hampering the study of the carcinogenic process induced by Cr(VI) in biologically relevant settings. For instance, exposure to chromates

---

<sup>1</sup> Atkinson's equation: Energy charge =  $([ATP] + \frac{1}{2}[ADP])/([ATP] + [ADP] + [AMP])$ .  
ADP, adenosine diphosphate; AMP, adenosine monophosphate; ATP, adenosine triphosphate.

induces primarily lung carcinomas and it is extremely difficult to have access to pre-cancerous and cancerous lung tissue from Cr(VI)-exposed workers, which would be of great value to accompany the molecular and cellular evolution of the disease [7]. To remain closer to the physiological situations, animal models might seem the most attractive alternative but, in addition to the high costs and ethical concerns always associated with this type of models, the restricted access to the tracheobronchial bifurcations remains a major problem. Cellular models are, thus, the preferred alternative to conduct the studies concerning the mechanisms underlying Cr(VI)-induced carcinogenesis.

As it is known that the human bronchial epithelium is the main target of Cr(VI) carcinogenicity *in vivo* (section 1.1.1), cell lines derived from this tissue are the systems with the most promising informative potential. Ideally, studies should be performed in primary cultures of human bronchial epithelial cells or in non-transformed cell lines obtained from those cells, as they are closer to the physiological situation. However, primary cultures and finite cell lines can only be maintained in culture for short periods as they rapidly become senescent, features that preclude long-term studies, which are essential to study multistage carcinogenesis [50]. In addition, their instability and high heterogeneity often leads to inconsistent results and, thus, many investigators prefer not to use them, even for the study of the early mechanistic events of carcinogenesis. In order to overcome these limitations, it is generally necessary to use continuous cell lines, either immortalized from primary cultures or obtained from biopsies of lung carcinomas.

Another important aspect to take into account is the type of medium used in cell culture. Different media present differences in several parameters, such as the presence of serum and of medium components capable of extracellularly reducing Cr(VI), and the absence of Asc, which can compromise the biological relevance of the results obtained [16]. For the culture of human bronchial epithelial cell lines, the use of LHC-9 medium might be a good option, as it was shown not to cause extracellular reduction of Cr(VI) [51].

Last but not least, the biological relevance of the experiments is also greatly influenced by the exposure regimen used to investigate the carcinogen under study, as different doses/concentrations and/or exposure times can evoke different molecular mechanisms.

Unfortunately, in many studies investigating Cr(VI)-induced carcinogenesis, these aspects are often overlooked and, thus, the inadequate choice of experimental

models and exposure regimens is one of the main causes behind the elusiveness of the molecular basis of this process, despite the numerous studies already performed [16]. For instance, a quick inspection of the literature reveals that only a few of those studies were carried out using human bronchial epithelial cell lines. It is also common to find the use of malignant cell lines, such as the A549 cell line [36], which is derived from a human lung adenocarcinoma [52], that introduce some confounding factors and difficult the interpretation of the results. This interpretation becomes even more complicated by the use of several different types of medium and culturing conditions, even for the same cellular model. In addition, one of the major problems of these investigations is the frequent use of extremely high Cr(VI) concentrations, which do not mimic the occupational exposure [16].

#### **1.1.4.1. The BEAS-2B cell line as a model system for human bronchial epithelium**

The BEAS-2B cell line is a continuous cell line derived from normal human bronchial epithelial (NHBE) cells cultured from explants of bronchial tissue obtained at the autopsy of a noncancerous individual [53]. This cell line was established in 1988, by the group of Curtis Harris. At the time, the investigators established it with the main purpose of studying multistage bronchial epithelial carcinogenesis, but, since then, this cell line has been increasingly used as a model for human bronchial epithelium, in extremely different investigations and areas of research, such as immunology, toxicology and many others [35, 54-61].

The immortalization of the cell line was achieved through infection of NHBE cells with a hybrid of the adenovirus 12 (Ad-12) with the simian virus 40 (SV40) [53]. The large T antigen (LT), one of the two proteins involved in the regulation of the SV40 life cycle, is the main responsible for the immortalization of cells infected with this virus [62]. After viral infection, LT inactivates the growth suppressors p53 and retinoblastoma protein (pRB), which are essential regulators of the mammalian cell cycle [63, 64]. It might be argued that the inactivation of these proteins can obscure some early mechanistic events of carcinogenesis. As an alternative, Wise and collaborators have proposed the use of lung fibroblasts [65], but these are not the primary targets of Cr(VI) *in vivo*.

It is true that this cell line cannot be considered normal, but it has been observed that BEAS-2B cells retain many of the features of human bronchial cells, only acquiring mild tumorigenic characteristics at high passages [66, 67]. Therefore, this cell line should be useful in the context of the studies investigating the carcinogenic effects of Cr(VI).

Some of the features that BEAS-2B cells retained from the NHBE cells include the polygonal shape, characteristic of epithelial cells, the presence of desmosomes and tight junctions and the ability to undergo squamous differentiation in response to serum [53, 68]. Due to this latter feature, a serum-free medium should be used for the maintenance of the BEAS-2B cell line. In the establishment of this cell line, the medium used was LHC-9 [53], a serum-free medium specially formulated for the growth of bronchial epithelial cells [50]. As previously explained, this medium is also adequate for investigating the effects of Cr(VI)-exposure (section 1.1.4).

The group of Curtis Harris reported that, at least until passage 29, BEAS-2B cells had an approximately diploid karyotype. They have also observed that, as immortalization progressed, there was an accumulation of a characteristic set of chromosomal alterations. For long, these studies were the only cytogenetic analysis of BEAS-2B cells available. Some years ago, our group performed an additional analysis of the karyotypic alterations of this cell line [59]. We observed the presence of a basal set of chromosomal alterations, which suffered some modifications with culture age. These aspects will be further discussed in section 3.1.3.

## 1.2. The importance of the stress response in biological systems

The stress response is the most ubiquitous and conserved response that cells developed to survive the stresses they might encounter in their environment, being present in the entire spectrum of organisms [49]. This response has been shown to also exert its protective effects in cancer cells. Unfortunately, in this case, the protective effects of the stress response at the cellular level do not translate into a beneficial effect at the organism level.

The stress response is essential to maintain cellular and organismal homeostasis not only under stressful conditions, but also in basal conditions. Its cytoprotective effects are essentially due to the action of a set of proteins, known as heat shock proteins (Hsps), which function as molecular chaperones and anti-apoptotic proteins [69, 70]. Mammals express many types of Hsps, which are commonly classified, according to their molecular weights, in 6 families: Hsp100, Hsp90, Hsp70, Hsp60, Hsp40 and small Hsps [71, 72]. The first four families are sometimes referred to as the high molecular weight Hsps and the other two families as the low molecular weight Hsps. The former are ATP-dependent, while the latter are ATP-independent [73, 74].

As chaperones, Hsps play a critical role in protein folding, in the assembly and disassembly of oligomeric protein complexes, in the translocation of proteins to their final subcellular locations and in the regulation of protein degradation [70].

In their environment, cells frequently encounter diverse phenomena that induce proteotoxic stresses, i.e. stresses that impose conformational alterations to proteins and eventually lead to their denaturation and/or aggregation. In these conditions, there is an overexpression of Hsps to allow the cells to manage the increase of damaged and aggregated proteins, which can trigger the programmed cell death pathways. In fact, the increased pool of Hsps will help in the refolding of the damaged proteins and protect them from aggregation or, if the damage is too extensive, and goes beyond a certain threshold where refolding is no longer possible, it will assist the sequestering and diversion of the severely damaged proteins to the proteasome, where they will be degraded [70, 75]. Ultimately, this induction of the stress response promotes the survival and adaptation of cells and organisms to conditions of stress.

The overexpression of Hsps is the result of a transient increase in the transcription of the genes that encode them, promoted by transcription factors known as heat shock factors (HSFs). HSFs promote transcription through binding to specific regions within

the promoters of the Hsp genes, called heat shock elements (HSEs) [70]. In mammals, there are several isoforms of HSFs, but the main regulator of the stress response is HSF1, which is homologous to the only HSF present in *Drosophila* [76], the organism where the stress response was initially discovered.

The reference to heat shock in the designations of the elements involved in the stress response is due to the fact that this response was initially named the heat shock response, after the first type of shock shown to induce it. Ritossa reported for the first time, in 1962, that a transient exposure to elevated temperature led to an increased transcriptional activity in specific regions of the polytene chromosomes of *Drosophila busckii* [77]. At the time, Ritossa also observed that the transcriptional activity in the same regions was increased upon incubation with 2,4-dinitrophenol (DNP), an uncoupler of oxidative phosphorylation, suggesting that heat shock and metabolic stress could be upregulating the transcription of the same set of genes. Nowadays, it is well established that this response is activated not only by heat shock, but also by cold shock, metabolic and oxidative stresses, exposure to heavy metals, pathological conditions and essentially every phenomenon capable of inducing proteotoxic stress [71, 78].

Considering the important role of the stress response in the maintenance of cellular homeostasis both in basal and stressful conditions, it is not surprising that its deregulation has been associated with aging and several pathologies, namely cancer (section 1.2.1), and neurodegenerative and autoimmune diseases [70, 71, 79].

### **1.2.1. The involvement of the stress response in carcinogenesis**

In the past few years, much effort has been dedicated to the study of the complex interplay between the stress response and carcinogenesis. Understanding this relationship is crucial because it is helping to shed light on the molecular mechanisms of cancer progression and is also allowing the development of new therapeutical approaches (section 1.2.2) [80-82].

Cancer cells are subjected, in their suboptimal cellular environment, to high levels of proteotoxic stresses that originate both from intrinsic and extrinsic factors. The intrinsic factors include the imbalance in protein production caused by aneuploidy, the presence of mutant oncoproteins and high levels of metabolic stress. The tumour microenvironment is the major responsible for the extrinsic stress as it subjects cancer

cells to extremely adverse conditions, including hypoxia, acidosis, nutrient deprivation and redox deregulation [83]. All these stresses could seriously compromise cell function and survival without a fully functional protective system, which is consistent with elevated levels of most Hsps and increased HSF1 activity consistently observed in several different types of tumours [80].

The activation of the stress response in cancer cells does not seem to be merely an adaptive response that enables survival to the multiple stresses to which they are subjected. On the contrary, it has been proposed that it is also an active driver of carcinogenesis [84]. In fact, due to its capacity to promote cellular proliferation and inhibit cell death pathways, the activation of the stress response has been implicated in tumour growth. Furthermore, it appears to be involved in the acquisition and maintenance of oncogenic hallmarks and also in chemotherapy resistance [73, 75, 80].

It is important to note that HSF1 activation might not be the only mechanism involved in the marked upregulation of Hsps observed in cancer cells. In fact, the activation of the promoters of some Hsps genes by the oncoprotein c-Myc and/or their derepression when tumour suppressor proteins, such as p53 or p63, lose their function have been proposed to also contribute to the above-mentioned upregulation [82]. Interestingly, HSF1 was shown to have several other functions in cancer cells (section 1.2.1.3) and is, along with Hsp90 and Hsp70, one of the components of the stress response that has received more attention in the context of carcinogenicity.

#### **1.2.1.1. Hsp90**

The Hsp90 family includes ubiquitous and abundant chaperones, with a molecular weight of approximately 90 kDa [85]. One of the features that distinguishes the proteins of the Hsp90 family from the other Hsps is that they act essentially to maintain the proper folding and to prevent the aggregation of conformationally labile proteins, while the other families have a role in promoting the correct folding of proteins synthesized *de novo* [75].

At least four members are included in the Hsp90 family: the two Hsp90 isoforms, Hsp90 alpha (Hsp90 $\alpha$ ) and beta (Hsp90 $\beta$ ), the TNF receptor-associated protein 1 (TRAP1), and the glucose-regulated protein 94 (GRP94). Hsp90 $\alpha$  and Hsp90 $\beta$  are found both in the cytosol and the nucleus, while TRAP1 and GRP94 are restricted to the mitochondria and the endoplasmic reticulum (ER), respectively [86, 87].

The two Hsp90 isoforms are constitutively expressed and Hsp90 $\alpha$  is also stress-inducible [88]. The two proteins are only active in the form of homodimers and the functional differences between them are not yet completely understood [89]. It was reported that the knockout of the genes encoding these two proteins is lethal to cells, suggesting that they both have an essential function in organismal homeostasis [75, 89, 90].

The set of proteins known to be activated and stabilized by Hsp90, i.e. the set of Hsp90 client proteins, is continuously increasing, and includes proteins involved in almost all cellular processes [80, 91]. Of note, Hsp90 interacts extensively and modulates the transcriptional activity of p53 [92, 93], a transcription factor known as the guardian of the genome [63].

The importance of Hsp90 function for the maintenance of cellular homeostasis is also reflected in the multiple mechanisms of regulation to which it is subjected. In addition to the transcriptional control of its expression, post-translational modifications, such as phosphorylation, acetylation and S-nitrosylation, are essential to regulate its activity [94, 95].

Similarly to the other high molecular weight Hsps, members of the Hsp90 family are dependent on ATP. In fact, in order for them to act as chaperones, ATP must bind to a specific site of their amino terminal domain (N-terminal domain) and suffer hydrolysis. It is thought that this binding and hydrolysis of ATP causes conformational alterations on Hsp90 that are essential for substrate binding [95, 96]. The ATP-binding pocket of this family of proteins contains the so called Bergerat motif, which belongs to the GHKL (bacterial Gyrase, Hsp90, histidine Kinase, MutL) superfamily, and is distinct from the one found on many kinases and on Hsp70 [97]. The biological relevance of this feature remains unclear [75], but it has been exploited for the development of drugs specifically targeting these proteins [98].

Hsp90 proteins have two other domains: the middle domain (M domain), which is highly charged, and is the docking site for the client proteins; and the carboxyl terminal domain (C-terminal domain), which is essential for dimerization, and possesses another ATP-binding site [96]. Currently, the role of this second ATP-binding site on the regulation of the chaperone function is not clear, but, interestingly, it is only shown upon nucleotide occupation of the N-terminal site [99].

Hsp90 proteins do not accomplish their tasks just on their own. In fact, it is considered that the chaperoning function of Hsp90 requires the assembly of an Hsp90

chaperone machine, a dynamic complex comprising not only Hsp90 homodimers, but also Hsp70 and proteic co-chaperones [95, 100]. The co-chaperones usually dock on the M domain, even though they can also interact with the other two domains, and mediate the interaction of Hsp90 with its client proteins [96]. Different complexes are assembled by association of different co-chaperones, and this diversity helps to explain how Hsp90 can chaperone so many distinct client proteins.

In addition to the chaperoning of client proteins, Hsp90 is also capable of modulating nuclear events, namely of regulating the activity of HSF1 (section 1.2.1.3). Hsp90 can also inhibit apoptosis by interacting with diverse components of the cytosolic apoptotic pathways [69].

It is interesting to note that, although Hsp90 is predominantly found in the intracellular environment, it has also been found in the cell surface in many cell types and it can be secreted to the extracellular environment. So far, extracellular Hsp90 seems to be essentially associated with regulation of cell mobility [100].

It is evident that Hsp90 has a plethora of functions that are essential to maintain cellular homeostasis. Thus, it is not surprising that Hsp90 has also been shown to be essential for cancer cells. In fact, Hsp90 has been consistently found overexpressed in many types of cancers, and this overexpression has been correlated with increased tumour growth, metastatic potential and chemotherapy resistance [73, 75, 80]. These observations have lead some investigators to propose that Hsp90 overexpression could be used as a marker of cellular malignancy [101] and that some cancers are addicted to Hsp90 [100].

An increased pool of Hsp90 is essential for cancer cells to recover essential proteins that became misfolded due to the extensive proteotoxic stresses to which they are subjected. It also facilitates the function of mutant oncoproteins, by protecting them from misfolding and degradation [75]. The mutant p53 proteins, which have been shown to exert functions that contribute to malignant progression [102], are an excellent example of oncoproteins known to be clients of Hsp90 [75]. In addition, Hsp90 is responsible for the chaperoning of many conformationally labile signaling proteins involved in the acquisition of the proposed hallmarks of cancer. Among these, it is worth mentioning several receptor tyrosine kinases and steroid hormone receptors, such as the human epidermal growth factor 2 (HER2) and the progesterone receptor, respectively, associated with uncontrolled cellular proliferation [75, 103], telomerase, an enzyme required for immortalization [104], Akt, involved in deregulation of the apoptotic response [105], hypoxia-inducible factor 1-alpha (HIF-1 $\alpha$ ), essential for angiogenesis [106] and matrix

metalloproteinases (MMPs) that promote tissue invasiveness and metastasis formation [107].

Interestingly, HIF-1 $\alpha$ , which is known to be activated by hypoxia and oxidative stress, was identified as a key regulator of Hsp90 $\alpha$  secretion. As it is well established that the tumour microenvironment is frequently hypoxic and that many tumours overexpress HIF-1 $\alpha$ , its new identified role in Hsp90 $\alpha$  secretion has been proposed as an explanation for the higher levels of extracellular Hsp90 found in cancer cells, in comparison to those of normal cells [73, 108]. Importantly, the increased levels of extracellular Hsp90 in cancer cells have been correlated with higher metastatic activity, which is likely due to the activation of MMP2 and of the HER2 signaling cascade that promotes cell motility and invasion [100, 108].

#### 1.2.1.2. Hsp70

Hsp70 is a family of multi-functional proteins, found in several subcellular compartments. All members of this family are structurally similar, presenting a conserved structure with an ATP-binding site in the N-terminal and a substrate binding domain in the C-terminal, connected by a short, flexible linker [109].

At least eight homologous chaperones belong to the Hsp70 family. There are two glucose-regulated proteins, GRP78 and GRP75, which are restricted to the ER and the mitochondria, respectively. The other six members reside in the cytosol and the nucleus. Among these, the best studied proteins are the constitutively expressed isoform, Hsp73, which has essential housekeeping functions, and the stress-inducible isoform, Hsp72, that is considered one of the most highly inducible among all Hsps [109, 110].

Members of the Hsp70 family are, unlike those of the Hsp90 family, essential for the folding of newly synthesized peptides. It is estimated that, in bacterial cells, these proteins assist the *de novo* folding of 10 to 20% of all proteins, and this value is likely higher in human cells [109]. In addition, Hsp70s can also facilitate the proteolytic degradation of unstable proteins [111]. Under stress conditions, Hsp70s, particularly the inducible Hsp72, have an essential role in the promotion of cell survival, due to their multifaceted anti-apoptotic function [69]. As previously mentioned (section 1.2), proteotoxic stresses cause protein denaturation and aggregation, which are powerful inducers of the programmed cell death pathways. The anti-apoptotic action of Hsp70s

deters these signaling pathways, allowing time for the repair of the proteome. Hsp70s interact with several proteins of the apoptotic signaling cascade and can inhibit both the extrinsic and the intrinsic apoptotic pathways. In addition, Hsp70s were shown to inhibit the lysosomal death pathway, dependent on the release of cathepsin proteases [80, 112].

To carry out these functions, ATP, co-chaperones and nucleotide exchange factors are required. ATP regulates the association of Hsp70 with short hydrophobic segments exposed in the non-native forms of its client proteins, by promoting conformational alterations in the substrate binding domain that increase its affinity for the substrates. Together with nucleotide exchange factors, co-chaperones control the ATPase activity of Hsp70, and, thus, the cycling of the protein between the active and inactive state. Co-chaperones also help in the targeting of Hsp70 to specific substrates, and, afterwards, in the release of the bound cargo [109, 111].

Overexpression of some members of the Hsp70 family, specially the stress-inducible isoform Hsp72, has been frequently observed in several cancers and correlated with poor prognosis [113, 114]. It has been suggested that the overexpression of Hsp70 might be associated with increased invasive and metastatic capacities and with resistance to chemotherapy. It is thought that cells overexpressing Hsp70 have an increased chance of survival, especially due to their capacity of inhibiting stress-induced apoptosis and suppressing senescence [73, 112].

Since the action of many chemotherapeutic agents is to promote the induction of programmed cell death, the capacity of Hsp70s to inhibit the apoptotic pathways is one of the keys to explain the resistance to those compounds. Avoiding apoptosis is also essential for cells that are initiating the metastatic process, and Hsp70 has been shown to influence the activity of proteins, such as focal adhesion kinases, Akt and Met, that regulate anoikis and amorphosis [114], particular types of apoptotic cell death that are induced by cell detachment from the extracellular matrix (ECM) and through disruption of cell shape, respectively [115, 116]. In addition, Hsp70 can also promote the secretion of MMPs, which also promote the invasive and metastatic capacities [114]. Interestingly, this role of Hsp70 in metastasis formation has been proposed to be mediated by extracellular Hsp70, in similarity to what has been observed for Hsp90 (section 1.2.1.1). In agreement, Hsp70 has shown to be present in the plasma membrane of solid tumours and metastasis, but not in the corresponding normal tissues [80].

Replicative senescence is thought to be counteracted by Hsp72, due to its capacity to stabilize and promote the activity of the ubiquitin ligase Hdm2. Hdm2 is one of the

inhibitors of the wild-type p53 protein, which has a pro-senescence activity [117]. Accordingly, siRNA-mediated depletion of Hsp72 in cancer cell lines resulted in a senescent phenotype, which included flattened cell morphology, decreased proliferation, and increased senescence-associated  $\beta$ -galactosidase staining [117]. This senescent phenotype seemed to be associated with the activation and stabilization of p53, due to reduced stability and activity of Hdm2, and the consequent induction of the cell cycle inhibitor p21, which is known to regulate p53-mediated senescence. In this study, Hsp72 depletion also triggered a p53-independent senescence program, which involved the inhibitory phosphorylation and downregulation of the cell cycle kinase Cdc2.

Members of the Hsp70 family have also been shown to bind and stabilize mutants of p53 in tumour cells, but the relevance of this interaction is not yet well established [71, 118]. In addition, they participate in the cytoplasmic sequestration of wild-type p53 in cancer cells. The cytoplasmic sequestration of wild-type p53 is a phenomenon observed in several types of tumours and correlates with poor prognosis [118].

Similarly to Hsp90, Hsp70 is also needed to stabilize HIF-1 $\alpha$  and, consequently, to promote angiogenesis [80, 81].

### 1.2.1.3. HSF1

Hsp expression is a highly regulated process, and HSFs are the primary regulators of this expression [119]. In vertebrates, HSF1 assumes a particularly important role, being considered the master regulator of the stress response, since it is the sole responsible for the increase in Hsps levels in response to stress [120]. In fact, it was observed that *HSF1* deletion in mammalian cells abrogates stress-induced expression of Hsps, even though the normal basal expression is maintained [121, 122]. HSF1 itself is also tightly regulated by intricate processes, controlled by multiple mechanisms that are not yet completely understood.

In unstressed cells, HSF1 is generally found in the cytosol, in an inactive state that consists of monomeric HSF1 complexed with Hsp90 [123]. The activation of this transcription factor requires the dissociation of HSF1 monomers from Hsp90 and their subsequent trimerization and phosphorylation, followed by nuclear translocation [124]. In the nucleus, HSF1 can finally coordinate and promote the expression of the inducible Hsps [125] (Figure 1.4). Generally, the activation of HSF1 occurs under conditions of

proteotoxic stress, induced by both physical and chemical agents. This stress leads to an accumulation of damaged proteins that require the chaperoning function of Hsp90, which, thus, disassociates from HSF1, allowing its activation [82, 123]. Inhibition of Hsp90 through binding of natural or synthetic compounds to its N-terminal ATP-binding pocket was reported to have a similar effect [123]. In turn, binding of Hsp70 to HSF1 trimers has been proposed as one of the steps required for the attenuation of its transcriptional activity (Figure 1.4). The stress response is, thus, partially auto-regulated by feedback mechanisms [119].

Several post-translational modifications, most notably phosphorylation, which is considered a key determinant of HSF1 transactivating potency [125], are essential for the conversion of HSF1 to an active form capable of being translocated to the nucleus and binding to HSEs in a productive manner [124]. In addition to phosphorylation, both sumoylation and deacetylation were shown to have a role in HSF1 activation. In turn, acetylation is involved in the attenuation of the transcriptional activity of this transcription factor [80].

The intracellular redox state can also modulate the activity of HSF1. In fact, it was shown that HSF1 possesses two crucial cysteine residues that act as sensors of the cellular redox state. An oxidative cellular environment will cause the oxidation of the sulfhydryl groups of these cysteine residues, leading to the formation of a disulfide bond that prompts trimerization and the DNA-binding activity of HSF1 [126]. Stressors that alter the redox balance, favoring the oxidation of the cysteine residues can, therefore, promote the activation of HSF1.

Structurally, HSF1, as well as the other HSFs, is organized in functional modules, which also reflect the complex regulation to which it is subjected [125]. The DNA binding domain, characteristic of transcription factors, is located in the N-terminal. This domain is followed by three arrays of hydrophobic heptad repeats (HR-A/B) that are essential for trimer formation. Adjacent to the C-terminal, another region of hydrophobic heptad repeats (HR-C) mediates the suppression of trimerization. The C-terminal also contains two distinct activation domains (AD 1 and 2), that are controlled by a centrally located heat-responsive regulatory domain (RD) [125].

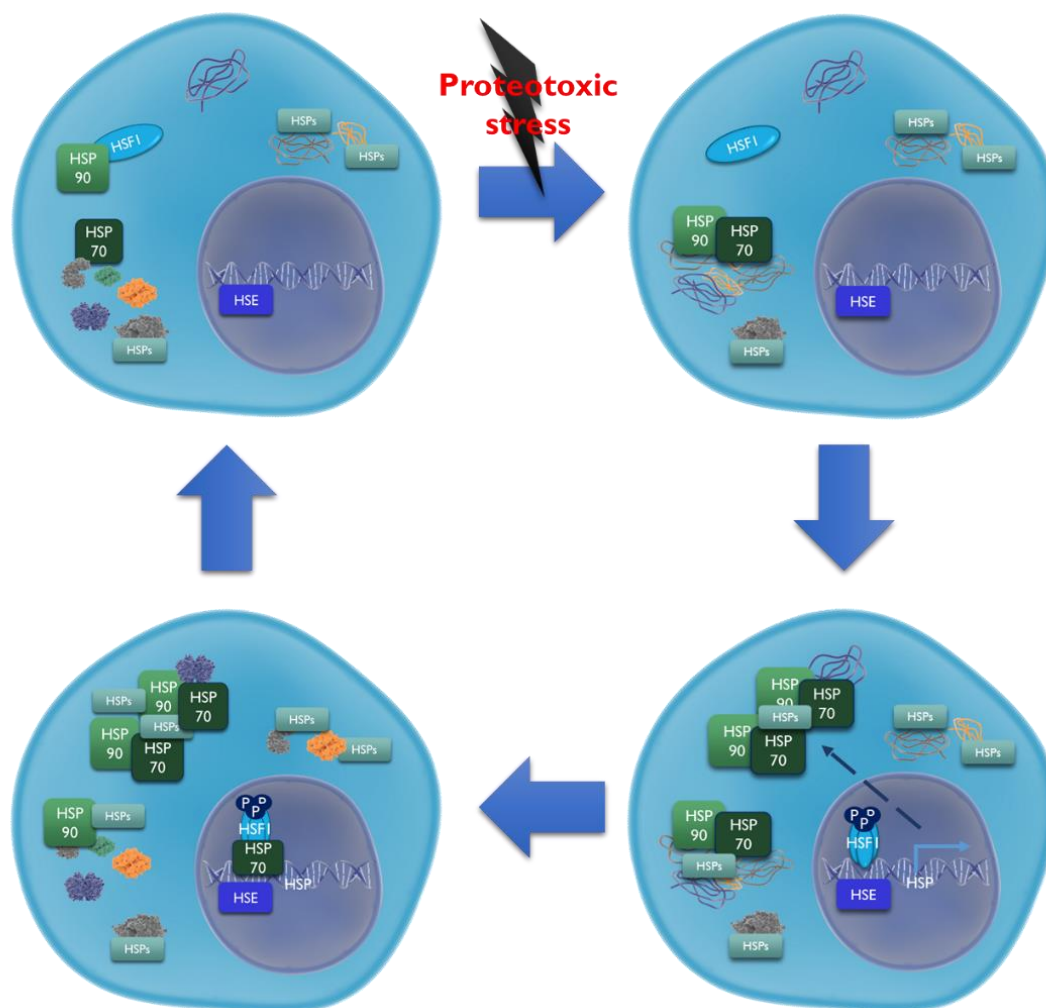


**Figure 1.4 | Schematic representation of the mechanisms involved in the activation and subsequent attenuation of HSF1 in response to a proteotoxic stress.** In unstressed cells, HSF1 is in an inactive state that consists of monomeric HSF1 complexed with Hsp90. Under conditions of proteotoxic stress, there is an accumulation of damaged proteins that require the chaperoning function of Hsp90, which, thus, disassociates from HSF1, allowing its activation. The activation of HSF1 involves its trimerization, phosphorylation (and other post-translational modifications not depicted in the figure) and nuclear translocation. In the nucleus, the transcriptionally active HSF1 coordinates and promotes the expression of the inducible Hsps, by binding to the heat shock elements (HSE) present in the HSPs genes. Upon restoration of cellular homeostasis, through the action of the increased pool of Hsps, the transcriptional activity of HSF1 is attenuated. This attenuation involves a negative feedback from Hsp70, which binds to HSF1 trimers, and also acetylation (not depicted in the figure).

It is interesting to note that HSF1 activity has been shown to not be restricted to the classical induction of the Hsps. Studies in yeast revealed that the direct transcriptional targets of HSF1 represent up to 3% of the genome and include genes involved in a broad range of cellular functions [127]. In humans, it has also been observed that HSF1 can

regulate a broad spectrum of non-Hsp genes [128]. Overall, HSF1 seems to control the expression of a set of genes that encode proteins with essential roles in cell survival [82].

Many studies have also shown that HSF1 is capable of facilitating neoplastic transformation and promoting cancer cell survival and proliferation [120, 129]. The first striking observations indicating the powerful role of HSF1 in carcinogenesis came from the group of Lindquist. In 2007, this group reported that HSF1 deficiency suppressed chemically induced skin carcinogenesis, as well as mutant p53-driven tumorigenesis and cellular transformation initiated by oncogenic *RAS* or proto-oncogenic platelet-derived growth factor B (*PDGF-B*) [120]. Depending on the nature of the oncogenic stimulus, HSF1 acted by increasing cellular proliferation and/or decreasing cell death. Interestingly, they also observed that HSF1 was capable of modulating glucose metabolism, and *HSF1*<sup>+/+</sup> cells had an increased glucose uptake and were more dependent on this nutrient to support the cellular energy needs than their *HSF1*<sup>-/-</sup> counterparts [120].

At the time, these observations were rather unexpected since HSF1 was traditionally considered to be an enhancer of organismal survival and longevity [129]. In the light of the new discoveries, HSF1 began to be seen as a double-edged sword, since it was also found to be capable of supporting carcinogenesis, a lethal phenomenon for the organism [120, 129].

For many years, it was believed that the effect of HSF1 on carcinogenesis was essentially indirect, acting mainly through the promotion of the expression of Hsps. As previously described, these proteins can potentiate oncogenesis by facilitating cellular adaptation to a constantly changing intracellular and extracellular milieu [120]. However, more recently, it was reported that, in highly malignant cells, HSF1 regulates a transcriptional program that is distinct from the one induced in response to heat shock [129]. Besides the Hsps genes, the HSF1-regulated cancer specific transcriptional program includes genes that are essential to support the oncogenic process, being involved in cell-cycle regulation, DNA repair, energy metabolism, cell adhesion, ECM formation and protein translation. This program was active in several human malignancies that have high morbidity and mortality rates associated, such as those of breast, lung and colon, and its activation correlated with poor prognosis and increased metastatic potential [129]. Therefore, activation of this transcription factor will have effects that go far beyond the upregulation of the Hsps, with the latter likely accounting for a smaller fraction of the role of HSF1 in tumorigenesis than initially expected.

Moreover, HSF1 was also found to induce the multidrug resistance phenotype, once more through a mechanism independent from the canonical stress response [130].

### **1.2.2. Hsps and HSF1 inhibitors as anticancer agents: a new therapeutic approach**

The observation that the stress response is activated in cancer cells has led many investigators to propose several elements of the stress response as new therapeutic targets in cancer. As such, much effort has been devoted to the development of inhibitors of those elements for therapeutic purposes [81].

Hsp90 inhibitors have received particular attention, fueled by the prospect of obtaining a simultaneous inhibition of the chaperoning of several oncogenic proteins crucial for the maintenance of each of the established cancer hallmarks [81, 100] (section 1.2.1.1). The great majority of inhibitors of Hsp90 that have been studied interacts with the N-terminal ATP-binding pocket with greater affinity than ATP. Binding of these compounds inhibits the ATPase activity of these chaperones [75], disrupting the chaperone cycle and probably causing client protein degradation [100]. Most of the compounds that have been developed and studied showed promising results in *in vitro* and *in vivo* models and some have already entered clinical trials, but, to this day, none has been approved for clinical use [131].

There have been some concerns about the safety of this therapeutic strategy. In fact, as Hsp90 is essential for normal cell function, its inhibition may be associated with undesirable side effects for normal cells. Interestingly, Hsp90 has been shown to have an approximately 100-fold greater affinity for its inhibitors in cancer cells than in normal cells, which leads to an accumulation of the inhibitors within the tumours [132]. It has been proposed that this differential affinity is due to the increased fraction of Hsp90 that, in cancer cells, is involved in multiprotein complexes. These complexes exhibit high ATPase activity, as a consequence of the augmented load of misfolded and mutant proteins in those cells. In turn, in normal cells, Hsp90 is found mostly as free dimers that have lower ATPase activity than the multiprotein complexes [75, 132]. These observations suggest the existence of a therapeutic window in which Hsp90 inhibitors will efficiently affect cancer cells without interfering with the function of normal cells.

To improve the efficacy of this therapeutic strategy, it might be important to choose cancers that are driven by Hsp90 client proteins and to use Hsp90 inhibitors synergistically with other therapeutic strategies [100]. Currently, there are, for instance, studies investigating the potential of combining Hsp90 inhibitors with inhibitors of the co-chaperones that are essential for Hsp90 function, of the proteasome or of angiogenesis [81, 100].

It is important to mention that inhibition of Hsp90 by N-domain targeting compounds has been shown to induce the expression of the cytoprotective Hsp70 and Hsp27 proteins [73]. This has raised concerns, because the overexpression of these proteins will protect cancer cells from some of the adverse effects of Hsp90 inhibitors. Accordingly, it was observed that sensitivity of cancer cells to a Hsp90 inhibitor, geldanamycin, can be substantially increased by silencing of Hsp70 and/or Hsp27 [100]. The induction of Hsp70 and Hsp27 is essentially a consequence of the interplay between Hsp90 and HSF1 (section 1.2.1.3). Inhibition of Hsp90 leads to the activation of HSF1 that, in turn, will promote the synthesis of the Hsps. Moreover, since, as previously discussed, HSF1 is also a powerful modulator of carcinogenesis, the consequences of this activation might extend far beyond the induction of the stress response.

To overcome the shortcomings associated with N-domain inhibitors, significant efforts are now being put in the development of C-terminal inhibitors, which do not seem to have the aforementioned drawbacks [73, 80]. Another possible strategy, is to combine inhibitors of Hsp90 with inhibitors of Hsp70 or of HSF1.

Inhibition of Hsp70 is, in fact, an anticancer strategy that has been taken into consideration, due to the known capacity of Hsp70 to regulate multiple protection mechanisms in cancer cells. Hsp70 inhibition might be useful in combination not only with Hsp90 inhibitors, but also with other common chemotherapeutic agents to abolish its anti-apoptotic effects [73, 133]. Unfortunately, the development and validation of pharmacological inhibitors of Hsp70 has been slower and more complicated than that of Hsp90 inhibitors [133]. All of the inhibitors that progressed to clinical trials had limited efficacy and presented severe toxicity [112].

HSF1 inhibitors have also a great potential as anticancer drugs, due to the multifaceted role of HSF1 in carcinogenesis [82, 120]. Some small compounds have been identified as inhibitors of the HSF1-induced upregulation of Hsps and other HSF1 targets. Their mechanisms of action are not completely understood, but apparently involve an indirect interference with HSF1 activity and not a direct targeting of this transcription

factor. All these compounds presented low potency and/or poor specificity in pre-clinical studies [82].

### **1.2.3. Heavy metals and the stress response**

Previous work, in a variety of *in vitro* and *in vivo* model systems, has shown that exposure to several heavy metals can lead to an induction of the expression of Hsps [55, 78, 134-137]. The pattern of alterations in the expression of Hsps and the tissue specificity of each metal depend on factors such as the route of metal uptake, distribution and accumulation among tissues, subcellular distribution within a tissue, and the capacity of the metal to generate secondary stressors. Therefore, it has been proposed that the alterations induced by a metal on the stress response might be used as a “biochemical fingerprint” of exposure or as a “toxicological signature” [134].

The effects of heavy metals on Hsps expression have been classified using those induced by heat shock as a reference. The classifications are the following: analogous induction, when the proteins induced by metals are the same as those induced by heat; subset induction, when the proteins induced by metals represent a subgroup of those induced by heat; and specific induction, when the proteins induced by metals, such as metallothionein, are not heat inducible [136]. These different classes of induction suggest that distinct mechanisms mediate the effects of heavy metals on the expression of Hsps. Heavy metals generally induce significant proteotoxicity and, thus, the classical mechanisms of activation of the stress response described in section 1.2.1.3 are likely the major mediators. Frequently, heavy metals also induce the generation of reactive species, such as ROS. These reactive species are known for their capacity to regulate transcription and it has been proposed that they might be partially responsible for the observed induction of the stress response upon exposure to metals [134, 136]. In support of this hypothesis it was reported, for instance, that the induction of Hsp70 in BEAS-2B cells exposed to divalent cadmium and mercury was inhibited by the addition of N-acetylcysteine, a known antioxidant [135].

### 1.2.3.1. The case of Cr(VI)

Cr(VI) is a heavy metal and, therefore, one would expect that it caused an increase in the expression of Hsps. However, the studies carried out so far have not always shown a correlation between Cr(VI)-exposure and increased expression of Hsps. Table 1.1 summarizes the observed effects of Cr(VI) on the expression of the different Hsps.

As can be seen in Table 1.1, the effects of Cr(VI) on Hsp90 expression were evaluated in three studies only, all in different systems. The results revealed both a downregulation of *HSP90AA1* messenger RNA (mRNA) [55], which encodes Hsp90 $\alpha$ , and a decrease of Hsp90 protein levels [138, 139]. On the other hand, *TRAP1* mRNA levels were found to be increased [41].

An increased expression, at both the mRNA and protein levels, was reported for Hsp27, in two different studies [140, 141]. Notwithstanding, one of these studies also revealed a reduced phosphorylation of this protein [141]. Since phosphorylation is a post-translational modification known to be essential for Hsp27 activation [141], it is possible that, despite the increased levels, the total activity of Hsp27 in those Cr(VI)-exposed cells was actually decreased. Interestingly, a distinct study reported an increase in Hsp27 phosphorylation [142], suggesting that Cr(VI)-effects on the activity of this protein might be dependent on the model system and exposure regimen employed.

The effects of Cr(VI) on Hsp70 are the most extensively studied so far, but there are some discrepancies, which might be due to the use of different systems and exposure regimens. At the protein level, there are two reports of increased Hsp70 levels [139, 140], and one of decreased levels of the constitutive isoform, Hsp73 [138]. Concerning mRNA levels, increases were reported for the mRNAs encoding both human [143] and rat inducible isoforms [144]; another study reported that the mRNA levels of *HSP-70* remained unchanged [145], but the authors did not specify the specific mRNA studied. There is also one study where an induction of the *HSP70* promoter was observed [137].

Two studies evaluated the effects of Cr(VI) on Hsp60 expression and obtained distinct results depending on whether mRNA or protein expression was evaluated. In fact, the mRNA levels were shown to be decreased [55], whereas those of protein were increased [40].

Table 1.1 | Cr(VI)-induced effects on the expression and activity of components of the stress response.

Protein family	System <sup>a</sup>	Exposure regimen		Effect <sup>c</sup>	Study
		Cr(VI) dose/concentration <sup>b</sup>	Duration		
Small Hsps	Rat lung epithelial cells	10 µM	24 h	Increased Hsp10 protein levels	[40]
	HaCaT cells	3.7 µM	24 h	Increased <i>HSPB1</i> mRNA and Hsp27 protein levels Reduced Hsp27 phosphorylation	[141]
	Human primary skin fibroblasts	1 µM	16 h	Increased Hsp27 phosphorylation	[142]
	BNL CL.2 cells	15 µM	3 h	Increased Hsp27 protein levels	[140]
Hsp40	ICR mice liver tissue	10 mg/kg, BW (IP inj)	8 weeks		
	BEAS-2B cells	10 µM	4 h	Decreased <i>DNAJB1</i> mRNA levels	[55]
Hsp60	BEAS-2B cells	10 µM	4 h	Decreased <i>HSPD1</i> mRNA levels	[55]
	Rat lung epithelial cells	10 µM	24 h	Increased Hsp60 protein levels	[40]
Hsp70	Sprague-Dawley rat lung tissue	0.25 mg/kg, BW (IT inst)	3 days	Increased levels of the rat inducible Hsp70 mRNA	[144]
	HT29	10 or 50 µM	6 h	Increased <i>HSPA1A</i> mRNA levels	[143]
	HepG2 cells	0.5 or 1.0 µM	48 h	Induction of <i>HSP70</i> promoter	[137]
		5 or 10 µM	3 h	Unchanged <i>HSP-70</i> mRNA levels <sup>d</sup>	[145]
		100 µM	12 or 24 h	Decreased Hsp73 protein levels	[138]
	Primary culture of rat granulosa cells	10 µM	24 h	Increased total Hsp70 protein levels	[139]
L-02 cells	16 or 32 µM	3 h	Increased Hsp70 protein levels <sup>d</sup>	[140]	
	ICR mice liver tissue	10 mg/kg, BW (IP inj)	8 weeks		
Hsp90	BEAS-2B cells	10 µM	4 h	Decreased <i>HSP90AA1</i> mRNA levels	[55]
	Primary culture of rat granulosa cells	16 or 32 µM	12 or 24 h	Decreased Hsp90 protein levels <sup>d</sup>	[138]
	L-02 cells	300 µM	24 h	Decreased total Hsp90 protein levels	[139]
Hsp100	A549	300 µM	2 h	Increased <i>TRAP1</i> mRNA levels	[41]
	Rat lung epithelial cells	10 µM	24 h	Increased Hsp105 protein levels	[40]

<sup>a</sup> A549, cell line derived from a human lung adenocarcinoma; BEAS-2B, cell line derived from human bronchial epithelial cells; BNL CL.2, cell line derived from embryonic murine liver cells; HaCaT, cell line derived from keratinocytes; HepG2, cell line derived from a human hepatocellular carcinoma; HT29, cell line derived from a human colorectal adenocarcinoma; L-02, cell line derived from human embryonic hepatocytes.

<sup>b</sup> Cr(VI) was added as a K<sub>2</sub>Cr<sub>2</sub>O<sub>7</sub> or Na<sub>2</sub>CrO<sub>4</sub> aqueous solution. BW, body weight; IP inj, intraperitoneal injection; IT inst, intratracheal instillation.

<sup>c</sup> Hsp, heat shock protein; *HSPB1*, heat shock 27 kDa protein 1; *DNAJB1*, DnaJ heat shock protein family (Hsp40) member B1; *HSPD1*, heat shock 60 kDa protein 1; *HSPA1A*, heat shock 72 kDa protein; *HSP90AA1*, heat shock 90kDa protein 1 alpha; *TRAP1*, TNF receptor-associated protein 1.

<sup>d</sup> No specific mRNA or isoform identified.

The effects of Cr(VI) on other Hsps have been addressed only once so far: the protein levels of Hsp10 and Hsp105 were found to be increased [40], whilst the levels of the mRNA that encodes Hsp40 decreased [55].

Overall, these studies strongly suggest that Cr(VI) can interfere with many components of the stress response, but the results appear to be dependent on the model system and the exposure regimen used and, thus, it has not been possible to establish a pattern for any of the components evaluated. Clearly, more investigations are required to characterize the alterations that Cr(VI) induces on the elements of the stress response under biologically relevant conditions. Furthermore, it would be important to investigate the molecular mechanisms underlying the observed alterations in the expression and activity of Hsps, what has not been done so far. Considering the involvement of the stress response in carcinogenesis (section 1.2.1), it would also be important to investigate the role that the observed alterations might have in terms of Cr(VI)-induced carcinogenesis.

To this date, the effects of Cr(VI) on HSF1 have not been studied. However, one may envisage that Cr(VI) could lead to its activation. In fact, it is possible that Cr(VI) promotes the oxidation of the sulfhydryl groups in the cysteine residues crucial for HSF1 activation [126] (section 1.2.1.3), as previous reports have shown that Cr(VI) interacts with those groups in other proteins [146, 147].

### 1.3. Genomic instability and cancer

Genomic instability is typically observed in most human cancers and its importance for cancer development and progression is, nowadays, undisputable [148, 149]. In their 2011 review on the hallmarks of cancer, Hanahan and Weinberg defined genomic instability and mutability as one of the characteristics of cancer cells that allows the acquisition of the core and emerging hallmarks [26] (section 1.1.3).

Different types of genomic instability have been identified in tumours [149]. Alterations in the structure and number of chromosomes, known as chromosomal instability (CIN), are the major form of genomic instability found in human cancers. MSI, which is characterized by alterations in the number of nucleotide repeats present in the microsatellite sequences, is another form of genetic instability commonly observed in tumours.

Many questions still remain concerning the molecular mechanisms underlying this phenomenon, the stage of carcinogenesis at which it arises and the exact contribute it gives for the development of distinct types of tumours [148].

In hereditary cancers, both CIN and MSI are generally associated with mutations in the so-called caretaker genes [150]. These genes encode multiple components of the DNA-maintenance machinery, ranging from those involved in the detection of DNA damage and activation of the DNA repair mechanisms to those that directly participate in DNA repair or in preventing the damaging action of mutagenic molecules [26]. For instance, germline mutations in breast cancer susceptibility 1 and 2 (*BRCA1* and *BRCA2*), BRCA1-interacting protein (*BRIP1*), Werner syndrome helicase (*WRN*) and several other genes involved in the repair of DNA DSBs or DNA interstrand cross-links increase the predisposition to certain types of cancer, such as those of the breast and ovary. On the other hand, mutations in DNA mismatch repair (MMR) genes lead to MSI in hereditary non-polyposis colon cancer [148]. These observations give support to the mutator hypothesis, which proposes that genomic instability is present in pre-cancerous lesions and promotes tumour development by increasing the spontaneous mutation rate [151]. On the contrary, mutations in caretaker genes are rarely found in sporadic cancers [148], suggesting a different molecular basis for the genomic instability observed in this type of cancers.

Sporadic cancers are more frequently characterized by the presence of gain-of-function mutations in oncogenes, such as *RAS* [148]. Some authors hypothesized that this

oncogene activation might be a trigger of genomic instability and proposed an “oncogene-induced DNA replication stress model” [148, 152]. According to this model, activation of oncogenes will lead, through mechanisms not yet completely defined, to the stalling collapse of DNA replication forks, i.e. to DNA replication stress, and, consequently, to DNA DSBs [152], the most dangerous type of DNA lesions [153]. This model is supported by studies indicating that activated oncogenes induce DNA DSBs in several cellular and animal models and that DNA DSBs are recurrently present in pre-cancerous and cancerous lesions [152]. Moreover, it was observed, in diverse experimental models and pre-cancerous human lesions with activated oncogenes, that genomic instability preferentially affects the regions in the genome, known as common fragile sites [154], that are particularly sensitive to DNA replication stress [155-157].

Currently, DNA DSBs can be easily visualized through indirect immunofluorescence techniques, which detect proteins that are recruited to the regions affected by these lesions as part of the DNA damage response. One of these proteins is the histone H2AX, which is phosphorylated to gamma-H2AX ( $\gamma$ -H2AX) by the kinases ataxia telangiectasia mutated (ATM) and ATM-Rad3-related (ATR), following direct DNA DSB induction and replication stress, respectively [158]. For each DNA DSB, hundreds to thousands of H2AX are phosphorylated in the nearby chromatin, leading to the formation of  $\gamma$ -H2AX foci, which are considered true markers of DNA DSBs [159].  $\gamma$ -H2AX has been shown to be essential for the recruitment and localization of DNA repair proteins [159], and the kinases ATM and ATR are also responsible for the phosphorylation of some of those proteins and of key regulators of cell cycle checkpoint signaling, such as p53 [160].

Activation of the cell cycle checkpoints in response to DNA damage triggers an arrest in either the S or G2 phase, particularly through p53-dependent mechanisms, giving the cells time to repair the damage and avoiding the replication of damaged DNA (G1/S checkpoint) or the segregation of abnormal chromosomes (G2/M checkpoint) [161]. If the damage is not repaired, p53 can also induce apoptosis or senescence, i.e. a permanent growth arrest. The activation of these mechanisms is of the utmost importance during the repair of DNA DSBs because the two major pathways involved in that repair, the non-homologous end-joining (NHEJ) and the homologous repair (HR), are slow and prone to errors [160]. These errors include the amplification or loss of chromosomal material and the translocation of chromosome segments in a reciprocal or non-reciprocal fashion. All of these errors can lead to tumorigenesis, because they can cause the deletion of one or

more regions encoding a tumour suppressor gene, amplify regions where oncogenes are located or create a fusion gene [162]. The activation of p53 by the DNA damage response constitutes, thus, a major block to the proliferation of cells with structural CIN and, consequently, a barrier to tumorigenesis [152] (Figure 1.5). Importantly, p53-dependent mechanisms are also involved in the blockade of numerical CIN, as they were shown to limit the proliferation of aneuploid cells [163]. Aneuploid cells can also be generated during the attempt to repair DNA DSBs. In fact, due to the slowness of the DNA DSB repair pathways, the cell cycle arrest is, sometimes, too prolonged, uncoupling centrosome duplication from cell cycle progression (Figure 1.5). In turn, this uncoupling leads to the generation of cells with aberrant centrosome numbers, which are more prone to undergo mitotic catastrophe and generate malignant aneuploid progeny [163]. From the beginning, aneuploidy will alter the dosage of key genes, namely tumour suppressor genes and oncogenes, leading to further instability and contributing to a faster tumorigenesis.

In light of these observations, the proponents of the oncogene-induced DNA replication stress model have argued that there might be a selective pressure for inactivation of p53. This would, for instance, help explain the high rates of mutation of *TP53* observed in human cancers [148, 152]. These investigators further speculated that, if p53 inactivation is essential for tumorigenesis, it is likely that mutations in other components of the p53 pathway are also present in tumours. So far, there are not enough data to firmly confirm this hypothesis, but the results from two high-throughput sequencing studies of human cancers gave a strong support [164, 165].



**Figure 1.5 | Role of DNA DSB repair in the acquisition of chromosomal instability (CIN).**

The major pathways for DNA DSB repair, the non-homologous end-joining (NHEJ) and the homologous repair (HR), are slow and prone to errors. The errors of these repair pathways, which include amplifications, deletions and translocations of chromosomal material, lead to the accumulation of mutations and are a source of structural CIN, while their slowness might trigger the uncoupling of centrosome duplication from cell cycle progression and, consequently, the generation of aneuploid cells and numerical CIN. Under normal conditions, p53-dependent mechanisms will induce a permanent cell cycle arrest or apoptosis to prevent the proliferation of cells with CIN. p53 activation constitutes, thus, a major block to tumorigenesis and it has been proposed that there might be a selective pressure for its inactivation.

### 1.3.1. The role of genomic instability in Cr(VI)-induced carcinogenesis

As previously mentioned, one of the distinguishable features of Cr(VI)-induced lung cancers is the frequent MSI [11, 12] (section 1.1). In terms of genomic instability, it is conceivable that CIN is also present in Cr(VI)-induced lung carcinomas [37] since, as discussed in section 1.1.3, Cr(VI) is a genotoxic agent, inducing a broad range of DNA lesions, namely DNA SSBs and DSBs, which have the greatest potential to cause this type of genomic instability.

For many years, the induction of DNA DSBs upon Cr(VI)-exposure was only suspected, with suspicions arising from observations of increased frequencies of chromosomal breaks and micronuclei [7]. More recently, undisputable evidence of the presence of DNA DSBs in Cr(VI)-exposed cells has been gathered by several groups [166-174], namely through indirect immunofluorescence studies for foci of  $\gamma$ -H2AX [159]. Noteworthy, a recent study reported that Cr(VI) selectively induces DNA DSBs in euchromatin, the transcriptionally active chromatin, where this type of lesions is most dangerous [171]. Some authors have proposed that DNA DSBs in Cr(VI)-treated cells were a consequence of damaged DNA processing, and not of a direct action of Cr(VI) [7]. In support to this hypothesis, it was observed that, upon exposure to Cr(VI), cells deficient for MLH1 (*MLH1*<sup>-/-</sup>), a key protein of the MMR system, presented much lower rates of  $\gamma$ -H2AX foci formation than *MLH1*<sup>+/+</sup> cells [167]. This suggested that the DNA DSBs were secondary lesions resulting from the processing of Cr(VI)-induced DNA damage by the MMR system. MMR-deficient cells were also less sensitive to the cytotoxic action of Cr(VI) [167]. Thus, it is possible that chronic exposure to Cr(VI) might result in the selective growth of cells with deficiencies in this repair system [7]. As MMR-deficient cells exhibit high rates of spontaneous mutagenesis, this hypothesis would also justify the high incidence of MSI in Cr(VI)-induced lung cancers [11, 12].

As mentioned in section 1.3, the attempt to repair DNA DSBs can lead to generation of cells with aberrant centrosome numbers and, thus, to numerical CIN. Evidence has been collected, specially by the group of John Wise, that this type of mechanism is frequently present Cr(VI)-exposed cells [175]. In fact, this group observed that, in telomerase-immortalized human lung fibroblasts (WTHBF-6 cells), exposures longer than 24 h to particulate forms of Cr(VI), specifically lead or zinc chromate, induced centrosome amplification, which triggered the clastogenic effects of Cr(VI),

namely the formation of aneuploid cells [176, 177]. In these studies, they have also observed tetraploid cells, which suggests that aneuploid cells might have also originated from an unstable tetraploid intermediary. This would be in agreement with the hypothesis of a link existing between tetraploidy, aneuploidy and cancer as it has been proposed by some investigators [178]. Induction of aneuploidy was also observed, by Wise's group, in immortalized human bronchial epithelial cells (BEP2D cells) exposed to lead chromate for 120 h [179], and, by another group, in human fibroblasts (MRC-5 cells) exposed for 30 h to soluble Cr(VI) (potassium dichromate) [180], but, in these cases, no tetraploid cells were observed. Two additional studies, which were investigating the possible genotoxic effects of particulate wear debris from cobalt chrome alloys used in orthopaedic joint replacements, have also reported induction of aneuploidy in primary human fibroblasts upon exposure to Cr(VI) [181, 182]. In contrast with these results, in a previous study from our group, an exposure of BEAS-2B cells to a low concentration of soluble Cr(VI) (potassium dichromate) for over 17 weeks failed to induce significant karyotypic alterations [59]. Interestingly, we observed cells with complex aneuploidies in a malignant cell strain, RenG2, established after selection and expansion of colony-forming cells obtained when BEAS-2B cells previously exposed to 1  $\mu$ M Cr(VI) for six weeks were cultured at clonal density. The karyotype of these cells, which contained many chromosomes in tetrasomy, suggests that they might have derived from a tetraploid intermediate. Of note, the malignant RenG2 strain did not present MSI. Overall, the results obtained seem to be dependent on the model systems and exposure regimens used. Thus, more studies are required to understand under which conditions numerical CIN might emerge in Cr(VI)-exposed cells.

It is important to note that some of the early molecular events that might be involved in the induction of numerical CIN due to uncoupling of cell cycle progression from centrosome duplication have been frequently observed in Cr(VI)-exposed cells. For instance, ATM and ATR activation upon Cr(VI)-exposure, along with activation of some of their physiological targets, has been widely reported [168, 169, 172, 183, 184]. Interestingly, while ATM was reported to be activated by low Cr(VI) concentrations, ATR was activated essentially by high Cr(VI) concentrations [7], although there is also one study where ATR activation was observed following exposure to low Cr(VI) concentrations [168].

In spite of significant progress made in recent years, great research effort is still required for the elucidation of the role that the observed genomic instability has on the

development and progression of Cr(VI)-induced carcinogenesis. For instance, several studies have reported extensive numerical chromosomal aberrations, but they did not identify which chromosomes were affected by those alterations. Without this information, is not possible to know which tumour suppressor genes, oncogenes, or other cancer-related genes have their expression altered. Even less is known concerning Cr(VI)-induced structural chromosomal alterations. It might be important to determine, for instance, if chromosomal translocations are induced by exposure to Cr(VI). These alterations are one of the main consequences of misjoined DNA DSBs and one of the major mechanisms for oncogene activation in human cancers [185], being, therefore, considered as standards for the evaluation and measurement of structural CIN [37]. Also of note is the fact that all of these studies have involved relatively short-term exposures to Cr(VI) and, thus, reveal essentially early mechanistic events of Cr(VI)-induced carcinogenesis.

## 1.4. Objectives

The main objective of the research work presented in this dissertation was to investigate the effects of Cr(VI) on the stress response and on genomic stability. This investigation included the evaluation of:

- the impact of a short-term exposure to Cr(VI) on the proliferation of cells subjected to an acute heat shock, on the modulation of the negative effects of this type of shock on the cellular energy status, and on the expression of key components of the stress response and of cancer-associated pathways also related to the stress response;
- the effects of a long-term exposure to Cr(VI) on genomic stability and cell morphology.

To address the question of biological relevance, the BEAS-2B cell line, a cellular model representative of the human bronchial epithelium, which is the main target of Cr(VI) carcinogenicity *in vivo*, was used throughout this work. The present investigation also had the objective of evaluating the impact of the culturing conditions and culture age on the growth characteristics and genomic stability of this cell line.

## **2. Materials and Methods**

---



## 2.1. General materials

All the materials used in the experimental work described in this dissertation are listed in Table 2.1. The manufacturer, reference and supplier of each material are specified in this table.

**Table 2.1 | List of materials used in the experimental work described in this dissertation.**

Material	Manufacturer	Reference	Supplier
<b>General materials</b>			
BEGM™ BulletKit	Lonza	CC-3170	VWR International, Lda, Carnaxide, Portugal
Bovine serum albumin (BSA, ≥ 96%)	Sigma-Aldrich®	A9647	Sigma-Aldrich® Química S.A., Sintra, Portugal
Bio-Rad Protein Assay Dye Reagent Concentrate	Bio-Rad Laboratories Lda.	500-0006	Bio-Rad Laboratories Lda, Amadora, Portugal
Collagen solution from bovine skin	Sigma-Aldrich®	C4243	Sigma-Aldrich® Química S.A., Sintra, Portugal
Dimethyl sulfoxide (DMSO, ≥ 99.9%)	Fisher Scientific	10213810	Fisher Scientific, Porto Salvo, Portugal
Fetal bovine serum (FBS)	Life Technologies™	10276-106	Alfagene®, Carcavelos, Portugal
Fibronectin from human plasma	Sigma-Aldrich®	F1056	Sigma-Aldrich® Química S.A., Sintra, Portugal
Gelatin from bovine skin	Sigma-Aldrich®	G9391	Sigma-Aldrich® Química S.A., Sintra, Portugal
Gibco® LHC-9 medium	Life Technologies™	12680-013	Alfagene®, Carcavelos, Portugal
Hydrochloric acid (HCl), 37%	Sigma-Aldrich®	320331	Sigma-Aldrich® Química S.A., Sintra, Portugal
Perchloric acid (PCA), 70%	Sigma-Aldrich®	244252	Sigma-Aldrich® Química S.A., Sintra, Portugal
Potassium chloride (KCl, ≥ 99 %)	Sigma-Aldrich®	P5405	Sigma-Aldrich® Química S.A., Sintra, Portugal
Potassium dichromate (K <sub>2</sub> Cr <sub>2</sub> O <sub>7</sub> , ≥ 99.5%)	Sigma-Aldrich®	P2588	Sigma-Aldrich® Química S.A., Sintra, Portugal

**Table 2.1 (cont.) | List of materials used in the experimental work described in this dissertation.**

Potassium hydroxide (KOH, $\geq 85\%$ )	Sigma-Aldrich®	221473	Sigma-Aldrich® Química S.A., Sintra, Portugal
Potassium phosphate monobasic (KH <sub>2</sub> PO <sub>4</sub> , $\geq 99.0\%$ )	Sigma-Aldrich®	P5379	Sigma-Aldrich® Química S.A., Sintra, Portugal
Sodium chloride (NaCl, 99.0-101.5%)	Sigma-Aldrich®	S9625	Sigma-Aldrich® Química S.A., Sintra, Portugal
Sodium hydroxide (NaOH, $\geq 98.0\%$ )	Sigma-Aldrich®	71689	Sigma-Aldrich® Química S.A., Sintra, Portugal
Sodium phosphate dibasic (Na <sub>2</sub> HPO <sub>4</sub> , $\geq 99\%$ )	Sigma-Aldrich®	S0876	Sigma-Aldrich® Química S.A., Sintra, Portugal
Trypan Blue solution, 0.4% (w/v)	Sigma-Aldrich®	T8154	Sigma-Aldrich® Química S.A., Sintra, Portugal
Trypsin solution from porcine pancreas, 2.5% (w/v)	Sigma-Aldrich®	T4549	Sigma-Aldrich® Química S.A., Sintra, Portugal
<b>Material for the quantification of metabolites</b>			
Kit L-Glutamine/Ammonia (Rapid)	Megazyme	K-GLNAM	Megazyme International Ireland, Bray, Ireland
<b>Materials for cytogenetic analysis</b>			
Acetic acid (glacial), 100%	Merck Millipore	1000632511	VWR International, Lda, Carnaxide, Portugal
Giemsa's azur eosin methylene blue solution	Merck Millipore	1092040500	VWR International, Lda, Carnaxide, Portugal
Gürr buffer tablets	Life Technologies™	10582-013	Alfagene®, Carcavelos, Portugal
Hanks' balanced salt solution (HBSS)	Life Technologies™	14170-088	Alfagene®, Carcavelos, Portugal
KaryoMAX® colcemid™ solution in PBS	Life Technologies™	15212-012	Alfagene®, Carcavelos, Portugal
Methanol	Merck Millipore	1060092511	VWR International, Lda, Carnaxide, Portugal
Trypsin (1:250), powder	Life Technologies™	27250-018	Alfagene®, Carcavelos, Portugal
<b>Materials for the quantification of individual protein levels</b>			
HSF1 ELISA Kit	Enzo Life Sciences® Inc.	ADI-900-198	Grupo Taper S.A., Sintra, Portugal
Hsp70 ELISA Kit	Enzo Life Sciences® Inc.	ADI-EKS-700B	Grupo Taper S.A., Sintra, Portugal
Hsp90 $\alpha$ ELISA Kit	Enzo Life Sciences® Inc.	ADI-EKS-895	Grupo Taper S.A., Sintra, Portugal

**Table 2.1 (cont.) | List of materials used in the experimental work described in this dissertation.**

Phosphatase inhibitor cocktail	Sigma-Aldrich®	P0044	Sigma-Aldrich® Química S.A., Sintra, Portugal
Protease inhibitor cocktail	Sigma-Aldrich®	P8340	Sigma-Aldrich® Química S.A., Sintra, Portugal
<b>Materials for the quantification of individual mRNA levels</b>			
Agarose (electrophoretic grade)	NZYTech	MB02702	NZYTech, Lisboa, Portugal
Aurum™ Total RNA Mini Kit	Bio-Rad Laboratories Lda	7326820	Bio-Rad Laboratories Lda, Amadora, Portugal
BlueJuice™ Gel Loading Buffer (10X)	Invitrogen™	10816-015	Alfagene®, Carcavelos, Portugal
Experion™ RNA StdSens Analysis Kit	Bio-Rad Laboratories Lda	7007103	Bio-Rad Laboratories Lda, Amadora, Portugal
GreenSafe Premium	NZYTech	MB13201	NZYTech, Lisboa, Portugal
HotStarTaq Master Mix Kit	Qiagen	203445	IZASA Portugal, Carnaxide, Portugal
iScript™ cDNA Synthesis Kit	Bio-Rad Laboratories Lda	1708890	Bio-Rad Laboratories Lda, Amadora, Portugal
MinElute PCR Purification Kit	Qiagen	28004	IZASA Portugal, Carnaxide, Portugal
Ready-Load™ 100 bp DNA Ladder	Invitrogen™	10380-012	Alfagene®, Carcavelos, Portugal
SsoFast™ EvaGreen® Supermix	Bio-Rad Laboratories Lda	1725201	Bio-Rad Laboratories Lda, Amadora, Portugal
TrackIt™ 100 bp DNA Ladder	Invitrogen™	10438-058	Alfagene®, Carcavelos, Portugal
<b>Cell culture materials</b>			
Disposable plastic material routinely used in cell culture	Orange Scientific	1	Frilabo, Maia, Portugal

<sup>1</sup> Consult the manufacturer website (<http://www.orangesci.com/>) for references of the different cell culture materials.

## 2.2. Biological material

The BEAS-2B cell line (Figure 2.1) was used in all the experiments presented in this dissertation. BEAS-2B cells were purchased from the European Collection of Cell Cultures (ECACC) (Salisbury, UK, Catalogue number: 95102433), as a cryopreserved cellular suspension. According to information obtained from the American Type Culture

Collection (ATCC), the official depositor of this cell line, the original depositor vials of these cells were at passage 31, and the current distribution lots are from passages 36 to 38. In the present work, passage 1 was defined as the thawed cells from the supplier. The cells were periodically assayed for mycoplasma contamination and no indication of such contamination was ever found.

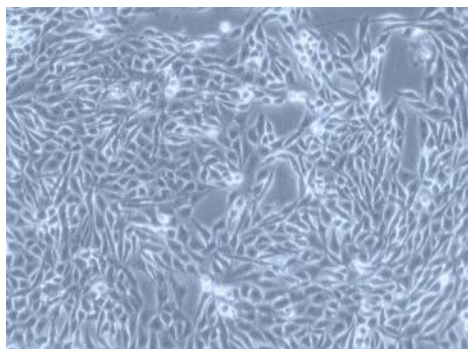


**Figure 2.1 | Representative micrograph (100× magnification) of BEAS-2B cells at passage 11, growing in monolayer.** This continuous cell line was established by immortalization of normal human bronchial epithelial cells with a hybrid of the adenovirus 12 (Ad-12) with the simian virus 40 (SV40).

### 2.3. Equipment

All the equipment used in the experimental work described in this dissertation is listed in Table 2.2. The manufacturer, reference and supplier of each material are specified in this table.

**Table 2.2 | List of equipment used in the experimental work described in this dissertation.**

Equipment	Manufacturer	Model	Supplier
Automated electrophoresis station	Bio-Rad Laboratories Lda	Experion™	Bio-Rad Laboratories Lda, Amadora, Portugal
Balance (analytical)	Acculab	ALC-810.2	Sartorius, S.A., Lisboa, Portugal
Balance (precision)	Acculab	ALC-210.4	Sartorius, S.A., Lisboa, Portugal
Bench autoclave	Prestige Medical	Omega Media	Ezequiel Panão Jorge, Electromédica, Coimbra, Portugal

**Table 2.2 (cont.) | List of equipment used in the experimental work described in this dissertation.**

Bench centrifuge	MPW Medical Instruments®	MPW-350R	MPW Medical Instruments®, Warsaw, Poland
Bench microcentrifuge	Eppendorf	Minispin	VWR International Lda., Carnaxide, Portugal
CO <sub>2</sub> incubator	Sanyo	COM-19AIC(UV)	Sanyo, San Diego, USA
Dry bath	Biogen Científica	AccuBlock Digital Dry Bath	Biogen Científica, Madrid, Spain
Epifluorescence microscope	Nikon	Nikon Eclipse E400	IZASA Portugal, Carnaxide, Portugal
HPLC column	Merck Millipore	5 µm Lichrospher 100 RP-18 column	Merck Millipore, Oeiras, Portugal
HPLC system	Beckman Coulter, Inc.	Beckman System Gold®	Beckman Coulter, Inc., Carnaxide, Portugal
Liquid nitrogen container	Cryo Diffusion S.A.S.	B2048	Cryo Diffusion S.A.S., Lery, France
Microplate reader	BioTek	µQuant	IZASA Portugal, Carnaxide, Portugal
Mr. Frosty™ freezing container	Thermo Scientific	5001-001	VWR International Lda., Carnaxide, Portugal
Optical microscope	Olympus	CKX41	Olympus, Center Valley, USA
pH meter	HANNA Instruments®	HI 110	Normax – Fábrica de vidros científicos, Lda., Marinha Grande, Portugal
Real-time PCR system	Bio-Rad Laboratories Lda	CFX96	Bio-Rad Laboratories Lda, Amadora, Portugal
Transilluminator	UVP Bioimaging Systems	BioSpectrum® Imaging System	VWR International Lda., Carnaxide, Portugal
UV-visible spectrophotometer	Thermo Scientific	Nanodrop 2000	VWR International Lda., Carnaxide, Portugal
Vertical laminar flux cabinet	Kojair	BW-100	Frilabo, Lda., Porto, Portugal
Visible spectrophotometer	Thermo Scientific	Genesys 20	VWR International Lda., Carnaxide, Portugal
Water purification system	Millipore S.A.	Slimplicity™	Interface, Equipamento e Técnica Lda., Amadora, Portugal

## 2.4. Culture of BEAS-2B cells

### 2.4.1. Solutions commonly used in the culture of BEAS-2B cells

All solutions used in the culture of BEAS-2B cells were sterilized prior to use. In this work, the 2% (w/v) bovine serum albumin (BSA) aqueous solution and the 100  $\mu$ M Cr(VI) solution were sterilized by filtration using a 0.2  $\mu$ m pore size filter. All other solutions were autoclaved at 121 °C and 1.39 atm.

Ultrapure water was used in the preparation of all solutions.

- **Phosphate-buffered saline (PBS), working solution**

- 1.37 M NaCl
- 27 mM KCl
- 100 mM Na<sub>2</sub>HPO<sub>4</sub>
- 20 mM KH<sub>2</sub>PO<sub>4</sub>

The solution pH was adjusted to 7.4 using solutions of NaOH or HCl.

Working solutions were prepared from stock solutions 10 times concentrated (PBS 10 $\times$ ), by dilution with water.

- **Trypsin, 0.25% (w/v) solution**

- 10 mL pancreatic porcine trypsin at 2.5% (w/v)
- 90 mL PBS

- **Fibronectin from human plasma, 0.1% (w/v) solution**

- 1 mg fibronectin from bovine skin
- 1 mL ultrapure water

Fibronectin was gently dissolved in water at 37 °C for 30 min.

- **Bovine skin gelatin, 2% (w/v) solution**

- 2 g gelatin from bovine skin

- 100 mL ultrapure water

Gelatin was gently dissolved in water, and the solution obtained was autoclaved.

After autoclaving, the solution was allowed to slowly cool to room temperature.

- **BSA, 2% (w/v) solution**

- 1 g BSA

- 50 mL ultrapure water

- **Fibronectin-containing coating solution (FNT(+) CS)**

- 0.5 mL fibronectin from human plasma at 0.1% (w/v)

- 0.5 mL collagen from bovine skin at 0.3% (w/v)

- 0.025 mL BSA solution at 2% (w/v)

- 48.975 mL culture medium

This coating solution contains 0.01 mg/mL fibronectin from human plasma, 0.03 mg/mL collagen from bovine skin and 0.01 mg/mL BSA.

- **Fibronectin-free coating solution (FNT(-) CS)**

- 25 mL bovine skin gelatin solution at 2% (w/v)

- 2.5 mL BSA solution at 2% (w/v)

- 22.5 mL PBS

This coating solution contains 10 mg/mL bovine skin gelatin and 1 mg/mL BSA in 0.45× PBS.

- **Cr(VI), 100  $\mu$ M solution**

- 0.74 mg  $K_2Cr_2O_7$

- 50 mL ultrapure water

## 2.4.2. Cell culture routine

Unless otherwise specified, BEAS-2B cells were grown as adherent monolayers in filter vented culture flasks pre-coated with FNT(–) CS, a solution containing bovine skin gelatin (a heterogeneous mixture of proteins present in collagen) and BSA in PBS. LHC-9 was used as cell culture medium. This medium is serum-free, an essential characteristic of media used in the culture of BEAS-2B cells, as they might undergo terminal differentiation in the presence of serum [53, 186]. LHC-9 was also the medium used in the establishment of the BEAS-2B cell line (section 1.1.4.1). The flasks were coated with an appropriate volume of FNT(–) CS (ca. 0.03 mL/cm<sup>2</sup>), 2 to 72 h before use. Immediately before seeding the cells, the excess of coating solution was removed, the flask was washed twice with PBS, and fresh, pre-warmed culture medium (about 0.2 mL/cm<sup>2</sup>) was added. Cells were maintained in an incubator at 37 °C and in a humidified atmosphere with 5% (v/v) CO<sub>2</sub>/95% (v/v) air.

For cultures initiated with a seeding density of 2000 cells/cm<sup>2</sup>, cell passage was performed once a week. All procedures of the cell passage were performed in a laminar flow chamber, in aseptic conditions. The procedure used for cultures grown in flasks with 75 cm<sup>2</sup> of growth area, which is schematically represented in Figure 2.2, was as follows. Initially, spent medium was discarded, cells were washed twice with 4 mL of PBS, and 2 mL of 0.25% trypsin were added and spread over the entire growth surface. Trypsin is essential to bring cells into suspension, because it will digest the extracellular and membrane proteins involved in cell adherence to the substrate and in cell to cell interactions [187]. The excess of trypsin was removed and cells were incubated at room temperature until evident dispersion was observed upon examination using an inverted microscope. Detached cells were easily detected, since they became round and smaller (Figure 2.3).

In addition to the extracellular and membrane proteins, trypsin can also digest intracellular proteins [187]. Thus, in order to avoid loss of cellular integrity and intracellular damage, trypsinization must be closely monitored. Frequently, cell culture medium is added to inhibit trypsin. However, LHC-9 is a serum-free medium, and this type of media does not inactivate trypsin [188]. Therefore, it was particularly important to remove the excess of trypsin shortly after its addition. After trypsinization, cells were collected in a centrifuge tube, using 8 mL of PBS. The cellular suspension was centrifuged at 590 g for 7 min at room temperature. The supernatant was discarded and

the pellet resuspended in an appropriate volume of culture medium (generally 8 or 9 mL). A small volume of cell suspension was removed and used for cell counting (section 2.5). Finally, the volume of cellular suspension needed to prepare a new vessel with the desired seeding density was calculated and, after homogenization of the cellular suspension, added to the vessel.

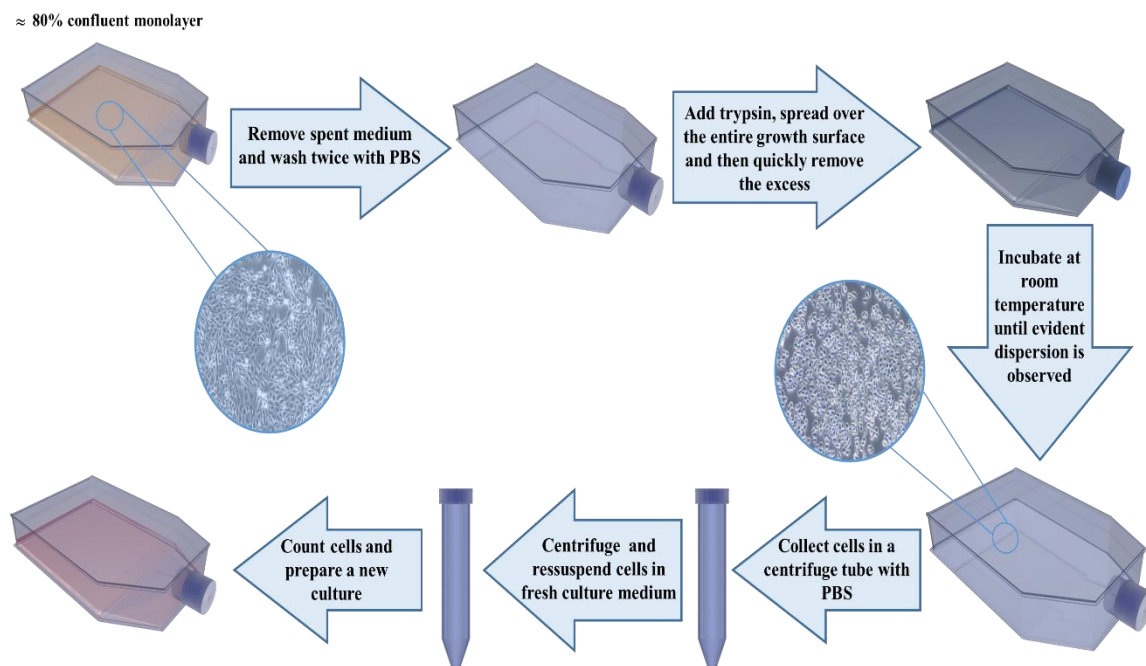


**Figure 2.2 | Schematic representation of the main steps required for cell subculturing.** Cell subculturing was performed in cultures approximately 80% confluent. Spent medium was removed and cells were washed twice with PBS. After trypsinization, cells were collected with PBS and centrifuged. The pellet was resuspended in culture medium and, after cell counting, an appropriate volume of cellular suspension was transferred to a new flask.

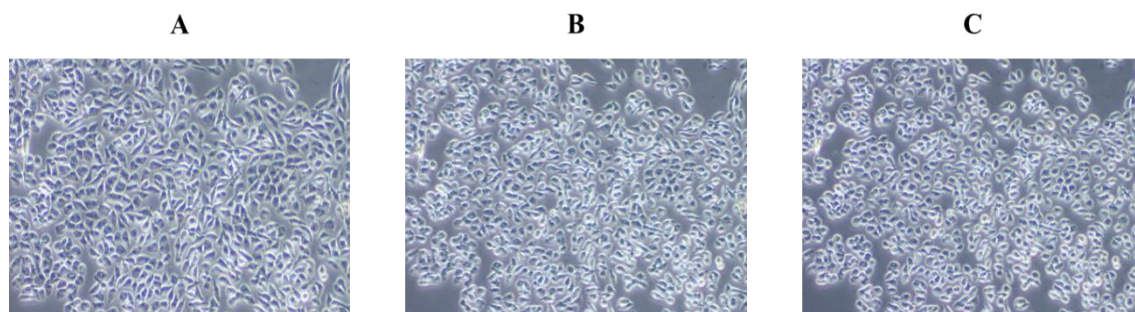


**Figure 2.3 | Effects of trypsin on BEAS-2B cells in culture.** Representative micrographs (100× magnification) of BEAS-2B cells at passage 24: (A) immediately after trypsin addition, (B) 1 min after trypsin addition, and (C) two minutes after trypsin addition. It is evident that cells become round and smaller.

### 2.4.3. Culture initiation

To initiate a culture of BEAS-2B cells, a frozen aliquot was thawed and transferred to a new pre-coated culture flask of 75 cm<sup>2</sup>, containing pre-warmed medium (Figure 2.4). Cells were then incubated for 24 h at 37 °C and 5% (v/v) CO<sub>2</sub>/95% (v/v) air. Afterwards, the culture medium was replaced in order to remove dimethyl sulfoxide (DMSO), a constituent of the freezing medium (section 2.4.4), and dead cells. An alternative for DMSO removal is the centrifugation of the cellular suspension, immediately after thawing. The DMSO remains in the supernatant, which is discarded. However, the centrifugation can be too aggressive to cells that have just been thawed, and are more fragile. Therefore, our group opted for the former procedure. Cells were then incubated again until the culture was ready for subculturing.

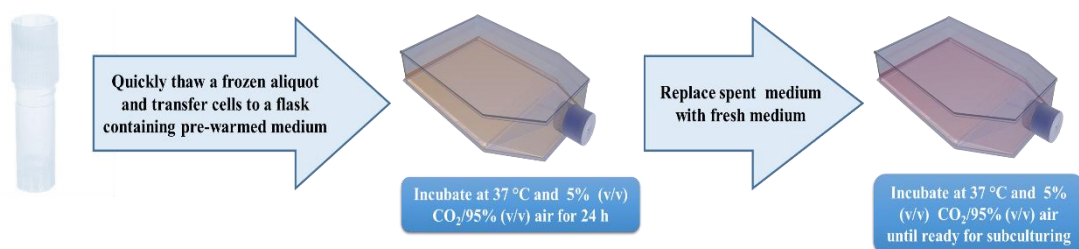


**Figure 2.4 | Essential steps for the initiation of a culture of BEAS-2B cells.** An aliquot of frozen cells was quickly thawed and transferred to a new flask with pre-warmed culture medium. After a 24 h incubation at 37 °C and 5% (v/v) CO<sub>2</sub>/95% (v/v) air, spent medium was replaced with fresh medium to remove DMSO and dead cells. The culture was incubated again at 37 °C and 5% (v/v) CO<sub>2</sub>/95% (v/v) air until ready for subculturing.

### 2.4.4. Cryopreservation of cells

Cryopreservation is a storage strategy that allows the preservation of viable cells for long periods of time, by maintaining them in liquid nitrogen, at a temperature of -196 °C [188, 189]. When needed, frozen cell aliquots can be simply thawed and cultured following the routine procedures.

It is important to maintain a frozen stock of cell lines at low passages to guard against genetic drift, i.e. the stochastic elimination of genes, observed in continuous cell lines upon continuous subculturing, and senescence or transformation in finite cell lines [188, 189]. In addition, the frozen cell aliquots can be used to replace cells that

accidentally died due to contaminations or technical failures, such as the breakdown of the incubator [188, 190].

The freezing process can, however, be lethal to cells if a cryoprotectant is not used. DMSO, a small molecule that easily diffuses into the cells, is the most commonly used cryoprotectant. Once inside the cells, DMSO will allow a gradual temperature reduction and cell dehydration, minimizing the formation of ice crystals, pH alterations and protein denaturation. However, this agent is cytotoxic and, therefore, should always be added in a proportion never exceeding 10% (v/v) [191, 192].

To prepare cells for freezing, cultures in flasks with 175 cm<sup>2</sup> of growth area were prepared. Before high confluence was reached, cells were harvested and centrifuged as described in section 2.4.4 (Figure 2.5). The pellet obtained from the centrifugation was resuspended in a solution containing culture medium, fetal bovine serum (FBS) and DMSO in a proportion of 7:2:1. Generally, aliquots of 1 mL, containing 1 to 4 million cells, were prepared. Aliquots were transferred to a Mr. Frosty™ freezing container, which was stored at -80 °C for 24 h. The freezing container was filled with isopropanol, which allowed cells to be cooled at a slow and constant rate [189]. Finally, aliquots were stored in a liquid nitrogen container, at -196 °C.

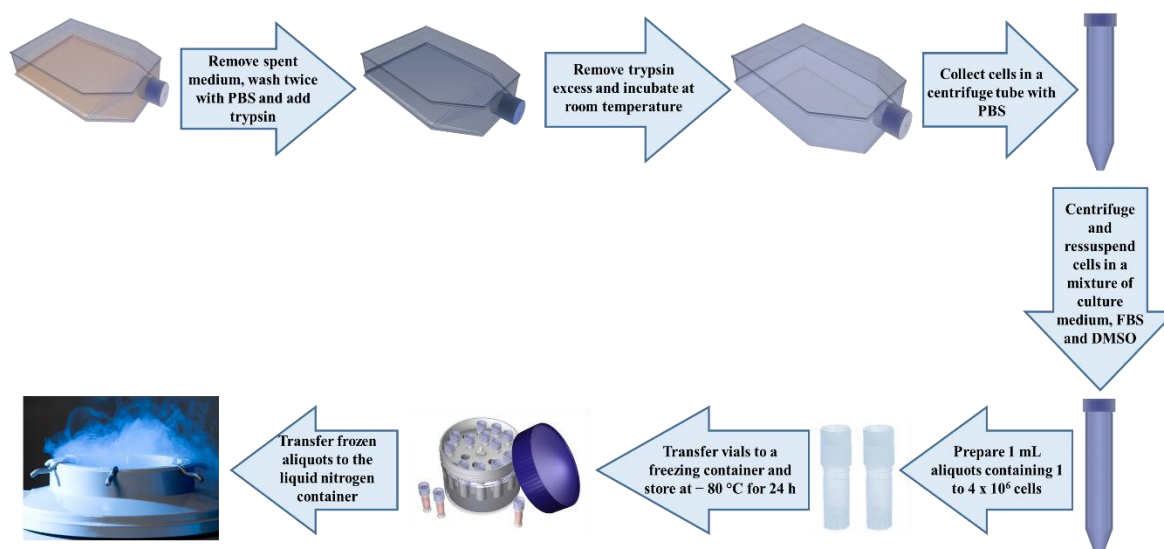


**Figure 2.5 | Schematic representation of the main steps required for cell freezing.** Cells were collected by trypsinization, and then centrifuged. The cell pellet was resuspended in a mixture of culture medium, FBS and DMSO in a proportion of 7:2:1. Aliquots of 1 mL, containing 1 to 4 million cells, were transferred to a freezing container that was stored at -80 °C for 24 h. After this period, the aliquots were transferred to a liquid nitrogen container.

## 2.5. Cell counting by the Trypan Blue exclusion method

Cell counting was done using an inverted microscope, a hemocytometer and the dye Trypan Blue. This method was used in routine cell culture, in the preparation of cultures for experiments, in the determination of doubling times (section 2.8), in cytotoxicity evaluations (section 2.11) and in heat shock assays (section 2.12).

Trypan Blue is a dye frequently used in cell counting because it offers the advantage of allowing the distinction between live and dead cells [193]. This dye easily permeates cells with damaged membranes, staining the cytoplasm of those cells blue. These cells are easily distinguished from live cells, whose membranes impede the penetration of the dye, appearing bright under microscope inspection [191, 193].

For cell counting, a small volume of the cellular suspension and of a 0.4% (w/v) solution of Trypan Blue were mixed in appropriate proportions (normally 100  $\mu\text{L}$  of cellular suspension and 20  $\mu\text{L}$  of Trypan Blue). Each hemocytometer chamber was filled with this mixture and the four corner squares of each chamber were counted following the rules depicted in Figure 2.6.

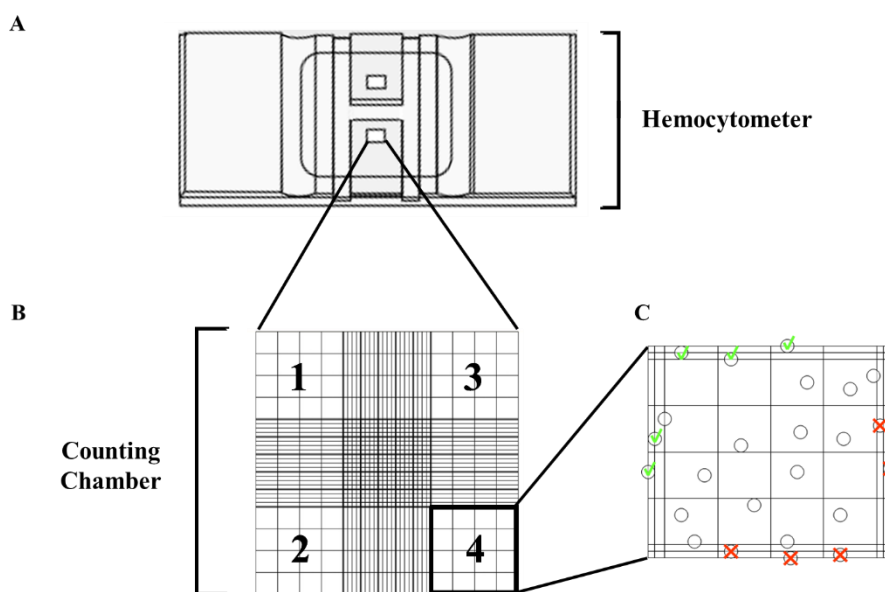


**Figure 2.6 | Schematic representation of a (A) hemocytometer and (B) one of its counting chambers.** For cell counting, a coverslip was placed over the hemocytometer, and a mixture of cellular suspension and Trypan Blue was added to both counting chambers. In each counting chamber, the cells in the four corner squares (1 to 4) were counted according to the rule depicted in panel (C), i.e. cells inside the grid and overlapping with the top and left edges (circles with green checkmark) were included in the counting, while cells overlapping with the bottom and right edges (circles with red cross) were excluded.

For both routine cell culture and preparation of experiments, at least two counts of each suspension were performed, in order to verify the homogeneity of the cellular suspension. Whenever those counts differed by more than 10%, a third count was done.

Each corner square in the counting chamber has a volume of  $1 \times 10^{-4}$  mL. Knowing this volume and the mean number of cells in the eight squares scored, and taking into account the dilution factor, it was possible to calculate the number of cells per milliliter of the cellular suspension, using equation 2.1.

$$\text{Cells/mL} = x \times \frac{\text{dilution factor}}{1 \times 10^{-4} \text{ mL}} \quad (2.1)$$

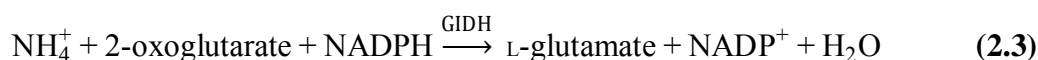
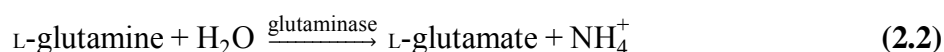
$x$  – mean number of cells counted in the eight corner squares of the two counting chambers.

## 2.6. Morphological studies

Cell morphology and the pattern of growth of BEAS-2B cultures were evaluated by phase-contrast microscopy. Cultures were observed with an Olympus CKX41 microscope equipped with an Olympus OD-20 camera, which was used for capturing micrographs.

## 2.7. Quantification of L-glutamine and ammonia in the culture medium

In the present work, L-glutamine and ammonia levels in the culture medium were determined using the kit L-Glutamine/Ammonia (Rapid). This kit is based on the two enzymatic reactions presented below (equations 2.2 and 2.3). The first promotes the deamination of L-glutamine to L-glutamate and ammonium, through the action of glutaminase (equation 2.2), and the second the formation of L-glutamate from the reaction of the ammonium ions with 2-oxoglutarate, in the presence of NADPH and glutamate dehydrogenase (GIDH) (equation 2.3).



As can be appreciated, the amount of NADPH consumed is equivalent to the total amount of L-glutamine and ammonia present in the sample. NADPH consumption is measured by the decrease in absorbance at 340 nm.

Samples of medium collected for analysis were heated for 15 min at 80 °C, to inactivate enzymes that might retain their activity outside the cellular environment. Samples were then stored at -20 °C until analysis.

For quantification of L-glutamine and ammonia, the procedure recommended by the supplier and described in Table 2.3 was followed.

**Table 2.3 | Procedure followed for quantification of L-glutamine and ammonia, using the kit L-Glutamine/Ammonia (Rapid).**

	Ammonia		L-glutamine	
	Blank	Sample	Blank	Sample
Sodium acetate buffer (μL)	0	0	100	100
Sample (μL)	0	50	0	50
Glutaminase solution (μL)	0	0	10	10
<b>Mixture and incubate for 5 min at room temperature</b>				
Ultrapure water (μL)	910	860	800	750
Triethanolamine buffer (μL)	150	150	150	150
NADPH solution (μL)	100	100	100	100
<b>Mixture and read absorbance (A<sub>1</sub>) at 340 nm after 4 min of incubation at room temperature</b>				
GIDH solution (μL)	10	10	10	10
<b>Mixture and read absorbance (A<sub>2</sub>) at 340 nm after 5 min of incubation at room temperature</b>				

In order to determine the concentrations of ammonia and glutamine in the samples, it was initially necessary to calculate the change in absorbance ( $\Delta A$ ) resulting from each analyte, according to the equations 2.4 to 2.6.

$$\Delta A_{\text{ammonia}} = (A_1 - A_2)_{\text{ammonia}} - (A_1 - A_2)_{\text{blank}} \quad (2.4)$$

$$\Delta A_{(\text{L-glutamine+ammonia})} = (A_1 - A_2)_{\text{L-glutamine}} - (A_1 - A_2)_{\text{blank}} \quad (2.5)$$

$$\Delta A_{\text{L-glutamine}} = \Delta A_{(\text{L-glutamine+ammonia})} - \Delta A_{\text{ammonia}} \quad (2.6)$$

These  $\Delta A$  values were then used to calculate the concentrations of the analytes, according to equation 2.7, using the molar extinction coefficient of NADPH at 340 nm ( $6300 \text{ M}^{-1} \text{ cm}^{-1}$ ).

$$c = \frac{V}{\epsilon \times d \times v} \times \Delta A \quad (2.7)$$

$c$ , concentration of the analyte;  $V$ , final volume (mL);  $\epsilon$ , molar extinction coefficient of NADPH at 340 nm ( $6300 \text{ M}^{-1} \text{ cm}^{-1}$ );  $v$ , sample volume (mL);  $\Delta A$ , change in absorbance at 340 nm.

## 2.8. Determination of doubling times

Doubling times were calculated based on total cell numbers in BEAS-2B cell cultures monitored for three days, during the exponential phase of growth. For each of the time points, triplicate cultures of each condition tested were prepared, at a seeding density of  $2000 \text{ cells/cm}^2$ , in 6-well plates. Total cell numbers were determined by the Trypan Blue exclusion method (section 2.5). Cells for this experiment were grown either in BEGM or LHC-9, and in vessels pre-coated with FNT(+) CS or FNT(-) CS.

At each time point, the medium of the corresponding cultures was removed and the cell monolayer was washed once with PBS. All residual PBS was removed using a micropipette. Afterwards,  $300 \mu\text{L}$  of trypsin were added to each well. Once the cells were trypsinized, an adequate volume of PBS was added (generally between  $200$  and  $500 \mu\text{L}$ ). Cells were resuspended, and the suspensions transferred to microcentrifuge tubes, which were kept on ice until the counting.

Plots of the natural logarithm of total cell numbers against time after seeding were constructed from the data obtained. The doubling time was calculated by dividing the natural logarithm of 2 by the slope of the line obtained in that plot.

## 2.9. Cytogenetic analysis

### *Preparation, spreading and banding of metaphase spreads<sup>2</sup>*

For the preparation of metaphase spreads, cells were cultured in 25 cm<sup>2</sup> culture flasks, at a seeding density of 4000 cells/cm<sup>2</sup>, and allowed to reach approximately 75% confluence. Cultures were then exposed to 100 µL of a 10 µg/mL colcemid solution for 3 h, to induce cell cycle arrest in pro-metaphase. After this incubation period, culture medium was collected in a centrifuge tube, to which a small amount of FBS was also added. The cell monolayer was then washed with 1 mL of Hank's balanced salt solution (HBSS), which was also transferred to the tube containing the spent medium and FBS. Cells were harvested by trypsinization, resuspended in the mixture containing culture medium/FBS/HBSS and collected in a centrifuge tube. The cellular suspension was centrifuged for 10 min at 280 g. The supernatant was discarded and the pellet resuspended in 1 mL of FBS. Subsequently, cell swelling was promoted by addition of 10 mL of a hypotonic solution of 5 mM potassium chloride (KCl) to the cell suspension, followed by a 20 min incubation at 37 °C, with the tube placed at 30° to promote cell spreading.

After the swelling, several steps of cell fixation were performed. The first step encompassed a pre-fixation with 40 µL of a 1:6 acetic acid/methanol fixation solution added to the hypotonic solution. After that, the suspension was homogenized by inversion and then centrifuged for 10 min at 280 g. Most of the supernatant was discarded and approximately 1 mL was used to resuspend the pellet. Cells were then sequentially fixed in 4 mL of 1:6, 1:3 and 1:1 acetic acid/methanol fixation solutions. Between each addition of the fixation solutions, cells were centrifuged for 10 min at 280 g. After addition of the 1:1 fixation solution, the cell suspension was incubated overnight at 4 °C, and only afterwards centrifuged. Most of the supernatant was discarded, and the pellet resuspended in the 200 to 300 µL remaining.

Cells were then spread in microscope slides, freshly immersed in distilled water, by pipetting one drop of the suspension (approximately 7 to 8 µL) to each end of the slide. This process was done in carefully controlled conditions of temperature and humidity (generally 22 °C and 42% humidity). Afterwards, the chromosomes were dehydrated by incubation of the slides at 80 °C for 3 h.

---

<sup>2</sup> With the exception of the preparation of cell cultures, all experimental procedures described in this subsection were performed by specialized technicians of the Laboratory of Cytogenetics and Genomics of the Faculty of Medicine of the University of Coimbra.

To facilitate the subsequent organization of the karyotypes and the identification of chromosomal alterations, the chromosomes were G-banded with trypsin and Giemsa (GTG-banding). This banding protocol is based on the selective action of trypsin on the different types of chromatin. Trypsin partially digests the euchromatin, which is in a more decondensed state, while it leaves the heterochromatin intact. Upon labelling with Giemsa the heterochromatic regions incorporate more dye than the euchromatic regions, appearing as darker bands under microscope observation. To obtain the GTG-banding, slides were sequentially immersed in a trypsin solution, a FBS solution (for trypsin inhibition), Gurr buffer, a Giemsa solution and once more in Gurr buffer. The period of time during which the slides were immersed in the trypsin and Giemsa solutions was optimized every time that the protocol was performed.

#### *Karyotype construction*

After banding, slides were observed under an optic microscope. For further karyotypic analysis, images of well spread metaphases were captured, with the aid of a camera incorporated in a Nikon Eclipse E400 microscope, and the Applied Imaging® CytoVision® software (Genetix, New Milton, United Kingdom). The same software was used to analyse the images obtained and construct the cells' karyotypes. For each condition analysed, at least 10 karyotypes were constructed.

## **2.10. Cellular treatment with Cr(VI)**

All treatments of the cell cultures with Cr(VI) were performed using a 100  $\mu$ M aqueous solution of Cr(VI). Cr(VI) additions were done only 24 h after the establishment of the culture, to allow the recovery of cells from the stress caused by the subculturing procedure and to allow enough time for their attachment to the substrate.

All conditions tested in each experiment, including the controls, which were prepared and established in parallel, received the same amount of addition vehicle (ultrapure water).

## 2.11. Cytotoxicity assays

The cytotoxic effects of a 48 h exposure to 1 and 2  $\mu\text{M}$  Cr(VI) were assessed in tetraplicate cultures established in 6-well plates and seeded at 4000 cells/cm<sup>2</sup> (Figure 2.7). Preparation of suspensions for determination of total cell numbers by the Trypan Blue exclusion method (section 2.5) was performed as described in section 2.8.

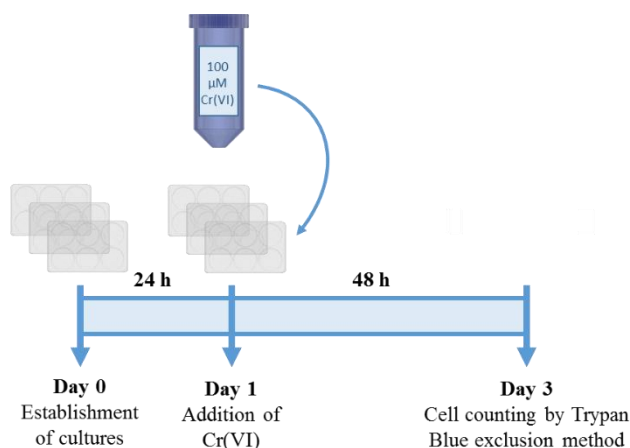


**Figure 2.7 | Protocol used in the evaluation of the cytotoxicity induced by Cr(VI) in BEAS-2B cell cultures.** Cr(VI) addition to cultures was performed as described in section 2.10.

## 2.12. Heat shock assays

The effect of an acute heat shock on the proliferation of BEAS-2B cells, grown in the absence or in the presence of 1  $\mu\text{M}$  Cr(VI), was assessed in tetraplicate cultures established in 6-well plates, at a seeding density of 4000 cells/cm<sup>2</sup> (Figure 2.8). Acute heat shock was induced by replacing spent medium with fresh pre-heated medium (43 °C) and putting the 6-well plates in a water bath (43 °C) for a short period of time (15 to 60 min). When the effect of the presence of Cr(VI) was being evaluated, Cr(VI) was added both 24 h after cell seeding and when the medium was replaced for induction of the heat shock. The relative growth of the cultures after the heat shock was determined based on the total number of cells immediately before and 24 h after the heat shock. Cell counting was done by the Trypan Blue exclusion method (section 2.5), in cell suspensions prepared as described in section 2.8.

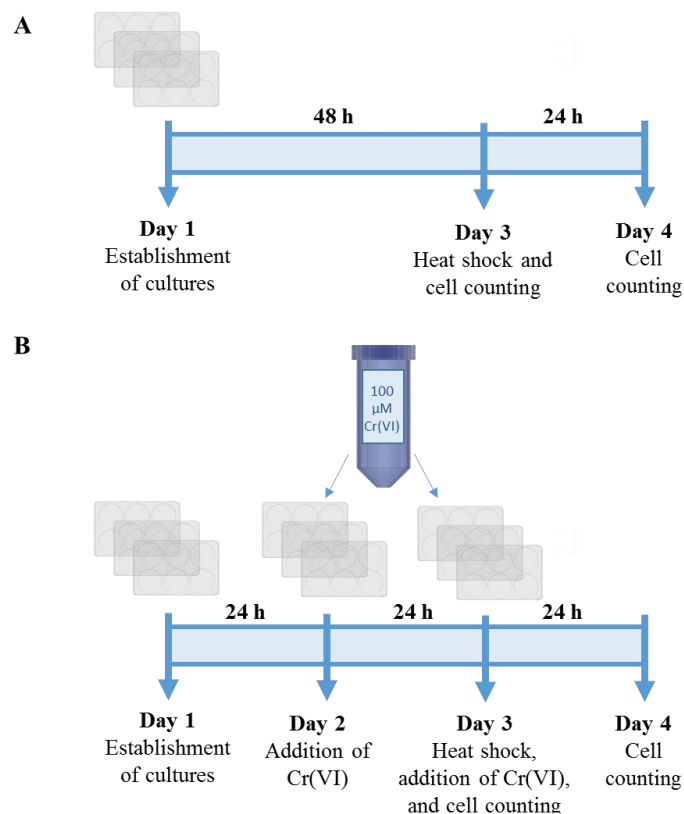


**Figure 2.8 | Schematic representation of the protocol used in the determination of the impact of an acute heat shock on the proliferation of BEAS-2B cell cultures grown in the (A) absence or in the (B) presence of Cr(VI). Cr(VI) addition to cultures was performed as described in section 2.10.**

### 2.13. Quantification of intracellular adenine nucleotide levels

For determination of the effects of an acute heat shock on the intracellular adenine nucleotide levels, the establishment of the cultures, the treatment with Cr(VI), and the induction of heat shock were performed as described in section 2.12 and schematically represented in Figure 2.9.

Intracellular adenine nucleotide levels were quantified by reverse-phase high performance liquid chromatography (RP-HPLC). RP-HPLC is the HPLC variant more commonly used for quantification of adenine nucleotides [194]. This technique has several advantages over other commonly used techniques, such as its high efficiency, reproducibility, and capacity to distinguish chemically similar compounds. In this variant, which involves the use of a hydrophobic stationary phase and a hydrophilic mobile phase [194, 195], molecules are eluted in order of increasing hydrophobicity. Thus, in the case of adenine nucleotides, those with more phosphate groups, which are more hydrophilic

than those that have fewer phosphate groups, establish a weaker interaction with the stationary phase and are eluted first.

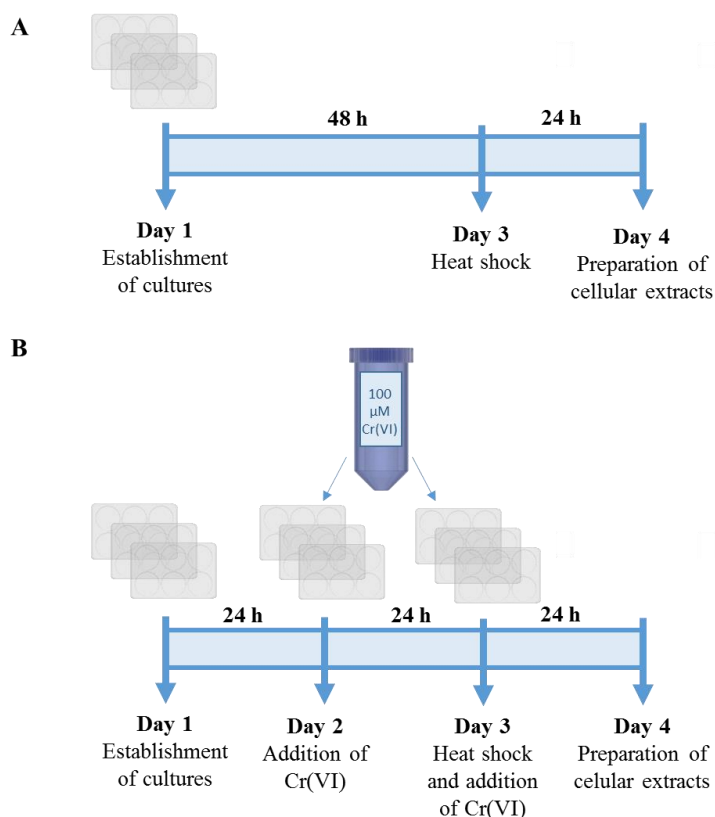


**Figure 2.9 | Schematic representation of the protocol used in the determination of the impact of an acute heat shock on the intracellular adenine nucleotide levels of BEAS-2B cells grown in the (A) absence or in the (B) presence of Cr(VI).** Cr(VI) addition to cultures was performed as described in section 2.10.

For the preparation of cellular extracts, the culture medium was removed from the wells, cultures were washed twice with PBS and 300  $\mu\text{L}$  of 0.3 M perchloric acid (PCA) were added to each well. Cells were scraped into the acid and the resulting extracts were centrifuged at 12100  $g$  for 5 min, to sediment the proteins in the sample. The sedimentation of the proteins not only facilitates their separation from the fraction containing the adenine nucleotides, but also ensures that enzymatic degradation of the adenine nucleotides does not occur. Each pellet, which corresponds to the protein fraction, was dissolved in 200  $\mu\text{L}$  of a 0.03 M sodium hydroxide (NaOH) solution. The resulting solution was later assayed for total protein levels (section 2.14). Supernatants were transferred to new centrifuge tubes and the extracts were neutralized by addition of 35  $\mu\text{L}$  of a 3 M potassium hydroxide (KOH) solution. In the presence of  $\text{K}^+$ ,  $\text{ClO}_4^-$  precipitates

as potassium perchlorate ( $\text{KClO}_4$ ). The sedimentation of the salt was promoted by incubating the centrifuge tubes on ice for 15 min, and then centrifuging them at 12100  $g$  for 5 min. The supernatants, which contained the adenine nucleotides, were transferred to new centrifuge tubes and stored at  $-80\text{ }^\circ\text{C}$  until their analysis by RP-HPLC. For the quantification, 20  $\mu\text{L}$  of sample were injected in the HPLC system (Figure 2.10). The calculated concentrations of the adenine nucleotides were also used to determine the energy charge according to the Atkinson's equation (section 1.1.3).

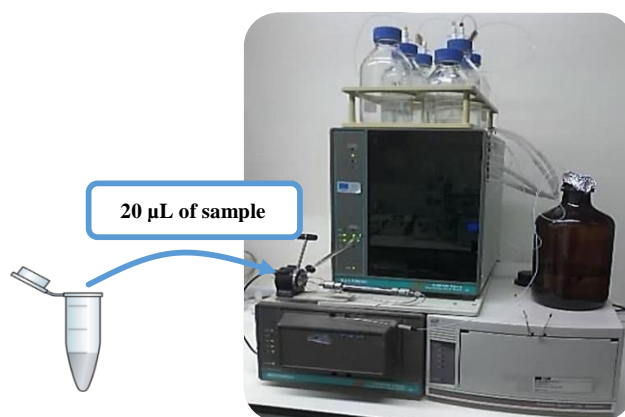


**Figure 2.10 | HPLC system Beckman System Gold<sup>®</sup>, with the column Lichrospher 100 RP-18 of 5  $\mu\text{m}$ , used in the quantification of intracellular adenine nucleotides.** For each run, 20  $\mu\text{L}$  of sample were injected in the system.

## 2.14. Total protein quantification

For normalization of the results obtained in the quantification of adenine nucleotides (section 2.13) and individual protein levels (section 2.15), total protein levels were determined using the Bradford method. Specifically, the Bio-Rad Protein Assay Dye Reagent Concentrate was used.

The Bradford or Coomassie Blue dye binding method is based on the interaction of the dye Coomassie Brilliant Blue G-250 with protein side chains containing basic and aromatic amino acids [196], which causes a shift in the maximal wavelength of absorption of the dye from 465 to 595 nm [197]. In the Dye Reagent concentrate, the dye is in a double protonated form that has a reddish-brown color. Upon interaction with proteins, the unprotonated form of the dye becomes more stable and the it acquires a blue color [198]. This method was chosen for its simplicity, rapidity, sensitivity and affordability.

BSA was used as standard, as it is one of the most commonly used calibration proteins, for its ready availability and low cost [199]. To obtain the standard curve (absorbance at 595 nm vs protein concentration), solutions of BSA, with concentrations ranging from 0 to 10 µg/mL, were prepared from a 1 mg/mL BSA stock solution. For protein quantification the procedure indicated in Table 2.4 was followed. The protein concentration in each extract was calculated using the standard curve (prepared for each experiment), after reading the absorbance at 595 nm, against the reagent blank, in a visible spectrophotometer.

**Table 2.4 | Procedure for the quantification of total protein levels, using the Bio-Rad Protein Assay Dye Reagent Concentrate.**

	Blank	Standards/Samples
Standard/Sample (µL) <sup>1</sup>	0	x
Ultrapure water (µL)	800	800-x
Reagent (µL)	200	
<b>Mixture by gentle inversion of the cuvette, and read the absorbance at 595 nm, after a 5 min incubation at room temperature.</b>		

<sup>1</sup> x, volume of standard or sample added to the cuvette.

## 2.15. Quantification of individual protein levels

Intracellular levels of Hsp90α, Hsp72 and HSF1 were determined using commercially available Enzyme-linked immunosorbent assay (ELISA) kits (Table 2.1). The use of these kits ensures a sensitive (limits of detection: Hsp90α – 50 pg/mL; Hsp72 – 200 pg/mL; HSF1 – 35 pg/mL), rapid and reliable quantification of the proteins of interest. The accurate quantification is possible due to the standard curve prepared for each assay from serial dilutions of a protein standard provided with the kit.

Cell lysates used in the assay were prepared from BEAS-2B cultures exposed to Cr(VI) for 48 h and control cultures established and maintained in parallel (Figure 2.11). Cells were seeded at 4000 cells/cm<sup>2</sup> in 25 cm<sup>2</sup> flasks for quantification of Hsp90α (one flask per lysate) and at 6000 cells/cm<sup>2</sup> in 175 cm<sup>2</sup> flasks for quantification of Hsp72 and HSF1 (two and four flasks per lysate, respectively).

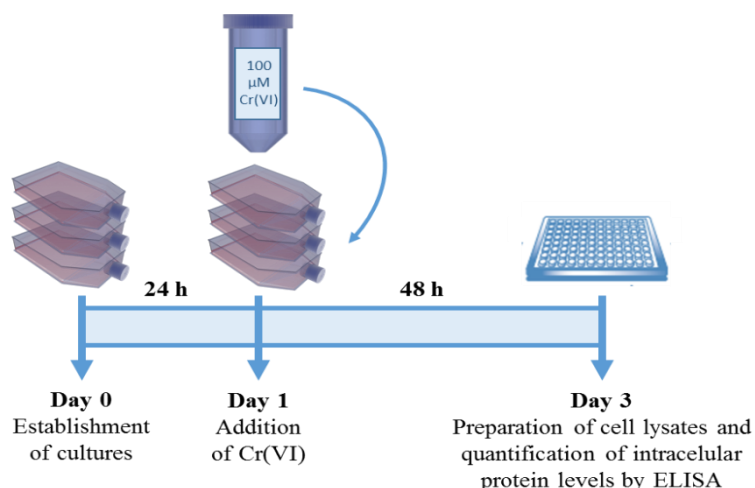


**Figure 2.11 | Protocol employed in the determination of the effects of Cr(VI) on the intracellular levels of Hsp90 $\alpha$ , Hsp72 and HSF1.** Cr(VI) addition to cultures was performed as described in section 2.10.

Preparation of the cell lysates was done according to the manufacturer's instructions, which had slight variations for each kit. The first steps of cell harvesting were equal for all experiments, and were performed as described in section 2.4.2.

For the quantification of Hsp90 $\alpha$  and Hsp72, after being collected in a centrifuge tube with PBS, cells were centrifuged at 590  $g$  for 7 min at 21  $^{\circ}C$ , while for HSF1 they were centrifuged at 250  $g$  for 7 min at 4  $^{\circ}C$ , and then washed once more with PBS and centrifuged again in the same conditions.

The pellets obtained were resuspended in an appropriate volume of extraction reagent, supplemented with a protease inhibitor cocktail in order to avoid degradation of the proteins. In the assays for HSF1 quantification, a phosphatase inhibitor cocktail was also added.

Cell suspensions were incubated on ice for 30 min with occasional mixing. Cell lysates were the supernatants of the subsequent centrifugation. For Hsp90 $\alpha$  and Hsp72 quantification assays, cell suspensions were centrifuged at 21000  $g$  for 10 min at 4  $^{\circ}C$ , and for HSF1, centrifugation was done at 16000  $g$  for 20 min at 4  $^{\circ}C$ .

A portion of the cell lysate was used in the assay, and another portion was stored at  $-20^{\circ}C$  to be used in the quantification of total protein levels (section 2.14) for

normalization. The remaining lysate was stored at  $-80\text{ }^{\circ}\text{C}$  to be used in posterior assays, if necessary.

All three kits used are quantitative sandwich ELISAs and use antibodies that are specific for the protein being quantified, not exhibiting cross-reactivity with related proteins, such as those belonging to the family of the protein of interest.

The assay plates provided in the kits were pre-coated with a specific monoclonal capture antibody that binds to the protein of interest present in the samples or in the standards. All the kits then use another antibody to detect the bound protein, but the strategy used in each kit is different. In the Hsp90 $\alpha$  kit, a monoclonal antibody conjugated to the enzyme horseradish peroxidase (HRP) is used. The Hsp72 kit uses a rabbit polyclonal antibody, which afterwards will be the target of an HRP conjugated anti-rabbit antibody. In the HSF1 kit, a polyclonal biotinylated antibody is used and, after the binding of the antibody to the protein, a solution of streptavidin (a protein with high specificity and affinity for biotin) conjugated to HRP is added. 3,3',5,5'-Tetramethylbenzidine (TMB) was the substrate of HRP used in the assays, being converted in a blue product through oxidation. TMB is one of the substrates more quickly oxidized by HRP, leading to rapid color development [200]. The development of the blue color is proportional to the amount of captured protein. An acidic solution is used to stop the color development, and convert the blue color to yellow. The intensity of the yellow color was read at 450 nm using a microplate reader.

Essentially, the protocol suggested by the supplier for each kit was followed. The detailed protocol of each type of assay is schematically represented in Figure 2.12.

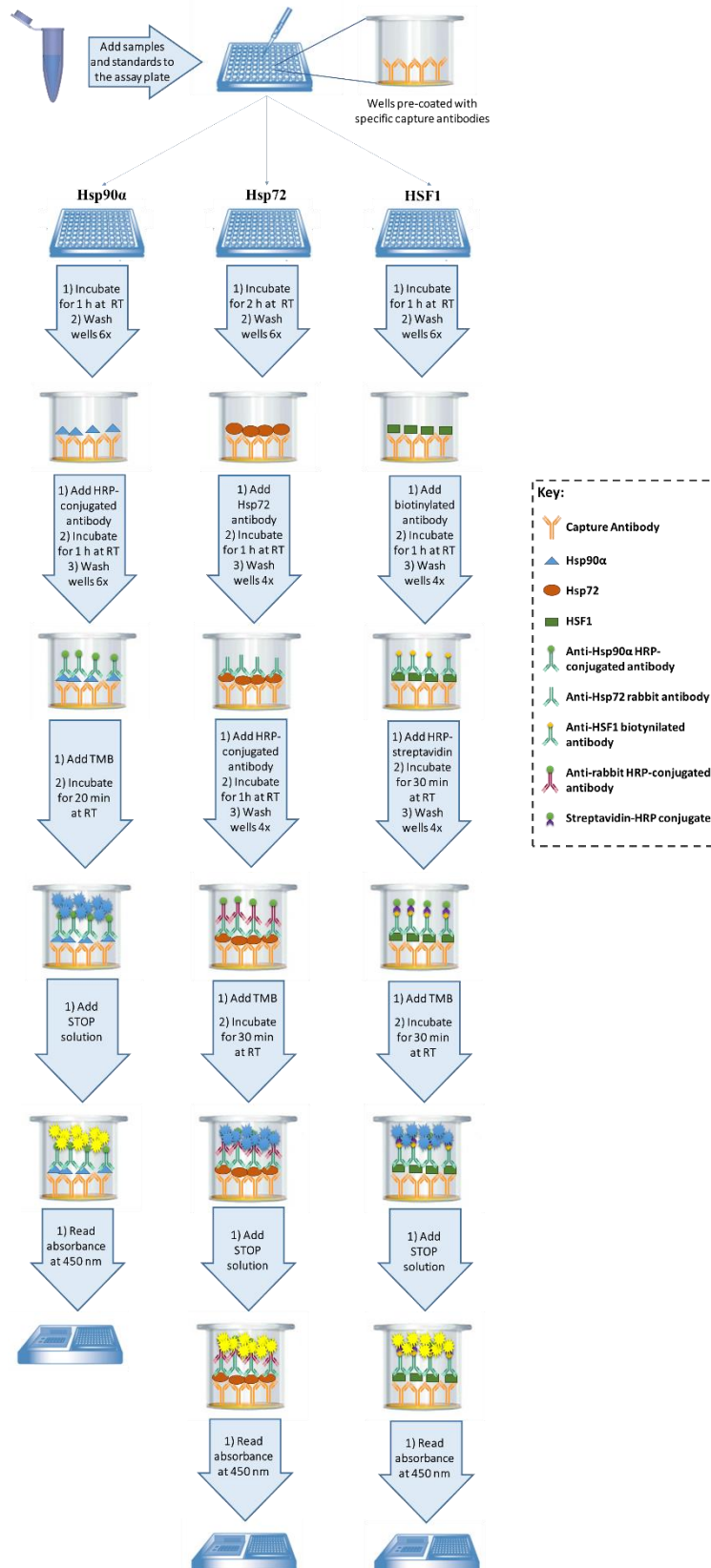


**Figure 2.12 | Schematic representation of the protocols followed for the quantification of Hsp90α, Hsp72 and HSF1 in cell lysates, using commercially available ELISA kits.** HRP, horseradish peroxidase; RT, room temperature; TMB, 3,3',5,5'-Tetramethylbenzidine.

## 2.16. Quantification of individual mRNA levels

In this work, quantitative reverse-transcription polymerase chain reaction (RT-qPCR) was used for the determination of individual mRNA levels. Several commercially available kits<sup>3</sup> were used for the preparation of samples and the RT-qPCR reactions (Table 2.1).

### *Total RNA extraction*

Cell pellets used for RNA extraction were prepared from BEAS-2B cultures exposed to Cr(VI) for 48 h and control cultures established and maintained in parallel (Figure 2.13). BEAS-2B cells were seeded at 8000 cells/cm<sup>2</sup> in flasks of 75 cm<sup>2</sup>. At the end of the treatment, cells were harvested and centrifuged as described in section 2.4.2. All the supernatant was removed, and cell pellets were stored at -80 °C until further processing.

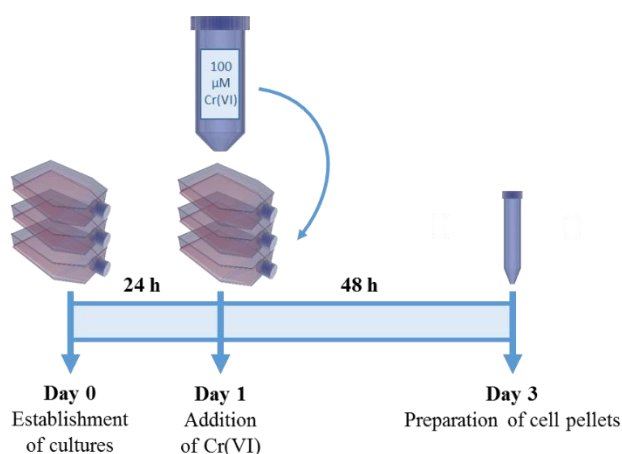


**Figure 2.13 | Protocol employed in the determination of the effects of Cr(VI) on the levels of selected mRNAs.** Cr(VI) addition to cultures was performed as described in section 2.10.

Total RNA was extracted using the Aurum™ Total RNA Mini Kit, following the manufacturer's protocol. Briefly, cell pellets were initially resuspended in 350 µL of lysis solution followed by addition of 350 µL of 70% ethanol. The resulting suspension was then transferred to a RNA binding column inserted inside a 2 mL capless tube and centrifuged at 10000 g for 30 s and at 25 °C. The flow-through was discarded and 700 µL

<sup>3</sup> The composition of the solutions and buffers supplied in these kits is not specified by the manufacturers.

of a low stringency solution were added to the column. After another centrifugation at 10000 *g* for 30 s, the flow-through was again discarded and 80  $\mu\text{L}$  of DNaseI solution were added directly to the membrane stack at the base of the column. The DNaseI was used to remove genomic DNA contamination from the sample. After a 15 min incubation, 700  $\mu\text{L}$  of a high stringency solution were added, and the column was centrifuged at 10000 *g* for 30 s. The flow-through was discarded and, after adding 700  $\mu\text{L}$  of low stringency solution, the column was centrifuged at 10000 *g* for 1 min. The flow-through was discarded, and the column was centrifuged at 10000 *g* for 2 min to remove residual low stringency solution. The column was transferred to a 1.5 mL microcentrifuge tube and 40  $\mu\text{L}$  of elution solution were added directly to the membrane stack at the base of the column. After a 1 min incubation, the column was centrifuged at 10000 *g* for 2 min.

The total RNA eluted was quantified using a Nanodrop spectrophotometer, with the elution solution as the blank. When not used immediately in downstream applications, total RNA was stored at  $-80\text{ }^{\circ}\text{C}$ .

#### *Evaluation of total RNA integrity*

The quality of the RNA has been shown to be one of the critical parameters determining the success of RT-qPCR experiments [201]. Thus, before using the extracted total RNA in downstream applications, its integrity was evaluated by an automated capillary-electrophoresis system using the Experion™ RNA StdSens Analysis Kit. In this type of system, RNA samples are electrophoretically separated on a micro-fabricated chip and subsequently detected via laser induced fluorescence detection [202]. This method is technically easy, fast and requires only a very small amount of sample, in comparison with other methods available for evaluation of RNA quality. An RNA ladder, optimized for automated electrophoresis, is used as a standard and allows the estimation of the RNA band sizes. The assessment of RNA integrity is based on the electrophoretic profile of the sample, particularly of the 18S and 28S ribosomal RNA (rRNA) bands. It is generally accepted that, in high quality samples of total RNA, the 28S rRNA peak area is approximately twice that of the 18S rRNA [201]. Based on the 28S/18S ratio, the software calculates the RNA quality indicator (RQI) which ranges from 1 (degraded RNA) to 10 (intact RNA).

Samples and the chip were prepared according to the manufacturer's instructions. Chip preparation requires its priming with the gel-staining solution. This solution was prepared by mixing 65  $\mu\text{L}$  of RNA gel, previously passed through a spin filter and

centrifuged at 1500 g for 10 min, with 1  $\mu\text{L}$  of RNA stain. For priming, 9  $\mu\text{L}$  of the gel staining solution were pipetted into the gel priming well on the chip. The chip was transferred to the priming station, where the pressure and time were set according to the alphanumeric code displayed in the chip. From the pool of samples, 12 samples, representative of each condition tested in the different independent experiments, were chosen to be analysed. Samples and the RNA ladder were denaturated for 2 min at 70  $^{\circ}\text{C}$  (1.5  $\mu\text{L}$  of total RNA and of RNA ladder were used). After denaturation, 1.5  $\mu\text{L}$  of sample were mixed with 7.5  $\mu\text{L}$  of Experion RNA loading buffer, which contains a 50 bp marker that is used for the proper alignment of samples to the RNA ladder. The chip was loaded by adding 9  $\mu\text{L}$  of gel, 9  $\mu\text{L}$  of gel staining solution, 1  $\mu\text{L}$  of RNA ladder and 6  $\mu\text{L}$  of each sample/loading buffer mixture to the respective wells, according to the labeling on the chip. The loaded chip was placed in the Experion vortex station for mixing of the components and then transferred to the Experion electrophoresis station where the run was initiated. All the RNA samples used presented RQI values within the high quality range (Appendix A.1).

#### *cDNA synthesis*

Total mRNA present in the samples was converted to cDNA by a conventional reverse transcription-PCR (RT-PCR), using the iScript™ cDNA Synthesis Kit. The reverse transcriptase provided in the kit is a modified Moloney Murine Leukemia Virus (MMLV) reverse transcriptase with a functional RNase H (RNase H<sup>+</sup>) domain, preblended with an RNase inhibitor. The use of this RNase guarantees greater sensitivity than that of RNase H<sup>-</sup> enzymes. The reaction mix contained both oligo(dT) and random hexamer primers, to ensure the conversion of a wide variety of targets.

Following the manufacturer's protocol, reactions were setup by mixing 8  $\mu\text{L}$  of 5 $\times$  iScript reaction mix, 2  $\mu\text{L}$  of iScript reverse transcriptase, a volume of RNA template containing 2  $\mu\text{g}$  of RNA (as determined by quantification using a Nanodrop spectrophotometer) and a volume of nuclease free water to make 40  $\mu\text{L}$  of total reaction volume. cDNA was synthesized by incubating the reaction mixtures for 5 min at 25  $^{\circ}\text{C}$ , followed by 30 min at 42  $^{\circ}\text{C}$  and 5 min at 85  $^{\circ}\text{C}$ . Part of the cDNA was diluted to a final concentration of 10 ng/ $\mu\text{L}$ , to be used in the qPCR reactions. Both the diluted and non-diluted cDNA were stored at  $-20^{\circ}\text{C}$ .

### Primer selection

The public databases RTPrimerDB [203] and PrimerBank [204] were used for the selection of primers to be used in the amplification of the target genes. These databases contain information about primers that have already been validated. The sequences of the primer pairs obtained from the databases were evaluated using the software Beacon Designer™ 8.13 (PREMIER Biosoft International, California, USA). Whenever the databases had no primers pairs for a specific target, or the primer pair obtained was classified as poor by the Beacon Designer™, the NCBI tool Primer-BLAST [205] was used to search for primer pair suggestions. These primer pairs were also evaluated using Beacon Designer™. The sequences of the primers used in this investigation, the annealing temperature used and the amplicon expected size are presented in Table 2.5. The primers are from Life Technologies™ and were obtained through Alfagene® (Carcavelos, Portugal).

**Table 2.5 | Identification of the target genes of this work and specifications of the primers used for their amplification by RT-qPCR.**

Gene Identification	Foward and Reverse Primer Sequence	ID Database	Ta (°C)	Amplicon (bp)
<i>ATM</i> (NM_000051)	Fwd: CAAACAGAAGAGCACCTAGGCTAA Rev: GAGCCTGAAGTACACAGAGAACAA	Primer-BLAST	60	200
<i>ATR</i> (NM_001184)	Fwd: TCCCTGAATACAGTGGCCTA Rev: TCCTTGAAAGTACGGCAGTTC	PB_157266316c3	59	131
<i>BRCA1</i> (NM_007294)	Fwd: AGGAACCTGTCTCCACAAAGTG Rev: ACTTTCTGTAGGCTCCTTTTGGT	Primer-BLAST	59	134
<i>HSP1</i> (NM_005526)	Fwd: ACCCCGTGTCCTGTGGTTT Rev: GGGAACGGGACAGTTGTGTAA	RTPDB_612	61	111
<i>HSP90AA1</i> (NM_001017963)	Fwd: AGCTCAAGCCTAAGAGACAAC Rev: AAGATGACCAGATCCTTCACAGA	RTPDB_3014	60	150
<i>HSPA1A</i> (NM_005345)	Fwd: GGGCCTTCCAAGATTGCTG Rev: TGCAAACACAGGAAATTGAGAACT	Primer-BLAST	60	95
<i>MYC</i> (NM_002467)	Fwd: GTCAAGAGGCGAACACACAAC Rev: TTGGACGGACAGGATGTATGC	PB_239582723c3	63	162
<i>PI4KB</i> (NM_002651)	Fwd: AACTTGCCCGAATGTGGTATT Rev: GCCTATGTCATCCACCGACC	PB_311771619c2	61	105
<i>TP53</i> (NM_000546)	Fwd: GGAGCACTAAGCGAGCACTG Rev: GGAACATCTCGAAGCGCTCA	Primer-BLAST	61	120
<i>YWHAZ</i> (NM_001135702)	Fwd: TGTAGGAGCCCGTAGGTCATC Rev: GTGAAGCATTGGGGATCAAGA	PB_208973243c2	61	179

Gene symbols: *ATM*, ataxia telangiectasia mutated; *ATR*, ataxia telangiectasia and Rad3-related protein; *BRCA1*, breast cancer 1 susceptibility protein; *HSP1*, heat shock factor 1; *HSP90AA1*, heat shock 90 kDa protein 1 alpha; *HSPA1A*, heat shock 72 kDa protein; *MYC*, v-Myc avian myelocytomatosis viral oncogene homolog; *PI4KB*, phosphatidylinositol 4-kinase, catalytic, beta; *TP53*, tumour protein p53; *YWHAZ*, tyrosine 3-monooxygenase/tryptophan 5-monooxygenase activation protein, zeta.

NM, GenBank accession number; PB, PrimerBank; RTPDB, RTPrimerDB; Ta, annealing temperature.

### *Preparation of standards*

Purified amplicons at known copy numbers were prepared to assess the amplification efficiency of the qPCR reactions for each set of primers and to construct a standard curve to be used in the determination of the starting quantity (SQ) of each transcript in the samples.

Highly concentrated amplicons were obtained through a hot-start PCR reaction using the HotStarTaq Master Mix Kit. This PCR variant was designed to increase the specificity of the PCR reaction and the yield of the specific PCR product [206]. According to the manufacturer's instructions, 50  $\mu\text{L}$  of reaction mix were prepared by mixing 25  $\mu\text{L}$  of HotStart master mix, 19  $\mu\text{L}$  of RNase-free water, 1  $\mu\text{L}$  of primer mix and 5  $\mu\text{L}$  of non-diluted cDNA. The primer mixes were prepared by diluting 10  $\mu\text{L}$  of forward primer and 10  $\mu\text{L}$  of reverse primer in 80  $\mu\text{L}$  of RNase-free water. The hot-start PCR protocol consisted of an initial activation step of 15 min at 95 °C, followed by 35 cycles of 30 s at 94 °C, 30 s at the adequate annealing temperature of the set of primers (Table 2.5), 20 s at 72 °C and by a final extension step of 10 min at 72 °C.

The PCR products obtained were then purified, to remove residual reaction components such as primers, unincorporated nucleotides, the polymerase and salts, using the MinElute PCR Purification Kit. Following the manufacturer's instructions, 250  $\mu\text{L}$  of Buffer PB were added to the 50  $\mu\text{L}$  of the hot-start PCR reaction. At this point, it was necessary to ensure that the pH of the mixture was lower than 7.5, as this is crucial for optimal DNA adsorption to the column membrane. The Buffer PB contains a pH indicator that at pHs lower than 7.5 presents a yellow color, and at pHs higher than 7.5 presents a violet color. As the mixture obtained presented a violet color, 10  $\mu\text{L}$  of a 3 M sodium acetate solution (pH 5.0) were added. The resulting mixture was then transferred to a MinElute column inserted in a 2 mL collection tube and centrifuged at 17900  $g$  for 1 min and at 25 °C. The flow-through was discarded and 750  $\mu\text{L}$  of Buffer PB were added to the column, which was again centrifuged at 17900  $g$  for 1 min. After discarding the flow-through, the column was subjected to an additional centrifugation at 17900  $g$  for 1 min, and then transferred to a 1.5 mL centrifuge tube. DNA was eluted by adding 10  $\mu\text{L}$  of Buffer EB directly to the membrane stack at the base of the column. After a 1 min incubation, the column was centrifuged at 17900  $g$  for 1 min and the DNA was recovered.

The eluted DNA was quantified using the Nanodrop, with the Buffer EB as the blank. Considering the molecular weight of each amplicon, calculated using the *Oligo*

*Calc: Oligonucleotide Properties Calculator* software [207], the number of copies was determined. From this concentrated solution, standards containing  $5 \times 10^9$  to  $5 \times 10^2$  copies were prepared by serial dilution. Standards were stored at  $-20^\circ\text{C}$ , until used in the qPCR reactions.

### qPCR

qPCR reactions were performed in 96-well PCR plates, in a CFX96 real time-PCR system. Immediately before the reaction, a mastermix sufficient for the number of planned reactions was prepared by mixing the SsoFast™ EvaGreen® Supermix with the primers and RNase free water. This supermix contains the DNA dye EvaGreen®, which has spectral properties similar to those of the commonly used SYBR® Green, but provides increased fluorescence, as it causes significantly less inhibition of the qPCR reaction. The performance of the qPCR reactions is also increased by the use of the Sso7 polymerase, which presents increased processivity and decreased reaction times, when compared to conventional DNA polymerases. Amplification of 25 ng cDNA was performed with an initial cycle of 2 min at  $98^\circ\text{C}$ , followed by 40 cycles of 5 s at  $98^\circ\text{C}$  plus 5 s at the appropriate annealing temperature for each set of primers (Table 2.5). At the end of each cycle, Eva Green® fluorescence was recorded to enable determination of the quantification cycle (Cq). No-reverse transcriptase and no-template controls were performed. All samples, except the standards, were assessed in duplicate. For quality control, the melting temperature of the PCR products was determined by performing melting curves. As mentioned, purified amplicons at known copy numbers were used to determine the amplification efficiency for each set of primers and to determine the SQ of each transcript in the samples from a standard curve that correlates the number of copies present in the standard with its Cq. Relative expression of the genes of interest was calculated by dividing their SQ by a normalization factor, which was the geometric mean of the SQs of the reference genes (*YWHAZ* and *PI4KB*<sup>4</sup>).

As an additional control, an electrophoresis with a representative sample of each amplicon was run to verify whether the reactions had yielded a single specific product

---

<sup>4</sup> The RefGenes tool from the software Genevestigator®, which contains public microarray data, was used to search for candidate reference genes, i.e. for genes that displayed stable expression in previous experiments with the BEAS-2B cell line. Primers for several of those genes were selected as described within the heading *Primer Selection* and optimization reactions were performed. The genes *YWHAZ* and *PI4KB* were chosen to be used as the reference genes in this work for presenting the best efficiencies and having an expression level within the expression range of the genes of interest.

with the expected amplicon size (Table 2.5). A 2.5% (w/v) agarose gel was prepared by melting 2.5 g of agarose in 100 mL of Tris-Borate-EDTA (TBE) buffer. The nucleic acid stain GreenSafe Premium was added to the gel to allow the detection of DNA at the end of the run. The gel was cast into the tray and, when solid, samples (10  $\mu$ L) and ladders (5  $\mu$ L) were added to the wells. Samples were prepared by mixing 5  $\mu$ L of qPCR reaction product with 3  $\mu$ L of water and 2  $\mu$ L of BlueJuice™ Gel Loading Buffer (10 $\times$ ). Electrophoresis was run in TBE buffer at 100 V for the time required to obtain satisfactory separation. DNA was visualised under UV light on a transilluminator and digitally photographed using the VisionWorks®LS Image Acquisition and Analysis Software (UVP Bioimaging Systems, California, USA). The electrophoresis showed that the primers were specific, as only one product was detected in each reaction and it had the expected amplicon size (Appendix A.2).

## 2.17. Statistical analysis

For statistical analysis of the experimental data obtained, the GraphPad Prism 5.00 software for Windows (GraphPad Software Inc, California, USA) was used. The statistical relevance of differences between groups was examined using the *t-student paired* test, when comparing two different conditions, or the *one-way ANOVA* method followed by the *Dunnet's* or *Bonferroni* multiple comparison tests, if three or more conditions were simultaneously tested. Differences with  $p < 0.05$  were considered statistically significant.

At least three independent experiments were performed for each parameter assessed, and the results are presented as mean  $\pm$  standard error of the mean (SEM).

## **3. Results and Discussion**

---



### 3.1. Impact of culturing conditions and culture age on the growth characteristics and genomic stability of the BEAS-2B cell line

As mentioned in section 1.4.1, since its establishment in 1988, the BEAS-2B cell line has been used as a model for human bronchial epithelium in extremely different experimental contexts. Interestingly, a quick inspection of the literature reveals that the recommendations for the routine culture of BEAS-2B cells published by ATCC [186], their official depositor, are rarely followed by the research groups that use this cell line, including our own [35, 46, 55-60, 208-210]. In our laboratory, by using a culture medium and coating solution different from those recommended by ATCC (Table 3.1), we were able to significantly reduce the costs associated with the use of this cell line. More recently, we have also altered the seeding density, so as to reduce the passage frequency to once a week (Table 3.1).

**Table 3.1 | Comparison of the culturing conditions recommend by ATCC for routine maintenance of BEAS-2B cells and those used in our laboratory.**

	ATCC	Our laboratory
<b>Culture medium</b>	BEGM	LHC-9
<b>Coating solution</b>	FNT(+) CS 0.01 mg/mL fibronectin 0.03 mg/mL collagen 0.01 mg/mL BSA (in BEGM)	FNT(-) CS 10 mg/mL gelatin 1 mg/mL BSA (in PBS)
<b>Seeding density<sup>1</sup></b>	1.5 to 3 × 10 <sup>3</sup> cells/cm <sup>2</sup>	2 × 10 <sup>3</sup> cells/cm <sup>2</sup>
<b>Passage routine</b>	Before reaching high confluence	7 days after seeding (~80% confluence)
<b>Medium renewal</b>	Every 2 to 3 days	None

<sup>1</sup>ECACC, the European supplier of this cell line, recommends 3 to 10 × 10<sup>3</sup> cells/cm<sup>2</sup>.

FNT(+) CS, fibronectin-containing coating solution; FNT(-) CS, fibronectin-free coating solution.

#### 3.1.1. Assessment of the culturing conditions adopted in our laboratory

The culturing conditions adopted in our laboratory (Table 3.1) consistently yielded apparently healthy cultures. As can be appreciated in Figure 3.1, the cells exhibited the polygonal shape and cobblestone growth typical of epithelial cells. Figure 3.1B also shows that, with our once a week passage routine, cultures did not reach

excessive confluence, which might have triggered terminal differentiation [186]. This observation was further confirmed by their growth curve (Figure 3.2), which showed that, at the time of subculturing (last time point on the growth curve), the culture viability was not yet decreasing (although cells were no longer at the exponential phase of growth).

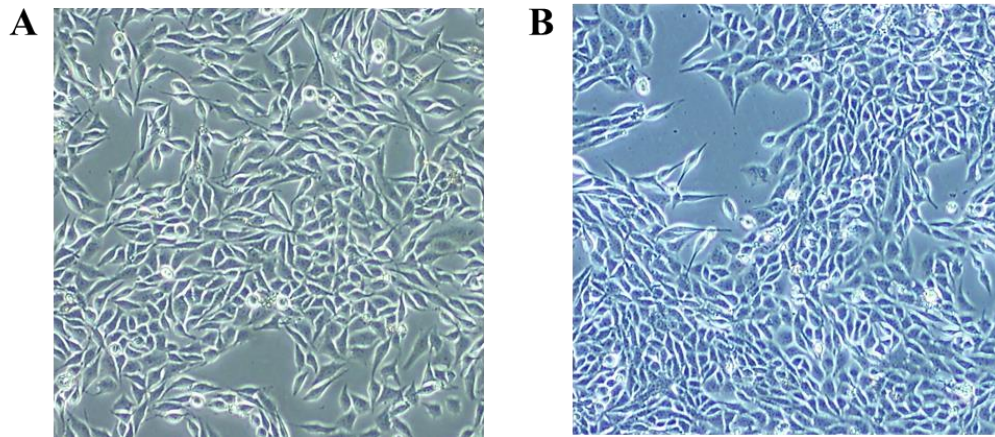


**Figure 3.1 | Representative micrographs (100× magnification) of BEAS-2B cells, grown using the culturing conditions adopted by our laboratory (Table 3.1), (A) 4 and (B) 7 days after subculturing. Cells were at passage 13.**

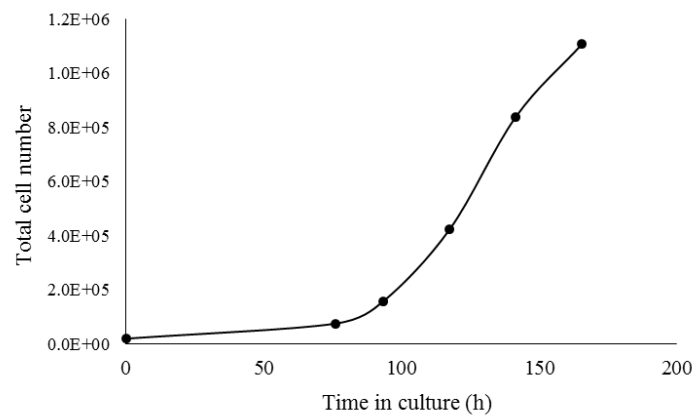


**Figure 3.2 | Representative growth curve of a culture of BEAS-2B cells. Cells were seeded at 2000 cells/cm<sup>2</sup> and their total numbers over time were determined by the Trypan Blue exclusion method (section 2.5). Cultures were monitored from day 3 to day 7 after seeding. Each time point represents the mean total cell number of triplicate cultures.**

The fact that the colour of the medium remained essentially unchanged throughout the interval between subcultures lends further support to the adequacy of our passage routine. We have also confirmed, in a previous study and in this one, that the levels of glucose and glutamine, nutrients present in the medium that are essential to assure cell survival, were not excessively depleted as a consequence of cellular proliferation. The levels of glucose were reduced from about 6 mM to approximately 2 mM over the seven day interval between passages [211] and those of glutamine were reduced from about 3 mM to approximately 1.5 mM (Figure 3.3A). Glutamine is an important energy source and biosynthetic precursor for *in vitro* cell cultures. On the contrary, ammonia, which is a by-product of the metabolism of this amino acid, is known to be toxic and capable of inhibiting cell growth [187]. As can be seen in Figure 3.3B, the levels of this by-product increased from about 0.7 mM at the time of seeding to 2.3 mM at the time of subculturing. Although significant, the observed decreases in the levels of glucose and glutamine and concomitant increase in the levels of ammonia did not seem to have compromised cell proliferation, as confirmed by the growth curve obtained (Figure 3.2).

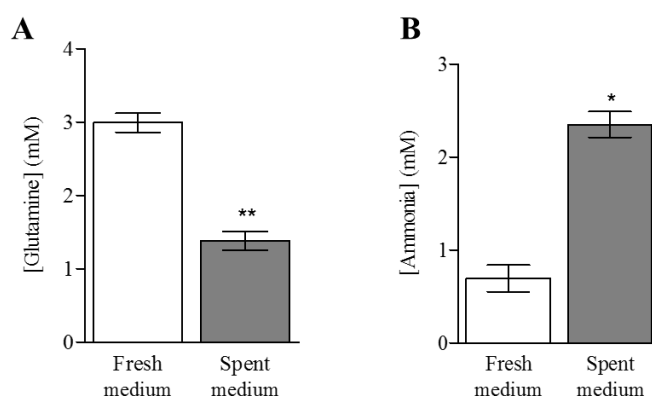


**Figure 3.3 | (A) Glutamine and (B) ammonia levels in the culture medium at the time of seeding (fresh medium) and of subculturing (spent medium).** Glutamine and ammonia levels were determined using the kit L-Glutamine/Ammonia (Rapid), as described in section 2.7. Results are presented as mean  $\pm$  SEM of three independent experiments. Experimental data were analysed with the software GraphPad Prism 5.00, using the *t-student paired* test: \*,  $p < 0.05$ ; \*\*,  $p < 0.01$ .

Altogether, these results indicate that the alterations introduced in our laboratory to the culturing conditions of BEAS-2B cells do not compromise cell growth and proliferation. Therefore, these culturing conditions were those used throughout the subsequent studies described in this thesis, unless otherwise stated.

### **3.1.2. Impact of culturing conditions on the growth characteristics of the BEAS-2B cell line**

It is well established that the culture medium and the nature of the substrate used for cell adhesion have a significant impact on the genotypes and phenotypes of epithelial cells grown *in vitro* [187]. Thus, we set out to analyse in some detail the impact of the changes we have introduced to the culturing conditions of BEAS-2B cells, taking cultures grown according to the ATCC recommendations as controls. To this end, we have established and cultured in parallel BEAS-2B cells under three different culturing conditions: (i) following the ATCC recommendations, i.e. using BEGM medium and the fibronectin-containing coating solution recommended by them (FNT(+) CS); (ii) replacing LHC-9 medium for BEGM medium, but maintaining the FNT(+) CS; (iii) replacing both the medium and coating solution recommended by ATCC by LHC-9 and the fibronectin-free coating solution routinely used in our laboratory (FNT(−) CS). The parameters assessed in this study were: cell morphology, pattern of growth and growth rate.

Inspection of the cultures under an inverted optic microscope revealed some cumulative changes in cell morphology and growth pattern induced by the two modifications introduced (Figure 3.4). These changes were rather subtle and, as such, may not be easily detected in the selected micrographs. Nonetheless, on closer inspection, it is possible to observe that these two changes led to reduced cell spreading and to more heterogeneous monolayers. The reduced cell spreading is in line with the observation that cultures grown in LHC-9 and in FNT(+) coated flasks were consistently more easily trypsinized than those grown under ATCC conditions, and that those grown in LHC-9 and in FNT(−) coated flasks were even more easily trypsinized. Overall, these results suggest that BEAS-2B cells cultured according to the ATCC specifications adhere more strongly to the substrate than those cultured with a different medium and/or coating solution. The presence of fibronectin in the coating solution recommended by ATCC is likely one of the key factors underlying this observation, as it has long been known that this protein is critical for cell adhesion [187]. The medium composition must also have had an important role, since medium replacement alone produced significant alterations. Most likely, the differential adhesion properties are evoked by quantitative differences in the media supplements that are added to the respective basal media (BEBM and LHC

basal media, for BEGM and LHC-9, respectively)<sup>5</sup>. However, in the absence of information regarding individual concentrations of these supplements, we can only speculate.

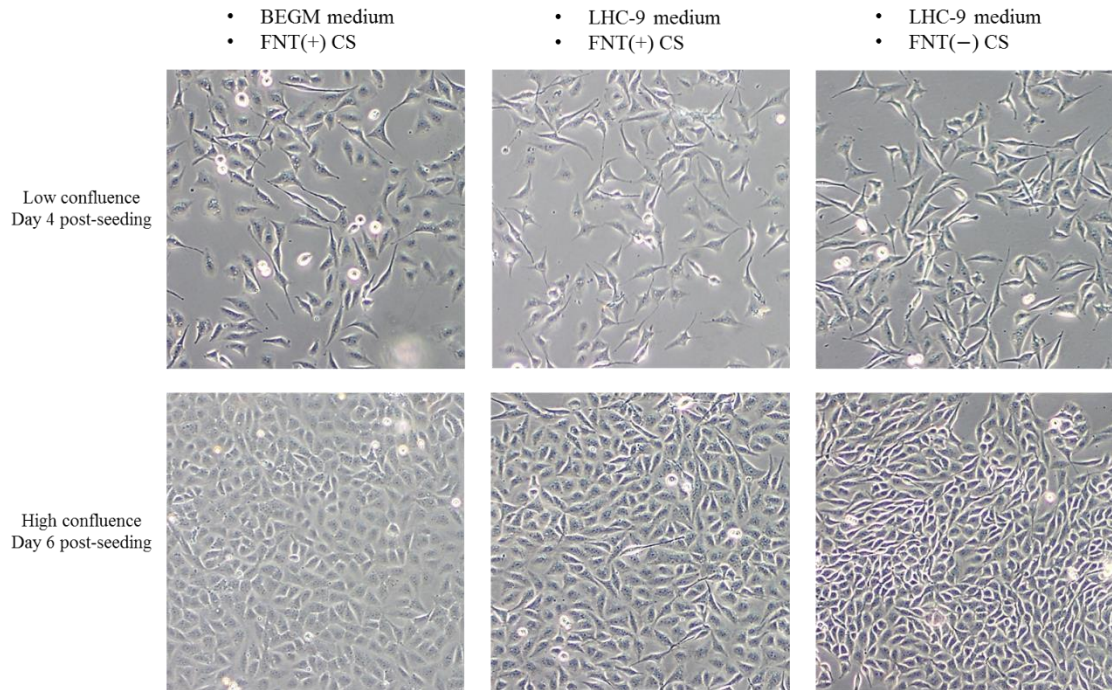


**Figure 3.4 | Effects of medium and coating solution on the morphology and growth pattern of BEAS-2B cells.** Representative micrographs (100× magnification) of BEAS-2B cells, at passage 13. For all conditions, the initial seeding density was 2000 cells/cm<sup>2</sup>. FNT(+) CS, fibronectin-containing coating solution; FNT(-) CS, fibronectin-free coating solution.

In terms of the growth rate of the cells, no significant changes were observed, with cells cultured under all three conditions presenting a similar doubling time (Figure 3.5).

<sup>5</sup> These supplements are the same for both media and include: epidermal growth factor, hydrocortisone, insulin, bovine pituitary extract, epinephrine, transferrin, triiodothyronine and retinoic acid.

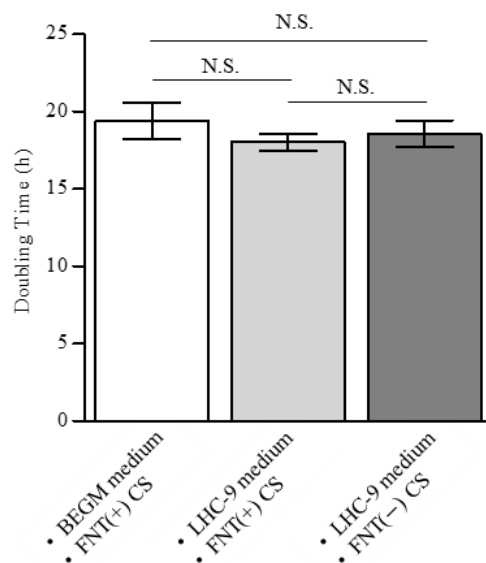


**Figure 3.5 | Effects of medium and coating solution on the growth rate of BEAS-2B cells.** For all conditions, the initial seeding density was 2000 cells/cm<sup>2</sup>. Doubling times were determined as described in section 2.8. Results are presented as mean  $\pm$  SEM of three independent experiments. Experimental data were analysed with the software GraphPad Prism 5.00, using the *one-way ANOVA* method followed by the *Bonferroni* multiple comparison test. No statistically significant differences were observed. FNT(+) CS, fibronectin-containing coating solution; FNT(-) CS, fibronectin-free coating solution; N.S., not significant.

Interestingly, there are several studies in the literature that do not mention coating [35, 56-58, 60, 208, 209] and, at least, one that specifically mentions that cultures were grown in the absence of coating [210]. The medium used in this latter case was BEGM. Thus, we have also tested the effects of the growth medium on cell attachment to non-coated surfaces. As can be appreciated in Figure 3.6A, cells grown in BEGM were able to adhere to the substrate in the absence of coating and form monolayers, although the cultures lost some of their homogeneity and the cells did not spread as extensively as in the presence of coating. This was not the case with the cultures grown in LHC-9, which, as can be seen in Figure 3.6B, lost their typical cobblestone growth and formed foci. This observation reinforces our notion that the BEGM formulation plays a key role in the promotion of the cell attachment to the substrate.

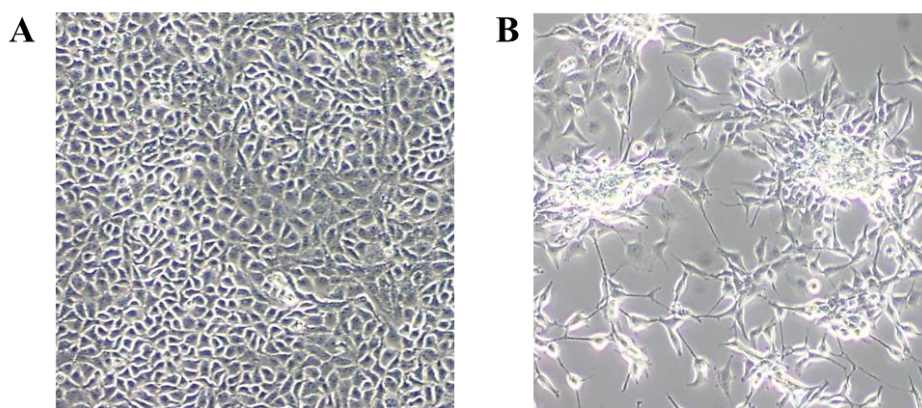


**Figure 3.6 | Effects of the growth medium on cell attachment to non-coated culture surface.** Representative micrographs (100× magnification) of BEAS-2B cells growing in uncoated 6-well plates, in (A) BEGM and (B) LHC-9. Cells were at passage 14 and the seeding density was 2000 cells/cm<sup>2</sup>.

Inspection of the literature also revealed that, against the ATCC recommendations [186], culture media supplemented with FBS are commonly used for routine maintenance of BEAS-2B cells [35, 58, 60, 208, 209]. This recommendation is likely based on an initial observation, from the group that established this cell line, that these cells underwent terminal squamous differentiation in response to serum [53]. However, in a subsequent study from the same group, where the effects of serum were extensively investigated, the authors isolated two subclones from a culture of BEAS-2B cells exposed to FBS and observed that only one of them was induced to undergo squamous differentiation. On the contrary, the other clone was mitogenically stimulated [212]. The isolated clones also differed in their morphology, but were karyotypically similar and presented marker chromosomes common to those observed in the parental BEAS-2B cell line, which seemed to indicate that they originated from a common cell. These observations suggest that cell cultivation might induce some heterogeneity in a population with a common origin, leading to the appearance of distinct phenotypes.

More recently, the impact of FBS on the phenotype of BEAS-2B cells was further investigated by Zhao and Klimecki, who have been using the BEAS-2B cell line as a model of arsenic-induced cytotoxicity [210]. Their study revealed that the addition of FBS to cultures grown in BEGM and in non-coated flasks caused alterations in the morphology, the epithelial identity (as revealed by the loss of E-cadherin protein, an epithelial marker), the mRNA expression of a significant number of genes and in the energy metabolism. The authors also investigated the sensitivity of BEAS-2B cells grown

in the presence of FBS to arsenic and concluded that FBS-exposed cells are more sensitive to arsenic-induced cytotoxicity. Thus, it would be important to assess the effect of FBS on other compounds whose cytotoxicity has also been investigated in BEAS-2B cells.

In the present study, we investigated the impact of FBS (1 or 10% (v/v)) on the morphology and growth pattern of BEAS-2B cells grown under the culturing conditions adopted in our laboratory (Table 3.1). As can be appreciated in Figure 3.7, FBS induced significant concentration and time-dependent changes in the morphology of the cells. Specifically, cells grown in the presence of FBS became bigger, more flattened and had a less clearly defined border, i.e. they acquired a more squamous appearance. These alterations were similar to those observed by Zhao and Klimecki in their aforementioned study [210]. FBS was also expected to have a growth inhibitory effect [212, 213], but we have not detected obvious changes in the proliferation rates of these cultures, over the five-week period that we monitored them.

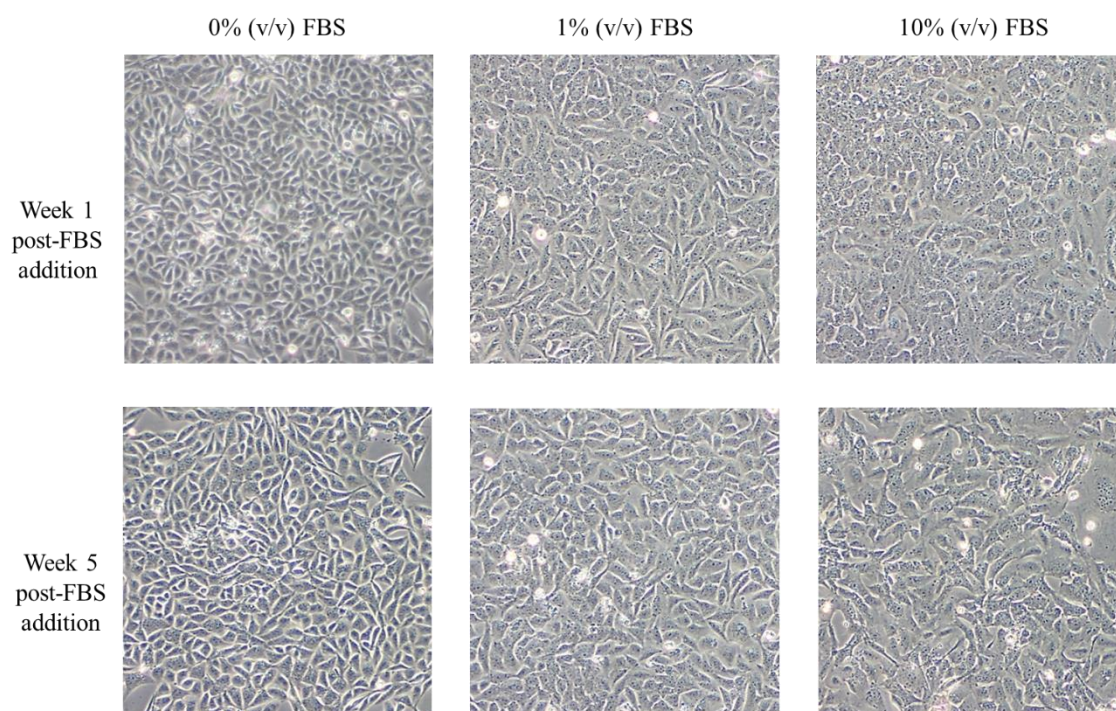


**Figure 3.7 | Effects of FBS on the morphology and pattern of growth of BEAS-2B cells.** Representative micrographs (100× magnification) of BEAS-2B cells, at passages 14 (week 1) and 18 (week 5). Cells were cultured in FTN(–) coated flasks, in LHC-9.

### **3.1.3. Impact of culture age on the growth characteristics and genomic stability of the BEAS-2B cell line**

BEAS-2B is a continuous cell line and it was specifically established for the study of carcinogenesis (section 1.1.4.1), a long-term process. However, it is well known that cultures grown *in vitro* over extended periods of time are subjected to selective pressures and undergo genetic drift, which can lead to significant alterations in the morphology, growth characteristics and gene expression of the cells [214]. BEAS-2B cell cultures are no exception and, in fact, the group that established this cell line reported that BEAS-2B cells underwent progressive changes over time in culture, which included the development of weak tumorigenicity [67]. In previous studies from our group, we have also observed progressive alterations, namely in the morphology, growth rate and chromosomal complement of BEAS-2B cells [59, 211]. One of the aims of the present study was to further extend our characterization of the impact of culture age on the morphology, pattern of growth and genomic stability of BEAS-2B cells, by monitoring these parameters over a considerably more prolonged period of time than in the previous studies. In addition, the impact of culture age on the sensitivity of these cells to FBS was also evaluated.

Under the culturing conditions adopted in our laboratory (Table 3.1), BEAS-2B cells appeared to have unlimited proliferative potential, as they could be subcultured for over 100 passages (corresponding to over 600 population doublings). Notwithstanding, we observed significant morphologic and karyotypic changes. Considering the morphology of the cells, it was possible to define three characteristic stages, that we named: the low passage stage (until passage 30), the transitional stage (from passage 30 to 60) and the high passage stage (from passage 60 onwards).

As can be appreciated in Figure 3.8, cells in the low passage stage presented the characteristic polygonal shape and the typical cobblestone growth of epithelial cells, while cells in the transitional stage lost these characteristics to a significant extent. In fact, over time in culture, cell shape became less defined and the cells became slightly bigger. Moreover, the monolayers lost their homogeneity and presented areas with extensive crisscrossing. Interestingly, in the high passage stage, crisscrossing was lost and the cultures recovered the homogeneity of the monolayer. On the other hand, the increase in

cell size became much more pronounced, and cells began to present a granular appearance.

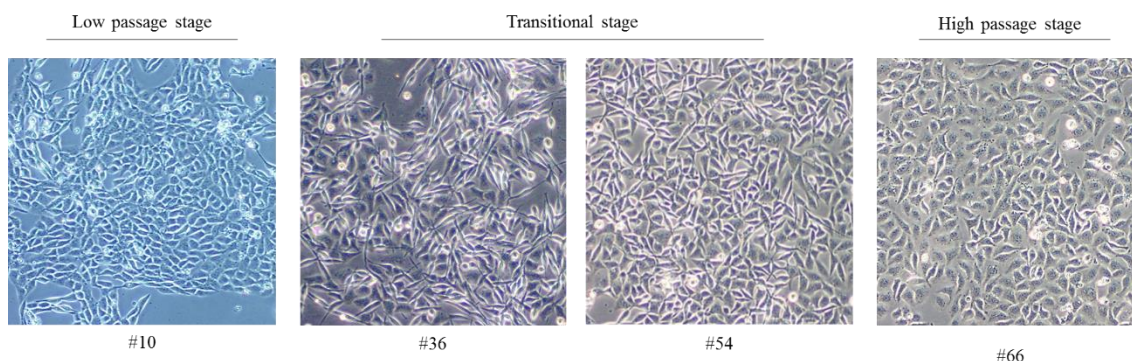


**Figure 3.8 | Impact of culture age on the morphology and pattern of growth of BEAS-2B cells.** Representative micrographs (100× magnification) of BEAS-2B cells, at the passages indicated at the bottom of each micrograph. Cells were cultured in FTN(–) coated flasks, in LHC-9. #, passage number.

As discussed in section 1.1.4.1, the cytogenetic characterization of the BEAS-2B cell line is somewhat incipient. The initial characterization, performed by Curtis Harris and collaborators, revealed that, while immortalization occurred, there was an accumulation of four abnormal chromosomes (additional material of unknown origin on the short arm of chromosomes 15 [(add(15)(p11.1)] and 16 [add(16)(p13)], a derivative of the long arm of chromosome 8 with the long arm of chromosome 9 [der(8;9)(q10;q10)] and a marker chromosome (mar)) and loss of one homolog of chromosomes 8, 15, 16, 21, and 22 [53, 66, 67]. Of note, the incidence of one of the alterations, the der(8;9)(q10;q10), decreased in the higher passages they analysed. To establish meaningful comparisons between the results obtained in the cytogenetic analysis carried out by the group of Curtis Harris and those carried out by us, we should compare karyotypes from cultures with an equivalent number of population doublings. Unfortunately, it is not possible to establish these numbers with accuracy, even more because we do not have any information concerning the passage routine adopted in the laboratory of Curtis Harris. Still, from the information available, namely that kindly provided by ATCC that cells were deposited at passage 31 and are currently being supplied at passages 36 to 38, it seems reasonable to assume that the population doublings of the higher passage cultures in the studies of Curtis Harris and collaborators were roughly equivalent to those of the cultures in our study that we classified as the low passage stage cultures.

The cytogenetic analysis of cells in the low passage stage previously carried out in our laboratory [59], showed some similarities with the analysis of the group of Curtis Harris, but also some significant differences. Concerning the similarities, we have also observed that chromosomes 15 and 16 exhibited additional material of unknown origin on their short arms (alterations designated in this study as 15p<sup>+</sup> and 16p<sup>+</sup>, respectively) [59], although we cannot state with certainty that these alterations correspond exactly to those they observed. Concerning the differences, we have observed five chromosomal alterations, four structural and one numerical, that Curtis Harris and collaborators did not report. The structural alterations comprised an isochromosome 5 [i(5)(q10)], additional material of unknown origin on the short arm of chromosomes 14 (14p<sup>+</sup>) and 22 (22p<sup>+</sup>) and a terminal deletion of the short arm of the X chromosome (Xp<sup>-</sup>). The numerical alteration was a trisomy of chromosome 20 [tri(20)]. Over time in culture, it was observed that the alterations 14p<sup>+</sup> and tri(20) tended to disappear, while two new alterations, a derivative of chromosome 2 and a terminal deletion on i(5)(q10), emerged. Interestingly, the tri(20), which was present with high incidence in our low passage cells, was also observed, by the group of Curtis Harris, in more than 25% of the cells from a tumorigenic cell line that this group had established from tumours induced by the injection of BEAS-2B cells into athymic nude mice [67]. Considering that tri(20) has also been frequently found in non-small cell lung carcinomas (NSCLCs) [215], the presence of this alteration in BEAS-2B cells could be seen as an indicator of tumorigenicity. However, the disappearance of this alteration in higher passages suggests that either tri(20) is not, in this case, directly related to tumorigenicity or that the tumorigenic potential of BEAS-2B cells is actually decreasing over time in culture.

In the present study, it was observed that the chromosomal complement of BEAS-2B cells suffered significant alterations with culture age, accompanying the morphologic changes (Table 3.2 and Figure 3.9). At the low passage stage, the cells presented the same set of chromosomal alterations that was reported in our previous study. Importantly, we have now identified the additional material on the short arm of chromosome 16 as the long arm of chromosome 17. This alteration is, thus, a derivative of the long arm of chromosome 16 with the long arm of chromosome 17 [der(16;17)].

**Table 3.2 | Incidence of the chromosomal alterations observed in BEAS-2B cells at different stages.**

Chromosomal alteration	Incidence			
	Low passage stage	Transitional stage		High passage stage
	#11 and 26	#48	#54	#104
der(2;9;14)	-	-	-	++
4p <sup>-</sup>	-	+++	+++	+++
4p <sup>+</sup>	-	-	-	-
i(5)(q10)	+++	++	-	-
der(5;9)	-	++	+++	+
der(5;15)	-	++	+++	+++
9q <sup>+</sup>	-	-	-	+++
14p <sup>+</sup>	+	+	-	-
15p <sup>+</sup>	+++	++	-	-
der(16;17)	+++	+++	+++	+++
18q <sup>-</sup>	-	++	+++	+++
22p <sup>+</sup>	+++	+++	+++	+++
tri(20)	+++	-	-	-
mono(20)	-	++	-	+
Xp <sup>-</sup>	+++	++	-	-
-Y	-	++	++	+

Incidence of the chromosomal alterations: -, chromosomal alteration present in less than 15% of the metaphases analysed; +, chromosomal alteration present in 15 to 40% of the metaphases analysed; ++, chromosomal alteration present in 40 to 80% of the metaphases analysed; + + +, chromosomal alteration present in more than 80% of the metaphases analysed. Number of metaphases analysed: #11 and 26 – 23 metaphases; #48 – 17 metaphases; #54 – 11 metaphases; #104 – 10 metaphases. Metaphase spreads were obtained as described in section 2.9. and the karyotypes constructed using the Applied Imaging<sup>®</sup> CytoVision<sup>®</sup> software. #, passage number; der(2;9;14), derivative of the chromosomes 2, 9 and 14; 4p<sup>-</sup> and Xp<sup>-</sup>, terminal deletion of the short arm of the respective chromosomes; 4p<sup>+</sup>, 14p<sup>+</sup>, 15p<sup>+</sup> and 22p<sup>+</sup>, additional material of unknown origin on the short arm of the respective chromosomes; i(5)(q10), isochromosome 5; der(5;9), derivative of the long arm of chromosome 5 with the long arm of the chromosome 9; der(5;15), derivative of the long arm of chromosome 5 with the long arm of the chromosome 15; 9q<sup>+</sup>, additional material of unknown origin on the long arm of chromosome 9; der(16;17), derivative of the long arm of chromosome 16 with the long arm of the chromosome 17; 18q<sup>-</sup>, terminal deletion of the long arm of chromosome 18; tri(20), trisomy of chromosome 20; mono(20), monosomy of chromosome 20; -Y, loss of chromosome Y.

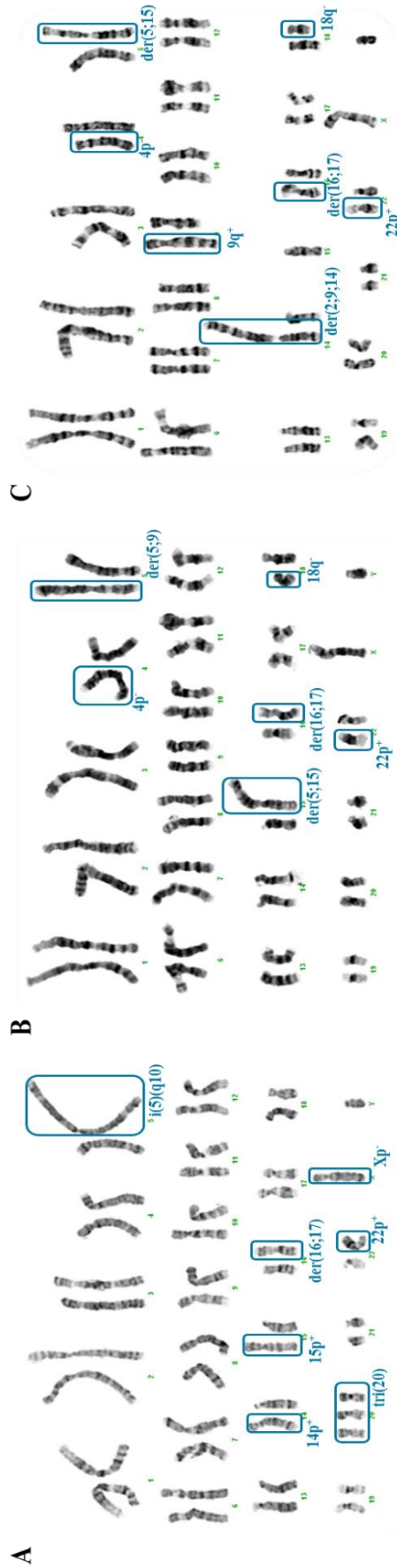


**Figure 3.9 | Representative G-banded karyotypes of BEAS-2B cells at the (A) low passage stage, (B) transitional stage, and (C) high passage stage.** Metaphase spreads were obtained as described in section 2.9 and the karyotypes constructed using the Applied Imaging<sup>®</sup> CytoVision<sup>®</sup> software. der(2;9;14), derivative of the chromosomes 2, 9 and 14; 4p<sup>-</sup> and Xp<sup>-</sup>, terminal deletion of the short arm of the respective chromosomes; i(5)(q10), isochromosome 5; der(5;9), derivative of the long arm of chromosome 5 with the long arm of the chromosome 9; der(5;15), derivative of the long arm of chromosome 5 with the long arm of the chromosome 15; 9q<sup>+</sup>, additional material of unknown origin on the long arm of chromosome 9; 14p<sup>+</sup>, 15p<sup>+</sup> and 22p<sup>+</sup>, additional material of unknown origin on the short arm of the respective chromosomes; der(16;17), derivative of the long arm of chromosome 16 with the long arm of the chromosome 17; 18q<sup>-</sup>, terminal deletion of the long arm of chromosome 18; tri(20), trisomy of chromosome 20.

During the transitional stage, dramatic alterations of the chromosomal complement took place, with most of the characteristic alterations observed in the low passage stage progressively disappearing, and several new alterations progressively emerging. The only chromosomal alterations from the set observed in the low passage stage whose incidence was not altered during the transitional stage were the der(16;17) and 22p<sup>+</sup>. The emerging alterations comprised four structural (terminal deletions of the short arm of chromosome 4 (4p<sup>-</sup>) and of the long arm of chromosome 18 (18q<sup>-</sup>), and derivatives of the long arm of chromosome 5 with the long arm of chromosome 9 [der(5;9)] or of chromosome 15 [der(5;15)]) and two numerical alterations (monosomy of chromosome 20 [mono(20)] and loss of chromosome Y (-Y)). Of note, the loss of chromosome Y is an alteration commonly found in NSCLCs [215, 216] and, thus, its presence might suggest that some cells could be progressing towards malignancy.

The tendency of the alterations 14p<sup>+</sup> and tri(20) to disappear over time had already been reported by our group [59], as discussed above. At that time, the disappearance of the other alterations was not observed, but this might be due to the fact that the cells analysed in that study had not undergone as many population doublings as the cells analysed in this study. On the other hand, none of the emerging alterations reported in that previous study were now observed.

From passage 54 to passage 104, which represent the high passage stage, the karyotypic changes were not as dramatic as those that occurred during the transitional stage. In fact, all alterations observed at passage 54 were still observed in the high passage stage, although the incidence of one of them, the der(5;9), was much reduced (Table 3.2). In addition, two new alterations were observed in the high passage stage: a derivative of the chromosomes 2, 9 and 14 [der(2;9;14)] and additional material of unknown origin on the long arm of chromosome 9 (9q<sup>+</sup>). It is interesting to note that, in this stage, all cells that did not present any of the two new structural alterations still had the der(5;9), i.e. they exhibited the karyotype of transitional stage cells. This observation suggests a certain heterogeneity in the culture, with cells at different stages of the karyotypic evolution.

Overall, these results reinforce the previous observations from our group and the group of Curtis Harris indicating that BEAS-2B cells present significant genomic instability, which leads to frequent alterations of their karyotype over time in culture. Thus, results obtained in long-term studies with these cells must be interpreted with great care. Moreover, it is critical that controls and exposed cultures are established from the same cell stock and cultured in parallel. In the future, it would be important to perform a

more precise characterization of the chromosomal alterations present in this cell line. This characterization will require the use of more advanced cytogenetic techniques, since the nature of some alterations could not be determined by conventional cytogenetics.

Concerning the impact of culture age on the sensitivity of BEAS-2B cells to FBS, no significant differences were observed between cultures in the low passage and in the transitional stage. In fact, as can be appreciated in Figure 3.10, the effects of FBS on the morphology and growth pattern of BEAS-2B cells in the transitional stage were very similar to those observed in low passage cells (Figure 3.7), including, once again, increased cell size, more flattened appearance and less definition of the cell border. The proliferation rate of the cultures grown in the presence of FBS remained apparently unaltered, over the five-week period of monitoring.

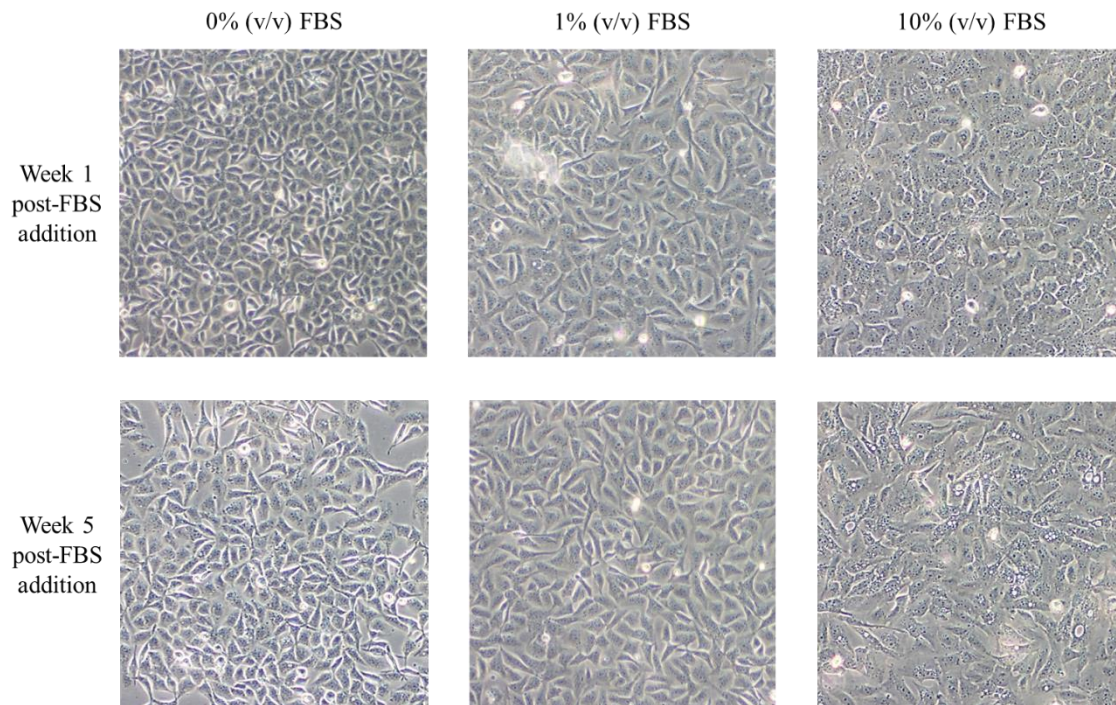


**Figure 3.10 | Effects of FBS presence on the morphology and growth pattern of BEAS-2B cells in the transitional stage.** Representative micrographs (100× magnification) of BEAS-2B cells, at passages 48 (week 1) and 52 (week 5). Cells were cultured in FTN(–) coated flasks, in LHC-9.

### **3.2. Effects of a short-term exposure to Cr(VI) on the stress response of BEAS-2B cells**

As discussed in section 1.1.3, cells exposed to Cr(VI) experience several types of cellular stresses, namely oxidative and metabolic stresses. In previous studies from our group, it was consistently observed that BEAS-2B cells that resisted to low concentrations of Cr(VI) (0.1 to 1  $\mu$ M) exhibited increased proliferation rates [46-48]. This suggested that, somehow, those cells were able not only to resist the several stresses induced by Cr(VI) exposure, but also gain a proliferative advantage over their non-exposed counterparts. This observation pointed to the possibility that Cr(VI) might also protect incipiently transformed cells from the additional stresses they will encounter during neoplastic transformation.

To assess this possibility, our group has been using acute thermal shocks as a model of induced cellular stress. In a previous study, we observed that, in BEAS-2B cells, exposure to Cr(VI) attenuated the transient growth arrest induced by an acute cold shock [217, 218], an observation that lends some support to our hypothesis.

In the present study, we set out to determinate if Cr(VI) could also confer a similar resistance against an acute heat shock (section 3.2.2). In addition, we evaluated whether Cr(VI) could protect against the negative effects of heat shock on the cellular energy status (section 3.2.3) and modulate the expression of some key elements of the stress response (section 3.2.4) and/or of cancer-associated pathways also related to the stress response (section 3.2.5).

#### **3.2.1. Establishment of the exposure regimen to Cr(VI) and to heat shock**

The use of inadequate cellular models and exposure regimens in the studies investigating Cr(VI)-induced carcinogenesis might be regarded as one of the main factors hampering the elucidation of the molecular basis of this process (section 1.1.4). In this study, we addressed this issue by using the BEAS-2B cell line, a cellular model representative of the human bronchial epithelium, which is the main target of Cr(VI) carcinogenicity *in vivo*, and an exposure regimen that presents low cytotoxicity.

As it was our objective to assess if the acquisition of resistance to stress could be one of the initiating events of Cr(VI)-induced cellular malignization, we opted for evaluating the effects of a short-term exposure of 48 h to Cr(VI). The concentration of Cr(VI) used in the cellular treatments was chosen based on our cytotoxicity evaluation.

Treatment of BEAS-2B cell cultures for 48 h with 1 and 2  $\mu\text{M}$  of Cr(VI) caused a 19 and 32% reduction of live cells in culture, respectively (Figure 3.11). Both concentrations produced statistically significant decreases, with the results being clearly concentration-dependent. The 2  $\mu\text{M}$  concentration was considered to be overly cytotoxic for the purpose of this study and, therefore, the concentration selected to be used in all further experiments was 1  $\mu\text{M}$  Cr(VI).

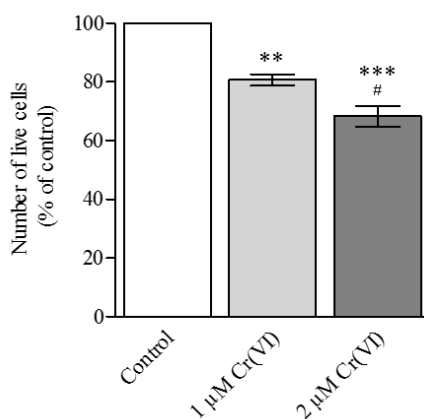


**Figure 3.11 | Cytotoxic effects of a 48 h exposure to 1 or 2  $\mu\text{M}$  Cr(VI) in BEAS-2B cells.** Cr(VI)-induced cytotoxicity was determined as described in section 2.11. Results are presented as mean  $\pm$  SEM of three independent experiments. Experimental data were analysed with the software GraphPad Prism 5.00, using the *one-way ANOVA* method followed by the *Bonferroni* multiple comparison test: \*\*,  $p < 0.01$ ; \*\*\*,  $p < 0.001$ , in comparison with control; #,  $p < 0.05$ , in comparison with 1  $\mu\text{M}$  Cr(VI).

To establish the exposure regimen to heat shock that would be used in subsequent experiments, the magnitude of the inhibitory effect on proliferation produced by acute heat shocks of different durations was determined.

As can be appreciated in Figure 3.12, heat shock caused a time-dependent decrease on cell proliferation (7, 18 and 44% for heat shocks of 15, 30 and 60 min, respectively). This decrease was statistically significant only for the 30 and 60 min heat shocks. In one experiment, we have also assessed the effects of a 2 h heat shock, but, in this case, the number of cells 24 h after the heat shock was lower than the number of cells immediately before the heat shock (Results not shown), indicating severe cytotoxicity.

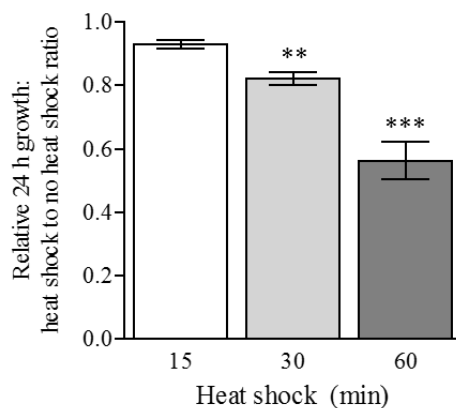


**Figure 3.12 | Effects of a 15, 30 or 60 min heat shock on the proliferation of BEAS-2B cells.** Heat shock assays were performed as described in section 2.12. Results are presented as mean  $\pm$  SEM of three independent experiments. Experimental data were analysed with the software GraphPad Prism 5.00, using the *one-way ANOVA* method followed by the *Dunnet's* multiple comparison test: \*\*,  $p < 0.01$ ; \*\*\*,  $p < 0.001$ .

The inhibitory effect on proliferation observed with the 60 min heat shock was similar to that induced by the cold shock conditions used in our previous studies. Thus, we opted for using a 60 min heat shock to study the effects of Cr(VI) on the proliferation of cells subjected to an acute heat shock.

### **3.2.2. Effects of Cr(VI) on the proliferation of BEAS-2B cells subjected to an acute heat shock**

Analysis of the results obtained for the relative growth of BEAS-2B cells subjected to an acute heat shock after treatment with 1  $\mu$ M Cr(VI) reveals that Cr(VI) conferred some resistance against the inhibitory effect on proliferation produced by the acute heat shock (Figure 3.13). In fact, whereas for control cells there was a 46% inhibition of proliferation, for Cr(VI)-exposed cells this inhibition was reduced to 38%. The difference between the two values, although not very pronounced, was statistically significant and consistently observed in all three independent experiments performed.

This result is in line with the one obtained in our laboratory while studying the effects of an acute cold shock [217, 218]. Thus, taken together, our results clearly suggest that Cr(VI) confers some resistance against acute thermal shocks. It is, therefore, tempting

to speculate that Cr(VI) might also confer some resistance to further stresses, namely those encountered during neoplastic transformation.

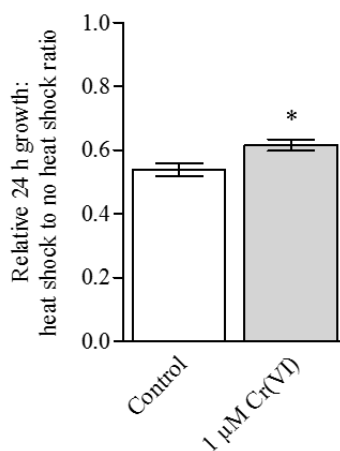


**Figure 3.13 | Exposure of BEAS-2B cells to 1  $\mu$ M Cr(VI) confers resistance against the inhibition of proliferation produced by an acute heat shock (1 h at 43  $^{\circ}$ C).** Heat shock assays were performed as described in section 2.12. Results are presented as mean  $\pm$  SEM of three independent experiments. Experimental data were analysed with the software GraphPad Prism 5.00, using the *t-student paired* test: \*,  $p < 0.05$ .

### 3.2.3. Effects of an acute heat shock on the energy status of BEAS-2B cells pre-incubated with Cr(VI)

As the major cellular energy currency, ATP is essential for cellular proliferation and survival. It is, thus, possible that a reduction of ATP levels might contribute to the inhibitory effect on proliferation produced by acute heat shocks. In agreement with this hypothesis, decreases in the intracellular ATP levels after heat shocks, concomitantly with reductions in cell proliferation, were observed in lower organisms, such as fungi [219] and protozoans [220], in mammalian cells in culture, namely rat thymocytes [221] and lymphoblasts [222], human peripheral lymphocytes [223] and leukaemia cells [224], and in *in vivo* mouse models [225-227]. However, there are also studies, specially in mammalian cells in culture, where no changes in the intracellular ATP levels after heat shock were observed [222, 228-230]. Overall, these results indicate that heat-induced variations in the intracellular ATP content might be highly dependent on the type of model system and heat shock-induction protocol used.

If heat shock does produce a negative effect on the energy status of our model system, it would be interesting to investigate whether Cr(VI) treatment might also

modulate this impact. Within this context, it is interesting to note that Cr(VI) has been shown to impact several aspects of mammalian cell bioenergetics, namely the cellular energy status, with decreases in the energy charge and ATP levels, and increases in ADP and AMP levels being reported in a variety of model systems [36]. Thus, we hypothesized that Cr(VI)-exposed cells could be somehow adapted to this metabolic stress and would, therefore, be less affected by the effects of the subsequent heat shock. This would help to explain the resistance conferred by Cr(VI) against the inhibitory effect on proliferation produced by the acute heat shock.

Figure 3.14 shows the impact of acute heat shocks on the intracellular levels of ATP, adenosine diphosphate (ADP), adenosine monophosphate (AMP) and on the energy charge. This latter parameter is one of the indexes used to measure the cellular energy status [45, 231]. Our results show some slight decreases in the intracellular levels of adenine nucleotides, although these were generally not statistically significant and did not show a consistent pattern in terms of time-dependency of the effects (Figure 3.14). The only statistically significant alterations observed were those induced by a 30 min heat shock on the levels of ADP (Figure 3.14B) and AMP (Figure 3.14C), but the same trend was not observed for the ATP levels (Figure 3.14A). Significantly, the energy charge remained essentially unaltered in all conditions tested (Figure 3.14D).

Although these results indicated a more pronounced effect of the 30 min heat shock on the cellular energy status, as the differences between the 30 min and 60 min heat shock were not very significant and we had previously used a 60 min heat shock to evaluate the effects of Cr(VI) on proliferation, we opted for using again the latter duration to investigate our hypothesis that Cr(VI)-exposed cells could be somehow adapted to this metabolic stress.

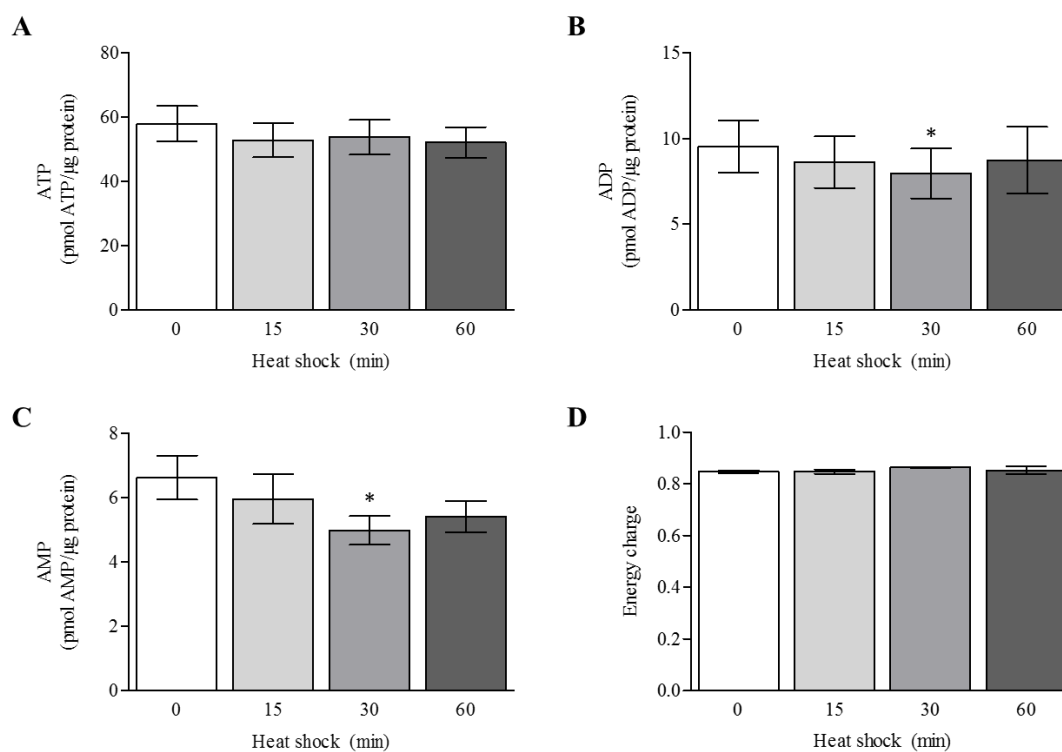


**Figure 3.14 | Effects of a 15, 30 or 60 min heat shock on the energy status of BEAS-2B cells.** Intracellular adenine nucleotides (A, B and C) were quantified by RP-HPLC, as described in section 2.13. The results were normalized to total protein levels, which were determined by the Bradford method (section 2.14). From the values obtained, the energy charge (D) was calculated according to Atkinson's equation (section 1.1.3). Results are presented as mean  $\pm$  SEM of three independent experiments. Experimental data were analysed with the software GraphPad Prism 5.00, using the *one-way ANOVA* method followed by the *Dunnet's* multiple comparison test: \*,  $p < 0.05$ .

In agreement with previous reports in the literature [36], exposure to Cr(VI) alone caused a decrease in the energy charge and in the ATP levels, as well as an increase in the levels of ADP and AMP (Results not shown). Of these changes, only the energy charge decrease had statistical significance. Contrary to what we hypothesized, pre-incubating cells with Cr(VI) did not protect against the negative effects of heat shock on the cellular energy status (Figure 3.15). In fact, the slight decreases in the adenine nucleotide levels were observed both in control and Cr(VI)-treated cells (Figure 3.15A) and were not translated to differences in the energy charge (Figure 3.15B). Thus, modulation of the cellular energy status of BEAS-2B cells does not seem to be the key to explain the Cr(VI)-conferred resistance against acute heat shocks.

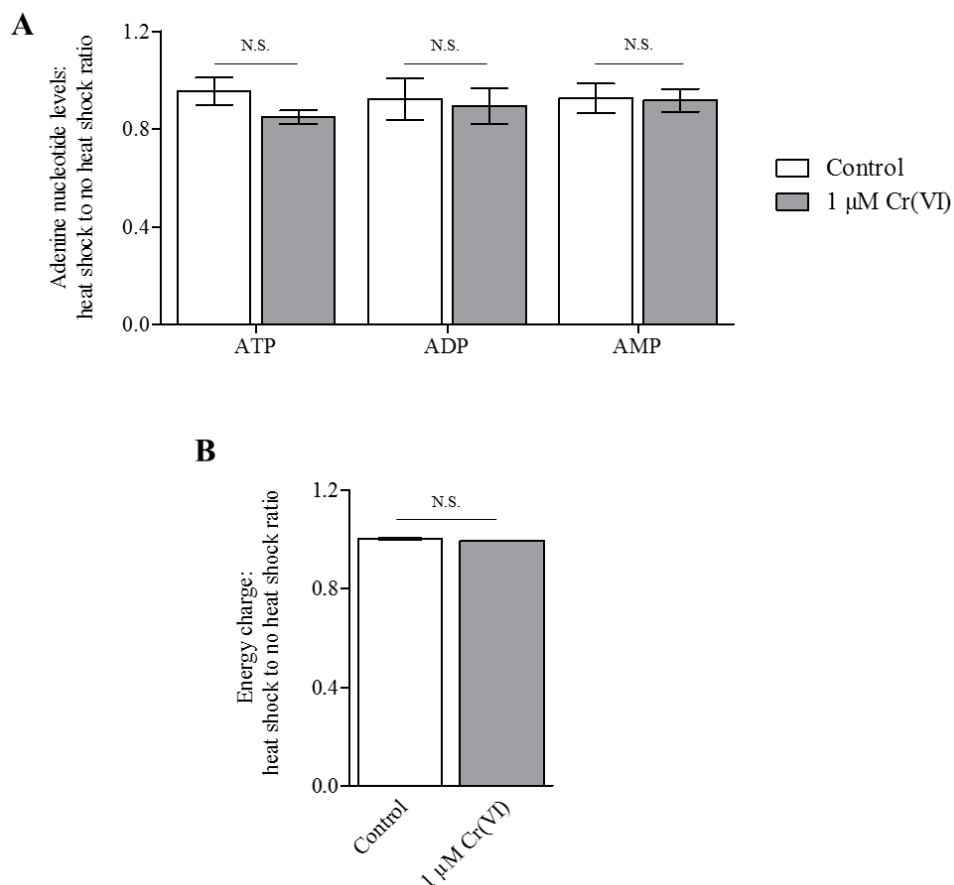


**Figure 3.15 | Effects of an acute heat shock on the energy status of BEAS-2B cells pre-incubated or not pre-incubated with Cr(VI).** Intracellular adenine nucleotides (A) were quantified by RP-HPLC, as described in section 2.13. The results were normalized to total protein levels, which were determined by the Bradford method (section 2.14). From the values obtained, the energy charge (B) was calculated according to Atkinson's equation (section 1.1.3). Results are presented as mean  $\pm$  SEM of three independent experiments. Experimental data were analysed with the software GraphPad Prism 5.00, using the *t-student paired* test. No statistically significant differences were observed. N.S., not significant.

### 3.2.4. Effects of Cr(VI) on the expression of key components of the stress response

Some reports of Cr(VI)-induced modulation of components of the stress response (section 1.2.3.1) suggest that Cr(VI) exposure might trigger this response. Thus, we hypothesized that the resistance conferred by Cr(VI) against acute thermal shocks could be the result of an activation of this ubiquitous cellular response to stress and set out to investigate the effects of a 48 h exposure to 1  $\mu$ M Cr(VI) on the expression of three of its

key components that have also been strongly implicated in carcinogenesis: Hsp90 $\alpha$ , Hsp72 and HSF1.

Inspection of Figure 3.16 shows that, at the protein level, Cr(VI) caused a significant decrease (ca. 60%) in the expression of Hsp90 $\alpha$ , while it had essentially no effect in the expression of Hsp72. The levels of HSF1 were extremely low, making their determination more difficult. As a consequence, only two of the experiments performed produced convincing results and these suggested that the levels of this transcription factor slightly decreased upon exposure to Cr(VI) (ca. 15%).

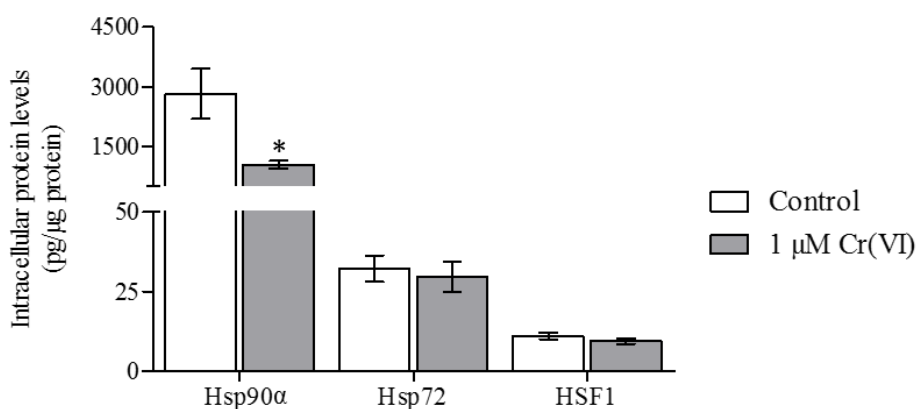


**Figure 3.16 | Effects of a 48 h exposure of BEAS-2B cells to 1  $\mu$ M Cr(VI) on the levels of Hsp90 $\alpha$ , Hsp72 and HSF1, three key components of the stress response.** Individual protein levels were determined using commercially available ELISA kits, as described in section 2.15. The results were normalized to total protein levels, which were determined by the Bradford method (section 2.14). Results are presented as mean  $\pm$  SEM of six independent experiments in the case of Hsp90 $\alpha$ , five in the case of Hsp72 and two in the case of HSF1. Experimental data were analysed with the software GraphPad Prism 5.00, using the *t-student paired* test: \*,  $p < 0.05$ .

The results obtained do not necessarily indicate that the heat shock response was not activated upon Cr(VI) exposure. For instance, it is possible that the protein levels of Hsp90 $\alpha$  and Hsp72 were initially increased and then decreased back to their basal levels (Hsp72) or even lowered levels (Hsp90 $\alpha$ ). As to HSF1, considering that it is a transcription factor, its activity might be mainly regulated at the post-translational level, for instance through phosphorylation (section 1.2.1.3), rather than at the translational level. Thus, many more studies, namely evaluation of the time course of the effect of Cr(VI) on the expression of these proteins and determination of the levels of phosphorylated HSF1, will be required to determine whether there is or not a correlation

between the capacity of Cr(VI) to modulate the stress response and to confer resistance against acute thermal shocks.

Of note, the observed decrease in Hsp90 $\alpha$  levels upon exposure to Cr(VI) was in line with earlier reports of decreased Hsp90 levels in primary cultures of rat granulosa cells [138] and in a cell line derived from human embryonic hepatocytes [139] (Table 1.1). On the contrary, there are two studies reporting increased Hsp70 levels upon exposure to Cr(VI) [139, 140]. There is one additional study where decreased levels of the constitutive isoform, Hsp73, were reported [138]. These results suggest that the effect of Cr(VI) might be isoform-specific and also dependent on the system and exposure regimen used. To the best of our knowledge, there are no studies where the effect of Cr(VI) on the expression of HSF1 was evaluated.

None of the above mentioned studies investigated the molecular mechanisms underlying the observed Cr(VI)-induced alterations on the expression of Hsps. Considering the plethora of effects that Cr(VI) is known to induce as a consequence of its intracellular reduction, due to the capacity of the species generated in this process to interact with all types of biomolecules (section 1.1.2), clarifying with precision those molecular mechanisms will, in all likelihood, be a daunting task. Within this context, it is worth mentioning the known capacity of Cr(III) to form complexes with ATP. These Cr(III)-ATP complexes are structurally similar to Mg(II)-ATP complexes, the predominant form of intracellular ATP, and have been shown to behave as competitive inhibitors of some ATP-dependent enzymes [232-235]. Both Hsp90 $\alpha$  and Hsp72 are ATP-dependent and, thus, it is possible that Cr(VI) inhibits the activity of these proteins, regardless of the impact it might have in terms of protein levels. On the other hand, exposure to Cr(VI) could lead to the activation of HSF1 since, as discussed in section 1.2.1.3, it might promote the oxidation of the sulfhydryl groups of the two cysteine residues crucial for the trimerization and DNA-binding activity of this transcription factor. It would be important to address these questions in future investigations, in order to more clearly understand the impact that Cr(VI) has on these key components of the stress response.

To further characterize the effects of Cr(VI) on the expression of Hsp90 $\alpha$ , Hsp72 and HSF1, and try to obtain some insights on the mechanisms involved in the observed downregulation of Hsp90 $\alpha$ , the impact of the same exposure (i.e. 48 h exposure to 1  $\mu$ M Cr(VI)) on the levels of the corresponding mRNAs was also investigated in this study.

In contrast with our findings at the protein level, we observed that the mRNA levels of *HSP90AA1* and *HSF1*, which encode Hsp90 $\alpha$  and HSF1, respectively, remained unaltered, whereas those of *HSPA1A*, which encodes Hsp72, were decreased (Figure 3.17). These results are also in contrast with those reported in previous studies (Table 1.1). For instance, there was one study reporting reduced levels of *HSP90AA1* in BEAS-2B cells exposed to Cr(VI) [55]. Of note, even though the cellular system was the same, the exposure regimen used was different, both in terms of Cr(VI) concentration (10  $\mu$ M) and exposure time (4 h). This suggests that the effects of Cr(VI) on the expression of this mRNA might be concentration and/or time-dependent. Concerning *HSPA1A*, there is one study reporting an increase in the levels of this mRNA in two distinct human cell lines exposed to different Cr(VI) concentrations [143]. In addition, there is also one study where increased levels of the mRNA encoding the rat inducible Hsp70 were observed in rat lung tissue [144]. Another study reported that no alterations were observed in the mRNA levels of *HSP-70*, but the authors did not identify the specific mRNA studied [145].

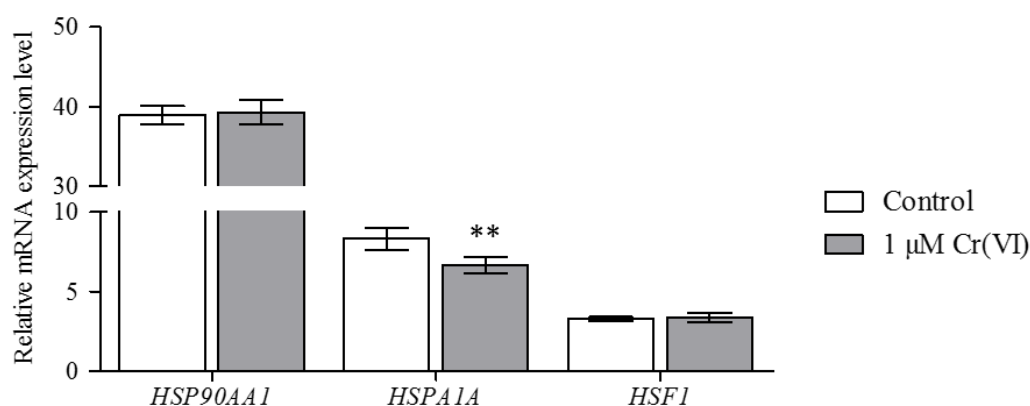


**Figure 3.17 | Effects of a 48 h exposure of BEAS-2B cells to 1  $\mu$ M Cr(VI) on the relative mRNA levels of *HSP90AA1*, *HSPA1A* and *HSF1*, which encode three key components of the stress response.** Individual mRNA levels were determined by RT-qPCR, as described in section 2.16. The results were normalized to the mRNA levels of *YWHAZ* and *PI4KB* and are presented as mean  $\pm$  SEM of four independent experiments. Experimental data were analysed with the software GraphPad Prism 5.00, using the *t-student paired* test: \*\*,  $p < 0.01$ . Gene symbols: *HSP90AA1*, heat shock 90 kDa protein 1 alpha; *HSPA1A*, heat shock 72 kDa protein; *HSF1*, heat shock factor 1.

The observation of contrasting results between protein and mRNA levels should not constitute a surprise. In fact, even though many investigators continue to use mRNA levels as indicators of the levels and activities of proteins, it has been reported that these

parameters generally show correlation coefficients of only  $\sim 0.4$ , meaning that only  $\sim 40\%$  of the variation in protein levels can be explained by variations in the respective mRNA levels [236]. The lack of a stronger correlation is attributed to the extensive regulation that occurs at the post-transcriptional, translational and post-translational levels. For instance, an increased translation rate, in Cr(VI)-treated cells, could explain the absence of differences in Hsp72 protein levels, when the levels of the corresponding mRNA were significantly decreased.

### **3.2.5. Effects of Cr(VI) on the mRNA levels of components of cancer-associated pathways related to the stress response**

In the context of the present work, we have also studied the effects of Cr(VI) exposure on the mRNA levels of some components of cancer-associated pathways that are somehow related to the stress response. Specifically, we determined the levels of the mRNAs encoding the proteins ATM, ATR and BRCA1, which have key roles in the DNA damage response, and the transcription factors p53 and c-Myc, generally regarded as major orchestrators of carcinogenesis. The expressions of ATM and ATR have been shown to be modulated by Hsp90 inhibitors, suggesting that Hsp90 plays a role in the stabilization of these proteins and/or of some of their upstream regulators [237, 238]. BRCA1 is one of the client proteins of Hsp90, and loss of Hsp90 function was reported to abolish BRCA1-dependent DNA DSB repair [239]. The chaperone activity of Hsp90 has also an important role in the stabilization of p53 and in the regulation of its transcriptional activity [92, 93]. Both ATR and p53 were shown to form complexes with HSF1 and both complexes modulate the transcriptional activity of p53 in response to DNA damage [240]. In addition, it was suggested that HSF1 is required for p53 nuclear translocation [241]. Finally, p53 and c-Myc have been shown to regulate the expression of some Hsps through modulation of the activity of the promoters of the genes that encode them; p53 represses the promoters, while c-Myc stimulates their activity [98] (section 1.2.1).

As can be appreciated in Figure 3.18, statistically significant differences, between control and Cr(VI)-exposed cells, were only observed in the levels *ATM* and *ATR*, with the first being downregulated and the second upregulated. The effects of Cr(VI) on ATM and ATR have been previously studied, but always in terms of the impact of this metal in

the activation of these proteins, which corresponds to their phosphorylation. All the studies so far have consistently reported an activation of both ATM and ATR, although the two proteins seem to respond differently to distinct Cr(VI) concentrations [7] (section 3.1.1). Our results suggest that Cr(VI) has an impact on these two kinases and, in future studies, it would be interesting to investigate if, with the conditions used in this study, Cr(VI) also affects the levels and/or activities of these proteins.

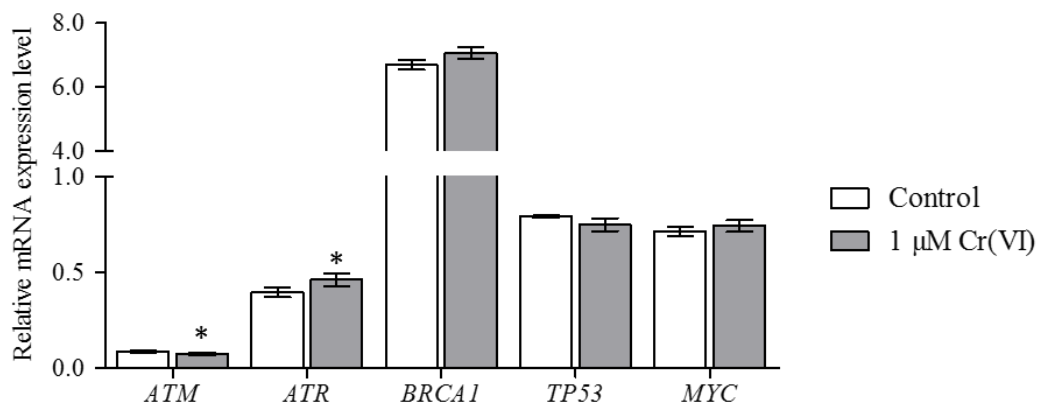


**Figure 3.18 | Effects of a 48 h exposure of BEAS-2B cells to 1  $\mu$ M Cr(VI) on the relative mRNA levels of *ATM*, *ATR*, *BRCA1*, *TP53* and *MYC*, components of cancer-associated pathways somehow related to the stress response.** Individual mRNA levels were determined by RT-qPCR, as described in section 2.16. The results were normalized to the mRNA levels of *YWHAZ* and *PI4KB* and are presented as mean  $\pm$  SEM of four independent experiments. Experimental data were analysed with the software GraphPad Prism 5.00, using the *t-student paired* test: \*,  $p < 0.05$ . Gene symbols: *ATM*, ataxia telangiectasia mutated; *ATR*, ataxia telangiectasia and Rad3-related protein; *BRCA1*, breast cancer 1 susceptibility protein; *TP53*, tumour protein p53; *MYC*, v-Myc avian myelocytomatosis viral oncogene homolog.

Considering our previously presented results on the impact of Cr(VI) in the levels of Hsp90 $\alpha$ , it is interesting to note that there is one report where an increase in the mRNA levels of *ATR* was observed after treatment of a diffuse B large cell lymphoma (DBLCL) cell line with an Hsp90 inhibitor [237]. In this cell line, Hsp90 was shown to complex with the transcriptional repressor BCL-6, whose target genes include *ATR* and *TP53*, promoting its stabilization. Upon Hsp90 inhibition, BCL-6 was no longer stabilized and its transcriptional targets were derepressed, leading to the increase in the mRNA levels of *ATR* and also of *TP53*. In the present study, we have observed a decrease in Hsp90 $\alpha$  levels after Cr(VI) exposure and, even though a decrease in the levels of a protein is not equivalent to its inhibition, the reduction in the pool of Hsp90 $\alpha$  will likely result in some destabilization in a fraction of its client proteins. The fact that we did not observe a similar

increase in the mRNA levels of *TP53* suggests that either there are more prevalent mechanisms regulating its transcription in our cells, or this BCL-6 destabilization mechanism is not relevant in our cells, and there is a different mechanism underlying the observed upregulation of *ATR*.

In terms of the effects of Cr(VI) on the expression of the other mRNAs tested in this study, the information found in the literature is quite sparse and not always very consistent. The effects on *BRCA1* were investigated in only one *in vivo* study, and an increased expression was reported in rat duodenal and jejunal cells [242]. Contrasting results were obtained in the two studies where the effect of Cr(VI) on *TP53* was evaluated. One *in vivo* study reported a decrease in the expression of *TP53* in rat stomach and colon cells [243], whereas an increase was observed in BEAS-2B cells [58]. Interestingly, at the protein level, both studies reported a decrease of p53. On the other hand, there are three studies reporting increased levels of p53 upon Cr(VI)-exposure [40, 244, 245], and one where no alterations were observed in two different cell lines [246]. Inconsistent results were also obtained in studies investigating the impact of Cr(VI) on *MYC* expression. Increases on *MYC* expression were observed *in vitro* in 10T1/2 mouse embryo fibroblasts [247] and in the malignant RenG2 cells [59] and *in vivo* in rat stomach and colon cells [243]. Interestingly, in the parental cell line of the malignant RenG2 cell strain, the BEAS-2B cell line, there are reports of both decreased *MYC* expression [55] and random variation over nine weeks of exposure [59]. Overall, the effects of Cr(VI) on these components of cancer-associated pathways seem to be strongly dependent on the model system and exposure regimen used. Although, in the present study, no Cr(VI)-induced alterations in the mRNA levels of these components were detected, it might be interesting to investigate whether there is an impact in levels and/or activities of the corresponding proteins. This might be particularly important for p53 and c-Myc, since, as previously discussed, these proteins are involved in the regulation of the expression of Hsps. Thus, alterations in their levels and/or activities could shed some light on the mechanisms underlying the alterations in the levels of Hsp90 $\alpha$  and *HSPA1A* mRNA observed in this study (section 3.2.4).

### **3.3. Effects of a long-term exposure to Cr(VI) on the genomic stability and morphology of BEAS-2B cells**

As discussed in section 1.3.1, the studies investigating the presence of CIN in Cr(VI)-exposed cells are still scarce and somewhat contradictory. In fact, while the group of Wise, along with other groups, reported significant inductions of numerical CIN after short-term exposures (24 to 120 h) to Cr(VI), our group did not observe Cr(VI)-induced karyotypic alterations during approximately 17 weeks of exposure of BEAS-2B cells to this agent [59]. These contradictions are, at least partially, accounted for differences in the model systems and exposure regimens used. For instance, in many studies of the other groups, fibroblasts were used as model systems, while we used epithelial cells and the uptake and intracellular metabolism of Cr(VI) might be different depending on the type of cell. Cr(VI) uptake is also dependent on the solubility of the compound used. In fact, soluble Cr(VI) compounds, such as potassium dichromate, which is used by our group, can be readily taken up by the cells, while particulate Cr(VI) compounds, such as zinc and lead chromate, which are normally used by the group of Wise, have to be extracellularly dissolved to release the soluble Cr(VI) oxyanion and, thus, persist for longer times in culture.

In this study, the effects of Cr(VI) on the chromosomal complement of BEAS-2B cells were evaluated by conventional cytogenetics, as in our previous study, but the duration of the exposure was significantly prolonged with the intent of more closely mimicking the chronic exposures that occur in occupational settings. Specifically, the impact of a 8 month exposure to 1  $\mu$ M Cr(VI) was investigated. As can be appreciated in Table 3.3 and Figure 3.19, no Cr(VI)-induced chromosomal alterations could be detected with the technique used. In fact, all chromosomal alterations, relative to the reference human karyotype, observed in Cr(VI)-exposed cells were also present, in similar frequencies, in the non-exposed counterparts, which were always maintained and processed in parallel. The cells analysed in this study were, according to the classification presented in section 3.1.3, in the transitional stage and presented all the eleven structural and three numerical alterations previously described. The frequencies of three alterations (14p<sup>+</sup>, 18q<sup>-</sup> and tri(20)) differed by more than 10% between the control and Cr(VI)-treated cultures, but, since the number of metaphases analysed was rather small (17 metaphases

for control cells and 16 for Cr(VI)-exposed cells), the biological relevance of these differences is questionable.

**Table 3.3 | Chromosomal alterations observed in BEAS-2B cells grown, for 8 months, in the absence or the presence of 1  $\mu$ M Cr(VI).**

Chromosomal alteration	Incidence	
	Control	1 $\mu$ M Cr(VI)
4p <sup>-</sup>	+++	+++
4p <sup>+</sup>	-	-
i(5)(q10)	++	++
der(5;9)	++	++
der(5;15)	++	++
14p <sup>+</sup>	+	-
15p <sup>+</sup>	++	++
der(16;17)	+++	+++
18q <sup>-</sup>	++	++
22p <sup>+</sup>	+++	+++
tri(20)	-	-
mono(20)	++	++
Xp <sup>-</sup>	++	++
-Y	++	++

Incidence of the chromosomal alterations: -, chromosomal alteration present in less than 15% of the metaphases analysed; +, chromosomal alteration present in 15 to 40% of the metaphases analysed; ++, chromosomal alteration present in 40 to 80% of the metaphases analysed; + + +, chromosomal alteration present in more than 80% of the metaphases analysed. Number of metaphases analysed: Control – 17 metaphases; Cr(VI)-exposed cells [1  $\mu$ M Cr(VI)] – 16 metaphases. Metaphase spreads were obtained as described in section 2.9. and the karyotypes constructed using the Applied Imaging<sup>®</sup> CytoVision<sup>®</sup> software. 4p<sup>-</sup> and Xp<sup>-</sup>, terminal deletion of the short arm of the respective chromosomes; 4p<sup>+</sup>, 14p<sup>+</sup>, 15p<sup>+</sup>, 22p<sup>+</sup>, additional material of unknown origin on the short arm of the respective chromosomes; i(5)(q10), isochromosome 5; der(5;9), derivative of the long arm of chromosome 5 with the long arm of the chromosome 9; der(5;15), derivative of the long arm of chromosome 5 with the long arm of the chromosome 15; der(16;17), derivative of the long arm of chromosome 16 with the long arm of the chromosome 17; 18q<sup>-</sup>, terminal deletion of the long arm of chromosome 18; tri(20), trisomy of chromosome 20; mono(20), monosomy of chromosome 20; -Y, loss of chromosome Y.

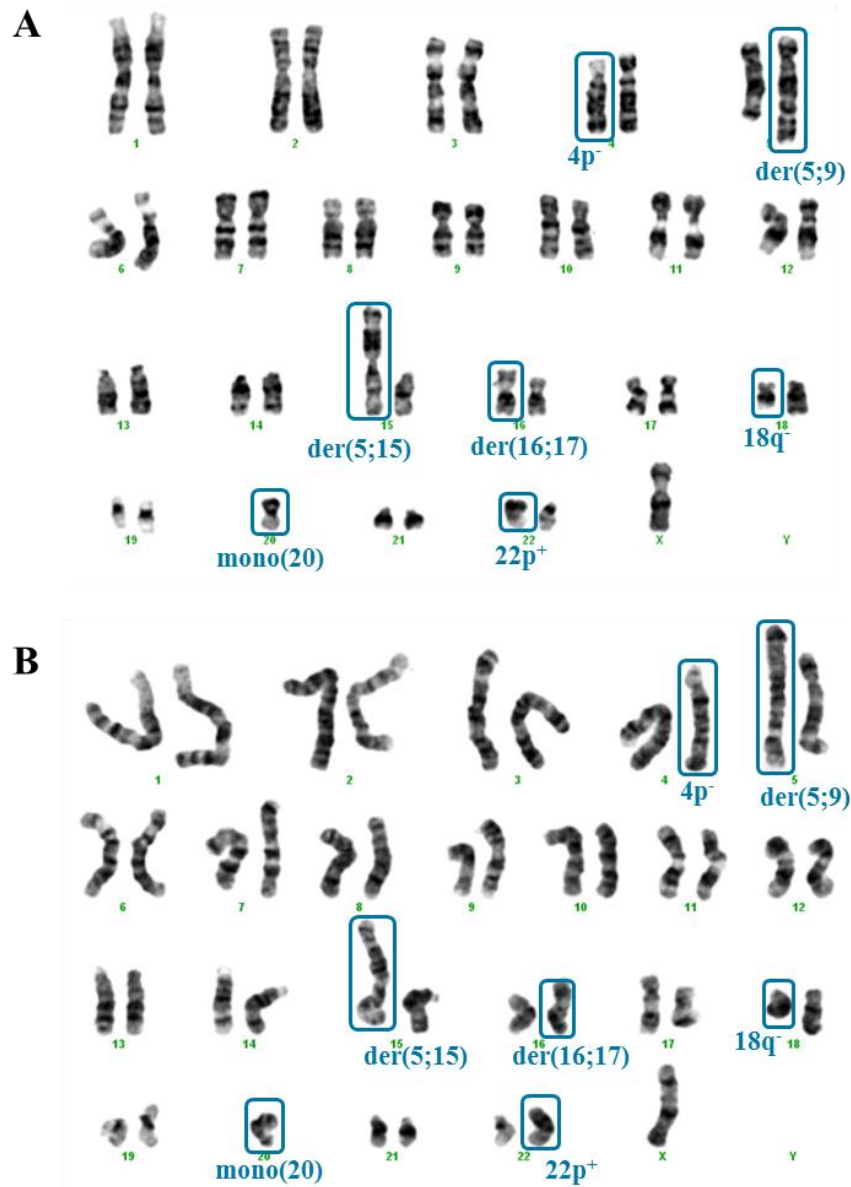


**Figure 3.19 | Representative G-banded karyotypes of BEAS-2B cells grown, for 8 months, in the (A) absence or in the (B) presence of 1  $\mu$ M Cr(VI). Metaphase spreads were obtained as described in section 2.9 and the karyotypes constructed using the Applied Imaging<sup>®</sup> CytoVision<sup>®</sup> software. 4p<sup>-</sup>, terminal deletion of the short arm of the chromosome; der(5;9), derivative of the long arm of chromosome 5 with the long arm of the chromosome 9; der(5;15), derivative of the long arm of chromosome 5 with the long arm of the chromosome 15; der(16;17), derivative of the long arm of chromosome 16 with the long arm of the chromosome 17; 18q<sup>-</sup>, terminal deletion of the long arm of chromosome 18; mono(20), monosomy of chromosome 20; 22p<sup>+</sup>, additional material of unknown origin on the short arm of chromosome 22.**

At first sight, the absence of Cr(VI)-induced alterations after such prolonged exposure might seem rather unexpected, considering the recognized genotoxic potential of Cr(VI) and the aforementioned observations by some groups indicating its capacity to induce aneuploidy. However, several aspects should be taken into consideration. First of all, apart from numerical alterations, conventional cytogenetic banding methods can only reliably detect structural alterations, such as deletions or duplications, that involve more than 10 megabases (Mb) of DNA [248]. Thus, the identification of potential submicroscopic structural alterations induced by Cr(VI) would require the use of more advanced molecular cytogenetic techniques, such as fluorescent *in situ* hybridization (FISH) or, for an even higher resolution (in the range of kilobases (kb)), comparative genome hybridization array (aCGH), which is currently the most powerful molecular cytogenetic technique [248, 249]. In addition, it must be stressed that the cells used in this study were at a critical phase of their karyotypic evolution (section 3.1.3), which might have masked potential Cr(VI) effects. It is also important to note that, as previously discussed, both the model system and the exposure regimen used in this study greatly differ from those used in the investigations of other groups.

It is generally accepted that alterations in cell morphology and pattern of growth are indicative of pre-neoplastic transformation. Thus, to try to correlate potential chromosomal alterations with pre-neoplastic transformation, we monitored, throughout the long term exposure, the morphology and growth pattern of Cr(VI)-treated cultures and of control cultures established and maintained in parallel. As can be appreciated in Figure 3.20, even after 10 months of continuous exposure, no Cr(VI)-induced changes in these parameters were observed. In fact, the alterations in the morphology and growth pattern observed in Cr(VI)-treated cultures were the same as those that occurred in control cultures over time in culture, and that have been discussed in section 3.1.3.

These results are not in agreement with previous reports, from our and other groups, indicating that Cr(VI)-treated cells present some characteristics of cells that undergo neoplastic transformation, such as altered morphology, loss of cell contact inhibition and growth in foci [46, 59, 179, 250]. Moreover, in some cases, cells derived from the obtained foci were shown capable of growing in an anchorage-independent manner, further confirming neoplastic transformation. Once more, it is likely that differences in the model system and exposure regimen account for the discrepancies between the results obtained in this study and those previous reports. For instance, the

culturing conditions used in the present study differ from those of the previous studies from our group reporting Cr(VI)-induced morphological alterations in two key aspects: the initial cell density and the type of culture medium used. In the present study, cells were seeded at 2000 cells/cm<sup>2</sup> and cultured in LHC-9, while in the other studies the initial seeding density was 4000 cells/cm<sup>2</sup> and the culture medium was BEGM [46, 59]. The use of different culture media might be particularly relevant taking into account our observation that the medium seems to play a role in cell adhesion to the substrate (section 3.1.1).

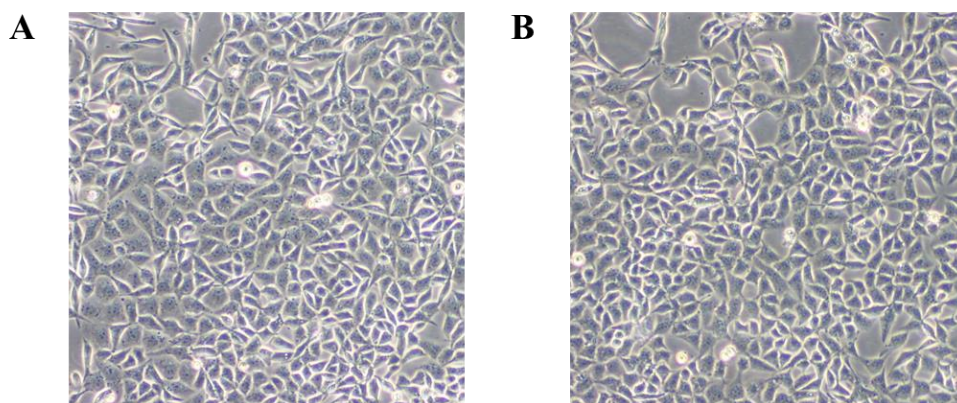


**Figure 3.20 | Effects of a 10 month exposure to 1  $\mu$ M Cr(VI) on the morphology and pattern of growth of BEAS-2B cells.** Representative micrographs (100 $\times$  magnification) of BEAS-2B cells, at passage 55, from (A) control cultures and (B) Cr(VI)-treated cultures. Cells were cultured in FNT(-) coated flasks, in LHC-9.

Taken together, the results presented in this section suggest that the exposure regimen used might not have been sufficient to induce the early stages of neoplastic transformation. Considering that our regimen included only a weekly addition of soluble Cr(VI), which is rapidly taken up by the cells, and that we have only assessed the effects of up to 10 months of exposure, while the chromate workers are subjected to a daily exposure for years in a row to particulate Cr(VI), it might be necessary to increase the number of cell treatments *per* week and/or to prolong the exposure period, in order to more closely mimic the conditions that lead to the development of Cr(VI)-induced carcinogenesis *in vivo*.



## **4. Conclusions and Future Perspectives**

---



Activation of the stress response and genomic instability have been frequently observed in cancer cells and proposed to have important roles in cancer development and progression. Within the context of Cr(VI)-induced carcinogenesis, little is known about the role that they might play. Concerning genomic instability, the studies investigating its presence in Cr(VI)-exposed cells are still scarce and somewhat contradictory. As for the stress response, some reports indicate that Cr(VI) might modulate the expression and/or activity of some of its components, but the relevance of these alterations for Cr(VI)-induced malignization have not been investigated. To gain further insight on these topics, the effects of a short-term exposure to Cr(VI) on the stress response and of a long-term exposure on genomic stability were investigated in the present study.

In all experiments performed the BEAS-2B cell line was used. This cell line was chosen as the cellular model for being representative of the human bronchial epithelium, which is the main *in vivo* target of Cr(VI) carcinogenicity. Initially, the impact of the culturing conditions and culture age on the growth characteristics and genomic instability of this cell line cell line was investigated. The results obtained showed that all modifications of the culturing conditions tested induced some alterations to the morphology and growth pattern of the cells. Changing the culture medium and/or the composition of the coating solution led to cumulative but rather subtle changes on these parameters, but did not alter the cellular growth rate. The growth medium also had a significant effect on cell attachment to no-coated surfaces. Growth of BEAS-2B cells in the presence of FBS induced profound alterations to the morphology and pattern of growth, but, apparently, did not inhibit cellular proliferation. The culture age also had a significant impact on the morphology, growth pattern and chromosomal complement of BEAS-2B cells. This observation indicates that the results from long-term studies with these cells have to be interpreted with great care.

A short-term exposure to a not-overly cytotoxic concentration of Cr(VI) conferred a certain resistance against the inhibitory effect on proliferation produced by an acute heat shock. This shock also had some negative effects on the cellular energy status, which might have contributed to the inhibitory effect on proliferation, but Cr(VI) did not protect against them. Apparently, the observed resistance was also not acquired through elevated protein levels of the components of the stress response evaluated in this study, Hsp90 $\alpha$ , Hsp72 and HSF1, since the only significant Cr(VI)-induced effect observed was a decrease in the levels of Hsp90 $\alpha$ . The levels of the corresponding mRNAs were also

evaluated and Cr(VI) induced a decrease in the levels of *HSPA1A*. In this study, the impact of Cr(VI) exposure on the mRNA levels of some components of cancer-related pathways also associated with the stress response were evaluated. The results obtained suggest that Cr(VI) might interfere with two key components of the DNA damage response, the kinases ATM and ATR, since the mRNA levels of *ATM* were found to be decrease in Cr(VI)-treated cells, while those of *ATR* were increased.

A long-term exposure, for over 8 months, to Cr(VI) did not induced chromosomal alterations that could be detected through conventional cytogenetics nor morphological alterations. These results suggest that the exposure regimen used was not sufficient to trigger neoplastic transformation.

It is important to note that research work presented in this dissertation was essentially a preliminary investigation and much more studies will be required to definitely establish the role played by alterations on the stress response and by genomic instability on Cr(VI)-induced carcinogenesis. In a first approach it would be important to perform some experiments that would allow a better understanding of the results obtained in this investigation. For instance, to determine whether there is or not a correlation between the capacity of Cr(VI) to modulate the stress response and to confer resistance against acute thermal shocks, the time course of the effect of Cr(VI) on the expression of the components of the stress response evaluated in this study should be investigated. It would be equally important to evaluate if Cr(VI) has the capacity to interfere with the activity of these proteins.

Concerning the effects of Cr(VI) on genomic stability, molecular cytogenetic techniques should be used to assess if, with the exposure regimen used in this study, Cr(VI) induced some submicroscopic structural chromosomal alterations. This analysis could reveal that the expression of some key cancer-related genes is altered, what would help to understand the molecular mechanisms underlying Cr(VI)-induced carcinogenesis. Molecular cytogenetic techniques should also be used to complete the cytogenetic characterization of the BEAS-2B cell line, since the nature of some chromosomal alterations could not be determined by conventional cytogenetics. With a complete cytogenetic characterization it will be easier to determine which phenotypic consequences can arise from the alterations observed at the karyotypic level, and evaluate the suitability of this cell line to be used in different experimental contexts.

Following these clarifications, several other aspects would worth investigation. Starting with the model system, it would be interesting to evaluate how the culturing

conditions might affect the sensitivity of BEAS-2B cells to Cr(VI), as this might help to explain discrepant results obtained by different groups when using similar exposure regimens.

Considering our present and past results clearly indicating that Cr(VI) confers resistance to acute thermal shocks, which were used as models of induced cellular stress, it is tempting to speculate that Cr(VI)-exposed cells might also be resistant to other types of stress. It would be interesting to address this possibility in further studies, particularly using models of relevant stresses in the context of carcinogenesis, such as hypoxia or nutrient deprivation. To understand the role that Cr(VI)-induced alterations on the stress response might have in carcinogenesis, it would be important to characterize in more detail the capacity of Cr(VI) to modulate the expression of some of its components. In particular, it might be interesting, considering that in most cancer cells Hsp90 is overexpressed, to investigate whether the decrease in Hsp90 $\alpha$  observed in this study is only characteristic of a short-term exposure or if it is also observable in cells malignantly transformed by Cr(VI), such as the malignant RenG2 strain, and/or in model systems that more closely mimic the physiological situation, namely co-culture systems or *in vivo* models.

In studies concerning the effects of Cr(VI) on genomic stability it might be important to use exposure regimens that involve an increased number of cell treatments *per* week and/or a more prolonged exposure period, since in the occupational settings there is a daily exposure for years in a row to particulate Cr(VI).



# References

---



1. Barceloux DG: **Chromium.** *J Toxicol Clin Toxicol* 1999, **37**:173-194.
2. Newman D: **A case of adeno-carcinoma of the left inferior turbinated body, and perforation of the nasal septum, in the person of a worker in chrome pigments.** *Glasgow Med J* 1980, **33**:469-470.
3. Langard S: **One hundred years of chromium and cancer: a review of epidemiological evidence and selected case reports.** *Am J Ind Med* 1990, **17**:189-215.
4. NTP (National Toxicology Program): **Chromium hexavalent compounds.** *Report on Carcinogens, Thirteenth Edition* 2014.
5. **Chromium, nickel and welding.** *IARC Monogr Eval Carcinog Risks Hum* 1990, **49**:1-648.
6. De Flora S: **Threshold mechanisms and site specificity in chromium(VI) carcinogenesis.** *Carcinogenesis* 2000, **21**:533-541.
7. Urbano AM, Rodrigues CFD, Alpoim MC: **Hexavalent chromium exposure, genomic instability and lung cancer.** *Gene Ther Mol Biol* 2008, **12B**:219-238.
8. Kondo K, Hino N, Sasa M, Kamamura Y, Sakiyama S, Tsuyuguchi M, Hashimoto M, Uyama T, Monden Y: **Mutations of the p53 gene in human lung cancer from chromate-exposed workers.** *Biochem Biophys Res Commun* 1997, **239**:95-100.
9. Ewis AA, Kondo K, Lee J, Tsuyuguchi M, Hashimoto M, Yokose T, Mukai K, Kodama T, Shinka T, Monden Y, Nakahori Y: **Occupational cancer genetics: infrequent ras oncogenes point mutations in lung cancer samples from chromate workers.** *Am J Ind Med* 2001, **40**:92-97.
10. Kondo K, Takahashi Y, Hirose Y, Nagao T, Tsuyuguchi M, Hashimoto M, Ochiai A, Monden Y, Tangoku A: **The reduced expression and aberrant methylation of p16(INK4a) in chromate workers with lung cancer.** *Lung Cancer* 2006, **53**:295-302.
11. Takahashi Y, Kondo K, Hirose T, Nakagawa H, Tsuyuguchi M, Hashimoto M, Sano T, Ochiai A, Monden Y: **Microsatellite instability and protein expression of the DNA mismatch repair gene, hMLH1, of lung cancer in chromate-exposed workers.** *Mol Carcinog* 2005, **42**:150-158.
12. Hirose T, Kondo K, Takahashi Y, Ishikura H, Fujino H, Tsuyuguchi M, Hashimoto M, Yokose T, Mukai K, Kodama T, Monden Y: **Frequent microsatellite instability in lung cancer from chromate-exposed workers.** *Mol Carcinog* 2002, **33**:172-180.
13. Witt KL, Stout MD, Herbert RA, Travlos GS, Kissling GE, Collins BJ, Hooth MJ: **Mechanistic insights from the NTP studies of chromium.** *Toxicol Pathol* 2013, **41**:326-342.
14. Cohen MD, Kargacin B, Klein CB, Costa M: **Mechanisms of chromium carcinogenicity and toxicity.** *Crit Rev Toxicol* 1993, **23**:255-281.
15. Costa M: **Toxicity and carcinogenicity of Cr(VI) in animal models and humans.** *Crit Rev Toxicol* 1997, **27**:431-442.

16. Urbano AM, Ferreira LM, Alpoim MC: **Molecular and cellular mechanisms of hexavalent chromium-induced lung cancer: an updated perspective.** *Curr Drug Metab* 2012, **13**:284-305.
17. De Flora S, Camoirano A, Bagnasco M, Bennicelli C, Corbett GE, Kerger BD: **Estimates of the chromium(VI) reducing capacity in human body compartments as a mechanism for attenuating its potential toxicity and carcinogenicity.** *Carcinogenesis* 1997, **18**:531-537.
18. Ishikawa Y, Nakagawa K, Satoh Y, Kitagawa T, Sugano H, Hirano T, Tsuchiya E: **"Hot spots" of chromium accumulation at bifurcations of chromate workers' bronchi.** *Cancer Res* 1994, **54**:2342-2346.
19. Ishikawa Y, Nakagawa K, Satoh Y, Kitagawa T, Sugano H, Hirano T, Tsuchiya E: **Characteristics of chromate workers' cancers, chromium lung deposition and precancerous bronchial lesions: an autopsy study.** *Br J Cancer* 1994, **70**:160-166.
20. Salnikow K, Zhitkovich A: **Genetic and epigenetic mechanisms in metal carcinogenesis and cocarcinogenesis: nickel, arsenic, and chromium.** *Chem Res Toxicol* 2008, **21**:28-44.
21. Connett P, Wetterhahn K: **Metabolism of the carcinogen chromate by cellular constituents.** *Struct Bond* 1983, **54**: 93-124.
22. Stearns DM, Kennedy LJ, Courtney KD, Giangrande PH, Phieffer LS, Wetterhahn KE: **Reduction of chromium(VI) by ascorbate leads to chromium-DNA binding and DNA strand breaks in vitro.** *Biochemistry* 1995, **34**:910-919.
23. Standeven AM, Wetterhahn KE: **Ascorbate is the principal reductant of chromium (VI) in rat liver and kidney ultrafiltrates.** *Carcinogenesis* 1991, **12**:1733-1737.
24. Standeven AM, Wetterhahn KE: **Ascorbate is the principal reductant of chromium(VI) in rat lung ultrafiltrates and cytosols, and mediates chromium-DNA binding in vitro.** *Carcinogenesis* 1992, **13**:1319-1324.
25. Hanahan D, Weinberg RA: **The hallmarks of cancer.** *Cell* 2000, **100**:57-70.
26. Hanahan D, Weinberg RA: **Hallmarks of cancer: the next generation.** *Cell* 2011, **144**:646-674.
27. Pritchard DE, Ceryak S, Ramsey KE, O'Brien TJ, Ha L, Fornsaglio JL, Stephan DA, Patierno SR: **Resistance to apoptosis, increased growth potential, and altered gene expression in cells that survived genotoxic hexavalent chromium [Cr(VI)] exposure.** *Mol Cell Biochem* 2005, **279**:169-181.
28. Nickens KP, Han Y, Shandilya H, Larrimore A, Gerard GF, Kaldjian E, Patierno SR, Ceryak S: **Acquisition of mitochondrial dysregulation and resistance to mitochondrial-mediated apoptosis after genotoxic insult in normal human fibroblasts: a possible model for early stage carcinogenesis.** *Biochim Biophys Acta* 2012, **1823**:264-272.
29. Son YO, Pratheeshkumar P, Wang L, Wang X, Fan J, Kim DH, Lee JY, Zhang Z, Lee JC, Shi X: **Reactive oxygen species mediate Cr(VI)-induced**

- carcinogenesis through PI3K/AKT-dependent activation of GSK-3beta/beta-catenin signaling.** *Toxicol Appl Pharmacol* 2013, **271**:239-248.
30. Beaver LM, Stemmy EJ, Constant SL, Schwartz A, Little LG, Gigley JP, Chun G, Sugden KD, Ceryak SM, Patierno SR: **Lung injury, inflammation and Akt signaling following inhalation of particulate hexavalent chromium.** *Toxicol Appl Pharmacol* 2009, **235**:47-56.
  31. Beaver LM, Stemmy EJ, Schwartz AM, Damsker JM, Constant SL, Ceryak SM, Patierno SR: **Lung inflammation, injury, and proliferative response after repetitive particulate hexavalent chromium exposure.** *Environ Health Perspect* 2009, **117**:1896-1902.
  32. Tessier DM, Pascal LE: **Activation of MAP kinases by hexavalent chromium, manganese and nickel in human lung epithelial cells.** *Toxicol Lett* 2006, **167**:114-121.
  33. Wang BJ, Sheu HM, Guo YL, Lee YH, Lai CS, Pan MH, Wang YJ: **Hexavalent chromium induced ROS formation, Akt, NF-kappaB, and MAPK activation, and TNF-alpha and IL-1alpha production in keratinocytes.** *Toxicol Lett* 2010, **198**:216-224.
  34. Ding SZ, Yang YX, Li XL, Michelli-Rivera A, Han SY, Wang L, Pratheeshkumar P, Wang X, Lu J, Yin YQ, et al: **Epithelial-mesenchymal transition during oncogenic transformation induced by hexavalent chromium involves reactive oxygen species-dependent mechanism in lung epithelial cells.** *Toxicol Appl Pharmacol* 2013, **269**:61-71.
  35. He J, Qian X, Carpenter R, Xu Q, Wang L, Qi Y, Wang ZX, Liu LZ, Jiang BH: **Repression of miR-143 mediates Cr (VI)-induced tumor angiogenesis via IGF-IR/IRS1/ERK/IL-8 pathway.** *Toxicol Sci* 2013, **134**:26-38.
  36. Abreu PL, Ferreira LM, Alpoim MC, Urbano AM: **Impact of hexavalent chromium on mammalian cell bioenergetics: phenotypic changes, molecular basis and potential relevance to chromate-induced lung cancer.** *Biometals* 2014, **27**:409-443.
  37. Holmes AL, Wise SS, Wise JP, Sr.: **Carcinogenicity of hexavalent chromium.** *Indian J Med Res* 2008, **128**:353-372.
  38. Zhitkovich A: **Importance of chromium-DNA adducts in mutagenicity and toxicity of chromium(VI).** *Chem Res Toxicol* 2005, **18**:3-11.
  39. De Flora S, Bagnasco M, Serra D, Zancchi P: **Genotoxicity of chromium compounds. A review.** *Mutat Res* 1990, **238**:99-172.
  40. Lei T, He QY, Cai Z, Zhou Y, Wang YL, Si LS, Chiu JF: **Proteomic analysis of chromium cytotoxicity in cultured rat lung epithelial cells.** *Proteomics* 2008, **8**:2420-2429.
  41. Ye J, Shi X: **Gene expression profile in response to chromium-induced cell stress in A549 cells.** *Mol Cell Biochem* 2001, **222**:189-197.
  42. Myers CR: **The effects of chromium(VI) on the thioredoxin system: Implications for redox regulation.** *Free Radic Biol Med* 2012, **52**:2091-2107.

43. Galluzzi L, Kepp O, Vander Heiden MG, Kroemer G: **Metabolic targets for cancer therapy.** *Nat Rev Drug Discov* 2013, **12**:829-846.
44. Warburg O: *The metabolism of tumors.* London: Constable & Co. Ltd; 1930.
45. Atkinson DE: **The energy charge of the adenylate pool as a regulatory parameter. Interaction with feedback modifiers.** *Biochemistry* 1968, **7**:4030-4034.
46. Costa AN, Moreno V, Prieto MJ, Urbano AM, Alpoim MC: **Induction of morphological changes in BEAS-2B human bronchial epithelial cells following chronic sub-cytotoxic and mildly cytotoxic hexavalent chromium exposures.** *Mol Carcinog* 2010, **49**:582-591.
47. Cerveira JF, Sanchez-Arago M, Urbano AM, Cuezva JM: **Short-term exposure of nontumorigenic human bronchial epithelial cells to carcinogenic chromium(VI) compromises their respiratory capacity and alters their bioenergetic signature.** *FEBS Open Bio* 2014, **4**:594-601.
48. Ferreira LMR, Guiomar AJ, Santos MS, Alpoim MC, Urbano AM: **Impact of carcinogenic chromium(VI) on the energy metabolism of human bronchial epithelial cells.** *Acta Med Port* 2012, **Suppl. 1/2011**:P45.
49. Lindquist S: **The heat-shock response.** *Annu Rev Biochem* 1986, **55**:1151-1191.
50. Lechner J, LaVeck M: **A serum-free method for culturing normal human bronchial epithelial cells at clonal density.** *J Tissue Cult Methods* 1985, **9**:43-48.
51. Borthiry GR, Antholine WE, Myers JM, Myers CR: **Reductive activation of hexavalent chromium by human lung epithelial cells: generation of Cr(V) and Cr(V)-thiol species.** *J Inorg Biochem* 2008, **102**:1449-1462.
52. Lieber M, Todaro G, Smith B, Szakal A, Nelson-Rees W: **A continuous tumor-cell line from a human lung carcinoma with properties of type II alveolar epithelial cells.** *Int J Cancer* 1976, **17**:62-70.
53. Reddel RR, Ke Y, Gerwin BI, McMenamin MG, Lechner JF, Su RT, Brash DE, Park JB, Rhim JS, Harris CC: **Transformation of human bronchial epithelial cells by infection with SV40 or adenovirus-12 SV40 hybrid virus, or transfection via strontium phosphate coprecipitation with a plasmid containing SV40 early region genes.** *Cancer Res* 1988, **48**:1904-1909.
54. Adamou JE, Wizemann TM, Barren P, Langermann S: **Adherence of *Streptococcus pneumoniae* to human bronchial epithelial cells (BEAS-2B).** *Infect Immun* 1998, **66**:820-822.
55. Andrew AS, Warren AJ, Barchowsky A, Temple KA, Klei L, Soucy NV, O'Hara KA, Hamilton JW: **Genomic and proteomic profiling of responses to toxic metals in human lung cells.** *Environ Health Perspect* 2003, **111**:825-835.
56. Kim JE, Koo KH, Kim YH, Sohn J, Park YG: **Identification of potential lung cancer biomarkers using an in vitro carcinogenesis model.** *Exp Mol Med* 2008, **40**:709-720.

57. Lau D, Xue L, Hu R, Liaw T, Wu R, Reddy S: **Expression and regulation of a molecular marker, SPR1, in multistep bronchial carcinogenesis.** *Am J Respir Cell Mol Biol* 2000, **22**:92-96.
58. Park YH, Kim D, Dai J, Zhang Z: **Human bronchial epithelial BEAS-2B cells, an appropriate in vitro model to study heavy metals induced carcinogenesis.** *Toxicol Appl Pharm* 2015, **287**:240-245.
59. Rodrigues CF, Urbano AM, Matoso E, Carreira I, Almeida A, Santos P, Botelho F, Carvalho L, Alves M, Monteiro C, et al: **Human bronchial epithelial cells malignantly transformed by hexavalent chromium exhibit an aneuploid phenotype but no microsatellite instability.** *Mutat Res* 2009, **670**:42-52.
60. Sun H, Clancy HA, Kluz T, Zavadil J, Costa M: **Comparison of gene expression profiles in chromate transformed BEAS-2B cells.** *PLoS One* 2011, **6**:e17982.
61. Veranth JM, Reilly CA, Veranth MM, Moss TA, Langelier CR, Lanza DL, Yost GS: **Inflammatory cytokines and cell death in BEAS-2B lung cells treated with soil dust, lipopolysaccharide, and surface-modified particles.** *Toxicol Sci* 2004, **82**:88-96.
62. Jha KK, Banga S, Palejwala V, Ozer HL: **SV40-mediated immortalization.** *Exp Cell Res* 1998, **245**:1-7.
63. Lane DP: **p53, Guardian of the genome.** *Nature* 1992, **358**:15-16.
64. Weinberg RA: **The retinoblastoma protein and cell cycle control.** *Cell* 1995, **81**:323-330.
65. Wise JP, Sr., Wise SS, Little JE: **The cytotoxicity and genotoxicity of particulate and soluble hexavalent chromium in human lung cells.** *Mutat Res* 2002, **517**:221-229.
66. Reddel RR, Salghetti SE, Willey JC, Ohnuki Y, Ke Y, Gerwin BI, Lechner JF, Harris CC: **Development of tumorigenicity in simian virus 40-immortalized human bronchial epithelial cell lines.** *Cancer Res* 1993, **53**:985-991.
67. Ohnuki Y, Reddel RR, Bates SE, Lehman TA, Lechner JF, Harris CC: **Chromosomal changes and progressive tumorigenesis of human bronchial epithelial cell lines.** *Cancer Genet Cytogenet* 1996, **92**:99-110.
68. **General Cell Collection: BEAS-2B.** Accessed January 2016. [http://www.phe-culturecollections.org.uk/products/celllines/generalcell/detail.jsp?refId=95102433&collection=ecacc\\_gc](http://www.phe-culturecollections.org.uk/products/celllines/generalcell/detail.jsp?refId=95102433&collection=ecacc_gc)
69. Takayama S, Reed JC, Homma S: **Heat-shock proteins as regulators of apoptosis.** *Oncogene* 2003, **22**:9041-9047.
70. Csermely PY, I. : **Heat shock proteins.** In *Molecular Pathomechanisms and New Trends in Drug Research*. London and New York: Taylor and Francis; 2002: 67-75
71. Jolly C, Morimoto RI: **Role of the heat shock response and molecular chaperones in oncogenesis and cell death.** *J Natl Cancer Inst* 2000, **92**:1564-1572.
72. Katschinski DM: **On heat and cells and proteins.** *News Physiol Sci* 2004, **19**:11-15.

73. Nahleh Z, Tfayli A, Najm A, El Sayed A, Nahle Z: **Heat shock proteins in cancer: targeting the 'chaperones'**. *Future Med Chem* 2012, **4**:927-935.
74. Saibil H: **Chaperone machines for protein folding, unfolding and disaggregation**. *Nat Rev Mol Cell Biol* 2013, **14**:630-642.
75. Whitesell L, Lindquist SL: **HSP90 and the chaperoning of cancer**. *Nat Rev Cancer* 2005, **5**:761-772.
76. Wu C: **Heat shock transcription factors: structure and regulation**. *Annu Rev Cell Dev Biol* 1995, **11**:441-469.
77. Ritossa F: **A new puffing pattern induced by temperature shock and DNP in Drosophila**. *Experientia* 1962, **18**:571-573.
78. Morimoto RI: **Cells in stress: transcriptional activation of heat shock genes**. *Science* 1993, **259**:1409-1410.
79. Macario AJ, Conway de Macario E: **Sick chaperones, cellular stress, and disease**. *N Engl J Med* 2005, **353**:1489-1501.
80. Ciocca DR, Arrigo AP, Calderwood SK: **Heat shock proteins and heat shock factor 1 in carcinogenesis and tumor development: an update**. *Arch Toxicol* 2013, **87**:19-48.
81. Soo ET, Yip GW, Lwin ZM, Kumar SD, Bay BH: **Heat shock proteins as novel therapeutic targets in cancer**. *In Vivo* 2008, **22**:311-315.
82. Whitesell L, Lindquist S: **Inhibiting the transcription factor HSF1 as an anticancer strategy**. *Expert Opin Ther Targets* 2009, **13**:469-478.
83. Wondrak G: **Introduction to Cell Stress Responses in Cancer: The Big Picture**. In *Stress Response Pathways in Cancer*. Springer Netherlands; 2015: 1-5
84. de Billy E, Travers J, Workman P: **Shock about heat shock in cancer**. *Oncotarget* 2012, **3**:741-743.
85. Jackson SE: **Hsp90: structure and function**. *Top Curr Chem* 2013, **328**:155-240.
86. Csermely P, Schnaider T, Soti C, Prohaszka Z, Nardai G: **The 90-kDa molecular chaperone family: structure, function, and clinical applications. A comprehensive review**. *Pharmacol Ther* 1998, **79**:129-168.
87. Felts SJ, Owen BA, Nguyen P, Trepel J, Donner DB, Toft DO: **The hsp90-related protein TRAP1 is a mitochondrial protein with distinct functional properties**. *J Biol Chem* 2000, **275**:3305-3312.
88. Wayne N, Bolon DN: **Dimerization of Hsp90 is required for in vivo function. Design and analysis of monomers and dimers**. *J Biol Chem* 2007, **282**:35386-35395.
89. Sreedhar AS, Kalmar E, Csermely P, Shen YF: **Hsp90 isoforms: functions, expression and clinical importance**. *FEBS Lett* 2004, **562**:11-15.
90. Wiech H, Buchner J, Zimmermann R, Jakob U: **Hsp90 chaperones protein folding in vitro**. *Nature* 1992, **358**:169-170.

91. McClellan AJ, Xia Y, Deutschbauer AM, Davis RW, Gerstein M, Frydman J: **Diverse cellular functions of the Hsp90 molecular chaperone uncovered using systems approaches.** *Cell* 2007, **131**:121-135.
92. Muller L, Schaupp A, Walerych D, Wegele H, Buchner J: **Hsp90 regulates the activity of wild type p53 under physiological and elevated temperatures.** *J Biol Chem* 2004, **279**:48846-48854.
93. Walerych D, Kudla G, Gutkowska M, Wawrzynow B, Muller L, King FW, Helwak A, Boros J, Zylicz A, Zylicz M: **Hsp90 chaperones wild-type p53 tumor suppressor protein.** *J Biol Chem* 2004, **279**:48836-48845.
94. Mollapour M, Neckers L: **Post-translational modifications of Hsp90 and their contributions to chaperone regulation.** *Biochim Biophys Acta* 2012, **1823**:648-655.
95. Wandinger SK, Richter K, Buchner J: **The Hsp90 chaperone machinery.** *J Biol Chem* 2008, **283**:18473-18477.
96. Pearl LH, Prodromou C: **Structure and mechanism of the Hsp90 molecular chaperone machinery.** *Annu Rev Biochem* 2006, **75**:271-294.
97. Dutta R, Inouye M: **GHKL, an emergent ATPase/kinase superfamily.** *Trends Biochem Sci* 2000, **25**:24-28.
98. Calderwood SK, Khaleque MA, Sawyer DB, Ciocca DR: **Heat shock proteins in cancer: chaperones of tumorigenesis.** *Trends Biochem Sci* 2006, **31**:164-172.
99. Soti C, Racz A, Csermely P: **A nucleotide-dependent molecular switch controls ATP binding at the C-terminal domain of Hsp90. N-terminal nucleotide binding unmask a C-terminal binding pocket.** *J Biol Chem* 2002, **277**:7066-7075.
100. Trepel J, Mollapour M, Giaccone G, Neckers L: **Targeting the dynamic HSP90 complex in cancer.** *Nat Rev Cancer* 2010, **10**:537-549.
101. Barrott JJ, Haystead TA: **Hsp90, an unlikely ally in the war on cancer.** *FEBS J* 2013, **280**:1381-1396.
102. Muller PA, Vousden KH: **Mutant p53 in cancer: new functions and therapeutic opportunities.** *Cancer Cell* 2014, **25**:304-317.
103. Ziemiecki A, Catelli MG, Joab I, Moncharmont B: **Association of the heat shock protein hsp90 with steroid hormone receptors and tyrosine kinase oncogene products.** *Biochem Biophys Res Commun* 1986, **138**:1298-1307.
104. Holt SE, Aisner DL, Baur J, Tesmer VM, Dy M, Ouellette M, Trager JB, Morin GB, Toft DO, Shay JW, et al: **Functional requirement of p23 and Hsp90 in telomerase complexes.** *Genes Dev* 1999, **13**:817-826.
105. Basso AD, Solit DB, Chiosis G, Giri B, Tsihchlis P, Rosen N: **Akt forms an intracellular complex with heat shock protein 90 (Hsp90) and Cdc37 and is destabilized by inhibitors of Hsp90 function.** *J Biol Chem* 2002, **277**:39858-39866.
106. Isaacs JS, Jung YJ, Mimnaugh EG, Martinez A, Cuttitta F, Neckers LM: **Hsp90 regulates a von Hippel Lindau-independent hypoxia-inducible factor-1 alpha-degradative pathway.** *J Biol Chem* 2002, **277**:29936-29944.

107. Eustace BK, Sakurai T, Stewart JK, Yimlamai D, Unger C, Zehetmeier C, Lain B, Torella C, Henning SW, Beste G, et al: **Functional proteomic screens reveal an essential extracellular role for hsp90 alpha in cancer cell invasiveness.** *Nat Cell Biol* 2004, **6**:507-514.
108. Li W, Sahu D, Tsen F: **Secreted heat shock protein-90 (Hsp90) in wound healing and cancer.** *Biochim Biophys Acta* 2012, **1823**:730-741.
109. Mayer MP, Bukau B: **Hsp70 chaperones: cellular functions and molecular mechanism.** *Cell Mol Life Sci* 2005, **62**:670-684.
110. Welch WJ: **Mammalian stress response: cell physiology, structure/function of stress proteins, and implications for medicine and disease.** *Physiol Rev* 1992, **72**:1063-1081.
111. Bukau B, Horwich AL: **The Hsp70 and Hsp60 chaperone machines.** *Cell* 1998, **92**:351-366.
112. Budina-Kolomets A, Basu S, Belcastro L, Murphy M: **The Hsp70 Family of Heat Shock Proteins in Tumorigenesis: From Molecular Mechanisms to Therapeutic Opportunities.** In *Stress Response Pathways in Cancer*. Springer Netherlands; 2015: 203-224
113. Ciocca DR, Calderwood SK: **Heat shock proteins in cancer: diagnostic, prognostic, predictive, and treatment implications.** *Cell Stress Chaperones* 2005, **10**:86-103.
114. Juhasz K, Lipp AM, Nimmervoll B, Sonnleitner A, Hesse J, Haselgruebler T, Balogi Z: **The complex function of hsp70 in metastatic cancer.** *Cancers* 2013, **6**:42-66.
115. Paoli P, Giannoni E, Chiarugi P: **Anoikis molecular pathways and its role in cancer progression.** *Biochim Biophys Acta* 2013, **1833**:3481-3498.
116. Martin SS, Vuori K: **Regulation of Bcl-2 proteins during anoikis and amorphosis.** *Biochim Biophys Acta* 2004, **1692**:145-157.
117. Yaglom JA, Gabai VL, Sherman MY: **High levels of heat shock protein Hsp72 in cancer cells suppress default senescence pathways.** *Cancer Res* 2007, **67**:2373-2381.
118. Zylicz M, King FW, Wawrzynow A: **Hsp70 interactions with the p53 tumour suppressor protein.** *The EMBO Journal* 2001, **20**:4634-4638.
119. Morimoto RI: **Regulation of the heat shock transcriptional response: cross talk between a family of heat shock factors, molecular chaperones, and negative regulators.** *Genes Dev* 1998, **12**:3788-3796.
120. Dai C, Whitesell L, Rogers AB, Lindquist S: **Heat shock factor 1 is a powerful multifaceted modifier of carcinogenesis.** *Cell* 2007, **130**:1005-1018.
121. McMillan DR, Xiao X, Shao L, Graves K, Benjamin IJ: **Targeted disruption of heat shock transcription factor 1 abolishes thermotolerance and protection against heat-inducible apoptosis.** *J Biol Chem* 1998, **273**:7523-7528.
122. Xiao X, Zuo X, Davis AA, McMillan DR, Curry BB, Richardson JA, Benjamin IJ: **HSF1 is required for extra-embryonic development, postnatal growth and**

- protection during inflammatory responses in mice. *EMBO J* 1999, **18**:5943-5952.**
123. Zou J, Guo Y, Guettouche T, Smith DF, Voellmy R: **Repression of heat shock transcription factor HSF1 activation by HSP90 (HSP90 complex) that forms a stress-sensitive complex with HSF1. *Cell* 1998, **94**:471-480.**
  124. Sarge KD, Murphy SP, Morimoto RI: **Activation of heat shock gene transcription by heat shock factor 1 involves oligomerization, acquisition of DNA-binding activity, and nuclear localization and can occur in the absence of stress. *Mol Cell Biol* 1993, **13**:1392-1407.**
  125. Pirkkala L, Nykanen P, Sistonen L: **Roles of the heat shock transcription factors in regulation of the heat shock response and beyond. *FASEB J* 2001, **15**:1118-1131.**
  126. Ahn SG, Thiele DJ: **Redox regulation of mammalian heat shock factor 1 is essential for Hsp gene activation and protection from stress. *Gene Dev* 2003, **17**:516-528.**
  127. Hahn JS, Hu Z, Thiele DJ, Iyer VR: **Genome-wide analysis of the biology of stress responses through heat shock transcription factor. *Mol Cell Biol* 2004, **24**:5249-5256.**
  128. Trinklein ND, Murray JI, Hartman SJ, Botstein D, Myers RM: **The role of heat shock transcription factor 1 in the genome-wide regulation of the mammalian heat shock response. *Mol Biol Cell* 2004, **15**:1254-1261.**
  129. Mendillo ML, Santagata S, Koeva M, Bell GW, Hu R, Tamimi RM, Fraenkel E, Ince TA, Whitesell L, Lindquist S: **HSF1 drives a transcriptional program distinct from heat shock to support highly malignant human cancers. *Cell* 2012, **150**:549-562.**
  130. Tchenio T, Havard M, Martinez LA, Dautry F: **Heat shock-independent induction of multidrug resistance by heat shock factor 1. *Mol Cell Biol* 2006, **26**:580-591.**
  131. Sidera K, Patsavoudi E: **HSP90 inhibitors: current development and potential in cancer therapy. *Recent Pat Anticancer Drug Discov* 2014, **9**:1-20.**
  132. Kamal A, Thao L, Sensintaffar J, Zhang L, Boehm MF, Fritz LC, Burrows FJ: **A high-affinity conformation of Hsp90 confers tumour selectivity on Hsp90 inhibitors. *Nature* 2003, **425**:407-410.**
  133. Evans CG, Chang L, Gestwicki JE: **Heat shock protein 70 (hsp70) as an emerging drug target. *J Med Chem* 2010, **53**:4585-4602.**
  134. Del Razo LM, Quintanilla-Vega B, Brambila-Colombres E, Calderon-Aranda ES, Manno M, Albores A: **Stress proteins induced by arsenic. *Toxicol Appl Pharmacol* 2001, **177**:132-148.**
  135. Han SG, Castranova V, Vallyathan V: **Comparative cytotoxicity of cadmium and mercury in a human bronchial epithelial cell line (BEAS-2B) and its role in oxidative stress and induction of heat shock protein 70. *J Toxicol Env Heal A* 2007, **70**:852-860.**

136. Goering PL, Fisher BR: **Metals and stress proteins.** In *Toxicology of Metals. Volume 115.* Springer Berlin Heidelberg; 1995: 229-266: *Handbook of Experimental Pharmacology.*
137. Tully DB, Collins BJ, Overstreet JD, Smith CS, Dinse GE, Mumtaz MM, Chapin RE: **Effects of arsenic, cadmium, chromium, and lead on gene expression regulated by a battery of 13 different promoters in recombinant HepG2 cells.** *Toxicol Appl Pharmacol* 2000, **168**:79-90.
138. Banu SK, Stanley JA, Lee J, Stephen SD, Arosh JA, Hoyer PB, Burghardt RC: **Hexavalent chromium-induced apoptosis of granulosa cells involves selective sub-cellular translocation of Bcl-2 members, ERK1/2 and p53.** *Toxicol Appl Pharmacol* 2011, **251**:253-266.
139. Xiao F, Li Y, Dai L, Deng Y, Zou Y, Li P, Yang Y, Zhong C: **Hexavalent chromium targets mitochondrial respiratory chain complex I to induce reactive oxygen species-dependent caspase-3 activation in L-02 hepatocytes.** *Int J Mol Med* 2012, **30**:629-635.
140. Lee J, Lim KT: **Inhibitory effect of SJSZ glycoprotein (38 kDa) on expression of heat shock protein 27 and 70 in chromium (VI)-treated hepatocytes.** *Mol Cell Biochem* 2012, **359**:45-57.
141. Zhang Q, Zhang L, Xiao X, Su Z, Zou P, Hu H, Huang Y, He QY: **Heavy metals chromium and neodymium reduced phosphorylation level of heat shock protein 27 in human keratinocytes.** *Toxicol In Vitro* 2010, **24**:1098-1104.
142. Rudolf E, Cervinka M: **Nickel modifies the cytotoxicity of hexavalent chromium in human dermal fibroblasts.** *Toxicol Lett* 2010, **197**:143-150.
143. Delmas F, Schaak S, Gaubin Y, Croute F, Arrabit C, Murat JC: **Hsp72 mRNA production in cultured human cells submitted to nonlethal aggression by heat, ethanol, or propanol. Application to the detection of low concentrations of chromium(VI) (potassium dichromate).** *Cell Biol Toxicol* 1998, **14**:39-46.
144. Izzotti A, Cartiglia C, Balansky R, D'Agostini F, Longobardi M, De Flora S: **Selective induction of gene expression in rat lung by hexavalent chromium.** *Mol Carcinog* 2002, **35**:75-84.
145. Majumder S, Ghoshal K, Summers D, Bai S, Datta J, Jacob ST: **Chromium(VI) down-regulates heavy metal-induced metallothionein gene transcription by modifying transactivation potential of the key transcription factor, metal-responsive transcription factor 1.** *J Biol Chem* 2003, **278**:26216-26226.
146. Myers JM, Antholine WE, Myers CR: **Hexavalent chromium causes oxidation of thioredoxin in human bronchial epithelial cells.** *Toxicology* 2008, **246**:222-233.
147. Sanadi DR, Langley M, White F: **Alpha-ketoglutaric dehydrogenase .7. Role of thioctic acid.** *J Biol Chem* 1959, **234**:183-187.
148. Negrini S, Gorgoulis VG, Halazonetis TD: **Genomic instability - an evolving hallmark of cancer.** *Nat Rev Mol Cell Biol* 2010, **11**:220-228.
149. Lengauer C, Kinzler KW, Vogelstein B: **Genetic instabilities in human cancers.** *Nature* 1998, **396**:643-649.

150. Vogelstein B, Kinzler KW: **Cancer genes and the pathways they control.** *Nat Med* 2004, **10**:789-799.
151. Loeb LA, Loeb KR, Anderson JP: **Multiple mutations and cancer.** *Proc Natl Acad Sci U S A* 2003, **100**:776-781.
152. Halazonetis TD, Gorgoulis VG, Bartek J: **An oncogene-induced DNA damage model for cancer development.** *Science* 2008, **319**:1352-1355.
153. Urbano AM, Ferreira LMR, Cerveira JF, Rodrigues CF, Alpoim MC: **DNA damage, repair and misrepair in cancer and in cancer therapy.** In *DNA damage, repair and misrepair in cancer and in cancer therapy*. InTech; 2011.
154. Durkin SG, Glover TW: **Chromosome fragile sites.** *Annu Rev Genet* 2007, **41**:169-192.
155. Bartkova J, Horejsi Z, Koed K, Kramer A, Tort F, Zieger K, Guldborg P, Sehested M, Nesland JM, Lukas C, et al: **DNA damage response as a candidate anti-cancer barrier in early human tumorigenesis.** *Nature* 2005, **434**:864-870.
156. Gorgoulis VG, Vassiliou LV, Karakaidos P, Zacharatos P, Kotsinas A, Liloglou T, Venere M, Ditullio RA, Jr., Kastrinakis NG, Levy B, et al: **Activation of the DNA damage checkpoint and genomic instability in human precancerous lesions.** *Nature* 2005, **434**:907-913.
157. Tsantoulis PK, Kotsinas A, Sfikakis PP, Evangelou K, Sideridou M, Levy B, Mo L, Kittas C, Wu XR, Papavassiliou AG, Gorgoulis VG: **Oncogene-induced replication stress preferentially targets common fragile sites in preneoplastic lesions. A genome-wide study.** *Oncogene* 2008, **27**:3256-3264.
158. Falck J, Coates J, Jackson SP: **Conserved modes of recruitment of ATM, ATR and DNA-PKcs to sites of DNA damage.** *Nature* 2005, **434**:605-611.
159. Kuo LJ, Yang LX: **Gamma-H2AX - a novel biomarker for DNA double-strand breaks.** *In Vivo* 2008, **22**:305-309.
160. Khanna KK, Jackson SP: **DNA double-strand breaks: signaling, repair and the cancer connection.** *Nat Genet* 2001, **27**:247-254.
161. Kastan MB, Bartek J: **Cell-cycle checkpoints and cancer.** *Nature* 2004, **432**:316-323.
162. Vamvakas S, Vock EH, Lutz WK: **On the role of DNA double-strand breaks in toxicity and carcinogenesis.** *Crit Rev Toxicol* 1997, **27**:155-174.
163. Godinho SA, Pellman D: **Causes and consequences of centrosome abnormalities in cancer.** *Philos Trans R Soc Lond B Biol Sci* 2014, **369**.
164. Ding L, Getz G, Wheeler DA, Mardis ER, McLellan MD, Cibulskis K, Sougnez C, Greulich H, Muzny DM, Morgan MB, et al: **Somatic mutations affect key pathways in lung adenocarcinoma.** *Nature* 2008, **455**:1069-1075.
165. Parsons DW, Jones S, Zhang X, Lin JC, Leary RJ, Angenendt P, Mankoo P, Carter H, Siu IM, Gallia GL, et al: **An integrated genomic analysis of human glioblastoma multiforme.** *Science* 2008, **321**:1807-1812.
166. Ha L, Ceryak S, Patierno SR: **Generation of S phase-dependent DNA double-strand breaks by Cr(VI) exposure: involvement of ATM in Cr(VI) induction of gamma-H2AX.** *Carcinogenesis* 2004, **25**:2265-2274.

167. Peterson-Roth E, Reynolds M, Quievryn G, Zhitkovich A: **Mismatch repair proteins are activators of toxic responses to chromium-DNA damage.** *Mol Cell Biol* 2005, **25**:3596-3607.
168. Xie H, Holmes AL, Young JL, Qin Q, Joyce K, Pelsue SC, Peng C, Wise SS, Jeevarajan AS, Wallace WT, et al: **Zinc chromate induces chromosome instability and DNA double strand breaks in human lung cells.** *Toxicol Appl Pharmacol* 2009, **234**:293-299.
169. Xie H, Wise SS, Holmes AL, Xu B, Wakeman TP, Pelsue SC, Singh NP, Wise JP, Sr.: **Carcinogenic lead chromate induces DNA double-strand breaks in human lung cells.** *Mutat Res* 2005, **586**:160-172.
170. Xie H, Wise SS, Wise JP, Sr.: **Deficient repair of particulate hexavalent chromium-induced DNA double strand breaks leads to neoplastic transformation.** *Mutat Res* 2008, **649**:230-238.
171. DeLoughery Z, Luczak MW, Ortega-Atienza S, Zhitkovich A: **DNA double-strand breaks by Cr(VI) are targeted to euchromatin and cause ATR-dependent phosphorylation of histone H2AX and its ubiquitination.** *Toxicol Sci* 2015, **143**:54-63.
172. Wakeman TP, Kim WJ, Callens S, Chiu A, Brown KD, Xu B: **The ATM-SMC1 pathway is essential for activation of the chromium[VI]-induced S-phase checkpoint.** *Mutat Res* 2004, **554**:241-251.
173. Reynolds MF, Peterson-Roth EC, Bespalov IA, Johnston T, Gurel VM, Menard HL, Zhitkovich A: **Rapid DNA double-strand breaks resulting from processing of Cr-DNA cross-links by both MutS dimers.** *Cancer Res* 2009, **69**:1071-1079.
174. Reynolds M, Stoddard L, Bespalov I, Zhitkovich A: **Ascorbate acts as a highly potent inducer of chromate mutagenesis and clastogenesis: linkage to DNA breaks in G2 phase by mismatch repair.** *Nucleic Acids Res* 2007, **35**:465-476.
175. Wise SS, Wise JP: **Aneuploidy as an early mechanistic event in metal carcinogenesis.** *Biochem Soc Trans* 2010, **38**:1650-1654.
176. Holmes AL, Wise SS, Pelsue SC, Aboueissa AM, Lingle W, Salisbury J, Gallagher J, Wise JP, Sr.: **Chronic exposure to zinc chromate induces centrosome amplification and spindle assembly checkpoint bypass in human lung fibroblasts.** *Chem Res Toxicol* 2010, **23**:386-395.
177. Holmes AL, Wise SS, Sandwick SJ, Lingle WL, Negron VC, Thompson WD, Wise JP, Sr.: **Chronic exposure to lead chromate causes centrosome abnormalities and aneuploidy in human lung cells.** *Cancer Res* 2006, **66**:4041-4048.
178. Ganem NJ, Storchova Z, Pellman D: **Tetraploidy, aneuploidy and cancer.** *Curr Opin Genet Dev* 2007, **17**:157-162.
179. Xie H, Holmes AL, Wise SS, Huang S, Peng C, Wise JP, Sr.: **Neoplastic transformation of human bronchial cells by lead chromate particles.** *Am J Respir Cell Mol Biol* 2007, **37**:544-552.

180. Seoane AI, Guerci AM, Dulout FN: **Malsegregation as a possible mechanism of aneuploidy induction by metal salts in MRC-5 human cells.** *Environ Mol Mutagen* 2002, **40**:200-206.
181. Figgitt M, Newson R, Leslie IJ, Fisher J, Ingham E, Case CP: **The genotoxicity of physiological concentrations of chromium (Cr(III) and Cr(VI)) and cobalt (Co(II)): an in vitro study.** *Mutat Res* 2010, **688**:53-61.
182. Tsaousi A, Jones E, Case CP: **The in vitro genotoxicity of orthopaedic ceramic (Al<sub>2</sub>O<sub>3</sub>) and metal (CoCr alloy) particles.** *Mutat Res* 2010, **697**:1-9.
183. Ha L, Ceryak S, Patierno SR: **Chromium (VI) activates ataxia telangiectasia mutated (ATM) protein. Requirement of ATM for both apoptosis and recovery from terminal growth arrest.** *J Biol Chem* 2003, **278**:17885-17894.
184. Wakeman TP, Xu B: **ATR regulates hexavalent chromium-induced S-phase checkpoint through phosphorylation of SMC1.** *Mutat Res* 2006, **610**:14-20.
185. Povirk LF: **Biochemical mechanisms of chromosomal translocations resulting from DNA double-strand breaks.** *DNA Repair* 2006, **5**:1199-1212.
186. **BEAS-2B (ATCC® CRL-9609™).** Accessed January 2016. [http://www.lgcstandards-atcc.org/products/all/CRL9609.aspx?geo\\_country=ro#culturemethod](http://www.lgcstandards-atcc.org/products/all/CRL9609.aspx?geo_country=ro#culturemethod)
187. Freshney RI: *Culture of animal cells : a manual of basic technique.* 5th edn. Hoboken, N.J.: Wiley-Liss; 2005.
188. ECACC: *Fundamental techniques in cell culture - laboratory handbook.* 2nd edn.
189. Harrison MA: **Cryopreservation of Cells.** *Encyclopedia of Life Sciences* 2001.
190. Pappas D: *Practical cell analysis.* C hichester, UK ; Hoboken, N.J.: Wiley; 2010.
191. Langdon SP: *Cancer cell culture : methods and protocols.* Totowa, N.J.: Humana Press; 2004.
192. Sinha B, Kumar, R.: *Principles of animal cell culture.* Bihar: International Book Distributing Co; 2008.
193. Coligan JE: **Current protocols in immunology.** New York: John Wiley and Sons.
194. Fallon A, Booth, R.F.G. e Bell; L.D.: *Applications of HPLC in Biochemistry.* 1987, Elsevier.
195. Aguilar MI: **Reversed-phase high-performance liquid chromatography.** *Methods Mol Biol* 2004, **251**:9-22.
196. Compton SJ, Jones CG: **Mechanism of dye response and interference in the Bradford protein assay.** *Anal Biochem* 1985, **151**:369-374.
197. Bradford MM: **A rapid and sensitive method for the quantitation of microgram quantities of protein utilizing the principle of protein-dye binding.** *Anal Biochem* 1976, **72**:248-254.
198. Kruger N: **The Bradford method for protein quantitation.** In *The Protein Protocols Handbook.* Humana Press; 2002: 15-21
199. Peterson GL: **Determination of total protein.** *Methods Enzymol* 1983, **91**:95-119.

200. Pierce TS: *Assay Development Technical Handbook*. US: Thermo Scientific Pierce; 2011.
201. Fleige S, Pfaffl MW: **RNA integrity and the effect on the real-time qRT-PCR performance**. *Mol Aspects Med* 2006, **27**:126-139.
202. Mueller O, Hahnenberger K, Dittmann M, Yee H, Dubrow R, Nagle R, Ilsley D: **A microfluidic system for high-speed reproducible DNA sizing and quantitation**. *Electrophoresis* 2000, **21**:128-134.
203. Pattyn F, Speleman F, De Paepe A, Vandesompele J: **RTPPrimerDB: the real-time PCR primer and probe database**. *Nucleic Acids Res* 2003, **31**:122-123.
204. Wang X, Seed B: **A PCR primer bank for quantitative gene expression analysis**. *Nucleic Acids Res* 2003, **31**:e154.
205. Ye J, Coulouris G, Zaretskaya I, Cutcutache I, Rozen S, Madden TL: **Primer-BLAST: a tool to design target-specific primers for polymerase chain reaction**. *BMC Bioinformatics* 2012, **13**:134.
206. Paul N, Shum J, Le T: **Hot start PCR**. *Methods Mol Biol* 2010, **630**:301-318.
207. Kibbe WA: **OligoCalc: an online oligonucleotide properties calculator**. *Nucleic Acids Res* 2007, **35**:W43-46.
208. Myers JM, Antholine WE, Myers CR: **The intracellular redox stress caused by hexavalent chromium is selective for proteins that have key roles in cell survival and thiol redox control**. *Toxicology* 2011, **281**:37-47.
209. Stueckle TA, Lu Y, Davis ME, Wang L, Jiang BH, Holaskova I, Schafer R, Barnett JB, Rojanasakul Y: **Chronic occupational exposure to arsenic induces carcinogenic gene signaling networks and neoplastic transformation in human lung epithelial cells**. *Toxicol Appl Pharmacol* 2012, **261**:204-216.
210. Zhao F, Klimecki WT: **Culture conditions profoundly impact phenotype in BEAS-2B, a human pulmonary epithelial model**. *J Appl Toxicol* 2015, **35**:945-951.
211. Ferreira DC: **Efeitos do crómio hexavalente no metabolismo energético de uma linha celular de epitélio brônquico humano**. University of Coimbra, Department of Life Sciences, MSc Thesis; 2015.
212. Ke Y, Reddel RR, Gerwin BI, Miyashita M, McMenamin M, Lechner JF, Harris CC: **Human bronchial epithelial cells with integrated SV40 virus T antigen genes retain the ability to undergo squamous differentiation**. *Differentiation* 1988, **38**:60-66.
213. Lechner JF, Haugen A, McClendon IA, Shamsuddin AM: **Induction of squamous differentiation of normal human bronchial epithelial cells by small amounts of serum**. *Differentiation* 1984, **25**:229-237.
214. Hughes P, Marshall D, Reid Y, Parkes H, Gelber C: **The costs of using unauthenticated, over-passaged cell lines: how much more data do we need?** *Biotechniques* 2007, **43**:575, 577-578, 581-574.
215. Matturri L, Lavezzi AM: **Recurrent chromosome alterations in non-small cell lung cancer**. *Eur J Histochem* 1994, **38**:53-58.

216. Testa JR, Liu Z, Feder M, Bell DW, Balsara B, Cheng JQ, Taguchi T: **Advances in the analysis of chromosome alterations in human lung carcinomas.** *Cancer Genet Cytogenet* 1997, **95**:20-32.
217. Urbano AM, Ferreira LM, Abreu PL: **P29. Effects of hexavalent chromium [Cr(VI)] on the stress response of a human bronchial epithelial cell line.** *Rev Port Pneumol* 2014, **20(Esp Cong 2)**:8-32.
218. Urbano AM, Ferreira LMR, Abreu PL: **Exposure of human bronchial epithelial cells to hexavalent chromium Cr(VI) decreases the expression of heat shock protein 90 alpha (Hsp90 alpha) and attenuates the transient growth arrest induced by an acute cold shock.** *FEBS Journal* 2013, **280**:239-239.
219. Lambowitz AM, Kobayashi GS, Painter A, Medoff G: **Possible relationship of morphogenesis in pathogenic fungus, *Histoplasma capsulatum*, to heat shock response.** *Nature* 1983, **303**:806-808.
220. Findly RC, Gillies RJ, Shulman RG: **In vivo phosphorus-31 nuclear magnetic resonance reveals lowered ATP during heat shock of *Tetrahymena*.** *Science* 1983, **219**:1223-1225.
221. Ohyama H, Yamada T: **Reduction of rat thymocyte interphase death by hyperthermia.** *Radiat Res* 1980, **82**:342-351.
222. Lunec J, Cresswell SR: **Heat-induced thermotolerance expressed in the energy metabolism of mammalian cells.** *Radiat Res* 1983, **93**:588-597.
223. Robins HI, Jonsson GG, Jacobson EL, Schmitt CL, Cohen JD, Jacobson MK: **Effect of hyperthermia in vitro and in vivo on adenine and pyridine nucleotide pools in human peripheral lymphocytes.** *Cancer* 1991, **67**:2096-2102.
224. Zhao QL, Fujiwara Y, Kondo T: **Mechanism of cell death induction by nitroxide and hyperthermia.** *Free Radic Biol Med* 2006, **40**:1131-1143.
225. Lilly MB, Ng TC, Evanochko WT, Katholi CR, Kumar NG, Elgavish GA, Durant JR, Hiramoto R, Ghanta V, Glickson JD: **Loss of high-energy phosphate following hyperthermia demonstrated by in vivo 31P-nuclear magnetic resonance spectroscopy.** *Cancer Res* 1984, **44**:633-638.
226. Evanochko WT, Ng TC, Lilly MB, Lawson AJ, Corbett TH, Durant JR, Glickson JD: **In vivo 31P NMR study of the metabolism of murine mammary 16/C adenocarcinoma and its response to chemotherapy, x-radiation, and hyperthermia.** *Proc Natl Acad Sci USA* 1983, **80**:334-338.
227. Francesconi R, Mager M: **Heat- and exercise-induced hyperthermia: effects on high-energy phosphates.** *Aviat Space Environ Med* 1979, **50**:799-802.
228. Henle KJ, Nagle WA, Moss AJ, Herman TS: **Cellular ATP content of heated Chinese hamster ovary cells.** *Radiat Res* 1984, **97**:630-633.
229. Knop RH, Chen CW, Mitchell JB, Russo A, McPherson S, Cohen JS: **Adaptive cellular response to hyperthermia: 31P-NMR studies.** *Biochim Biophys Acta* 1985, **845**:171-177.

230. Nagle WA, Moss AJ, Baker ML: **Increased lethality from hyperthermia at 42°C for hypoxic Chinese hamster cells heated under conditions of energy deprivation.** *Natl Cancer Inst Monogr* 1982, **61**:107-110.
231. Berg JM, Tymoczko JL, Stryer L: *Biochemistry*. 7th edn. New York: W. H. Freeman; 2012.
232. DePamphilis ML, Cleland WW: **Preparation and properties of chromium (3)-nucleotide complexes for use in the study of enzyme mechanisms.** *Biochemistry* 1973, **12**:3714-3724.
233. Janson CA, Cleland WW: **The specificity of chromium nucleotides as inhibitors of selected kinases.** *J Biol Chem* 1974, **249**:2572-2574.
234. Janson CA, Cleland WW: **The inhibition of acetate, pyruvate, and 3-phosphoglycerate kinases by chromium adenosine triphosphate.** *J Biol Chem* 1974, **249**:2567-2571.
235. Pauls H, Serpersu EH, Kirch U, Schoner W: **Chromium(III)ATP inactivating (Na<sup>+</sup> + K<sup>+</sup>)-ATPase supports Na<sup>+</sup>-Na<sup>+</sup> and Rb<sup>+</sup>-Rb<sup>+</sup> exchanges in everted red blood cells but not Na<sup>+</sup>,K<sup>+</sup> transport.** *Eur J Biochem* 1986, **157**:585-595.
236. Vogel C, Marcotte EM: **Insights into the regulation of protein abundance from proteomic and transcriptomic analyses.** *Nat Rev Genet* 2012, **13**:227-232.
237. Cerchietti LC, Lopes EC, Yang SN, Hatzi K, Bunting KL, Tsikitas LA, Mallik A, Robles AI, Walling J, Varticovski L, et al: **A purine scaffold Hsp90 inhibitor destabilizes BCL-6 and has specific antitumor activity in BCL-6-dependent B cell lymphomas.** *Nature Medicine* 2009, **15**:1369-U1363.
238. Makhnevych T, Houry WA: **The role of Hsp90 in protein complex assembly.** *Biochim Biophys Acta* 2012, **1823**:674-682.
239. Stecklein SR, Kumaraswamy E, Behbod F, Wang W, Chaguturu V, Harlan-Williams LM, Jensen RA: **BRCA1 and HSP90 cooperate in homologous and non-homologous DNA double-strand-break repair and G2/M checkpoint activation.** *Proc Natl Acad Sci USA* 2012, **109**:13650-13655.
240. Logan IR, McNeill HV, Cook S, Lu X, Meek DW, Fuller-Pace FV, Lunec J, Robson CN: **Heat shock factor-1 modulates p53 activity in the transcriptional response to DNA damage.** *Nucleic Acids Res* 2009, **37**:2962-2973.
241. Li Q, Feldman RA, Radhakrishnan VM, Carey S, Martinez JD: **Hsf1 is required for the nuclear translocation of p53 tumor suppressor.** *Neoplasia* 2008, **10**:1138-1145.
242. Kopec AK, Kim S, Forgacs AL, Zacharewski TR, Proctor DM, Harris MA, Haws LC, Thompson CM: **Genome-wide gene expression effects in B6C3F1 mouse intestinal epithelia following 7 and 90days of exposure to hexavalent chromium in drinking water.** *Toxicol Appl Pharmacol* 2012, **259**:13-26.
243. Tsao DA, Tseng WC, Chang HR: **The expression of RKIP, RhoGDI, galectin, c-Myc and p53 in gastrointestinal system of Cr(VI)-exposed rats.** *J Appl Toxicol* 2011, **31**:730-740.
244. Carlisle DL, Pritchard DE, Singh J, Owens BM, Blankenship LJ, Orenstein JM, Patierno SR: **Apoptosis and P53 induction in human lung fibroblasts exposed**

- to chromium (VI): effect of ascorbate and tocopherol.** *Toxicol Sci* 2000, **55**:60-68.
245. Xiao F, Feng X, Zeng M, Guan L, Hu Q, Zhong C: **Hexavalent chromium induces energy metabolism disturbance and p53-dependent cell cycle arrest via reactive oxygen species in L-02 hepatocytes.** *Mol Cell Biochem* 2012.
246. Reynolds M, Zhitkovich A: **Cellular vitamin C increases chromate toxicity via a death program requiring mismatch repair but not p53.** *Carcinogenesis* 2007, **28**:1613-1620.
247. Landolph JR: **Molecular mechanisms of transformation of C3H/10T1/2 Cl 8 mouse embryo cells and diploid human fibroblasts by carcinogenic metal compounds.** *Environ Health Perspect* 1994, **102 Suppl 3**:119-125.
248. Shaffer LG, Bejjani BA: **A cytogeneticist's perspective on genomic microarrays.** *Hum Reprod Update* 2004, **10**:221-226.
249. Oostlander AE, Meijer GA, Ylstra B: **Microarray-based comparative genomic hybridization and its applications in human genetics.** *Clin Genet* 2004, **66**:488-495.
250. Patierno SR, Banh D, Landolph JR: **Transformation of C3H/10T1/2 mouse embryo cells to focus formation and anchorage independence by insoluble lead chromate but not soluble calcium chromate: relationship to mutagenesis and internalization of lead chromate particles.** *Cancer Res* 1988, **48**:5280-5288.



# **Appendices**

---



## A.1. Evaluation of RNA integrity

The integrity of the RNA used in the RT-qPCR reactions was evaluated, as described in section 2.16, by an automated capillary-electrophoresis system. The virtual RNA gel image and the RNA quality indicators obtained from the Experion™ software at the end of the run are presented in Figure A.1. All samples analyzed presented the highest RQI possible and were, therefore, considered adequate for use in downstream applications.

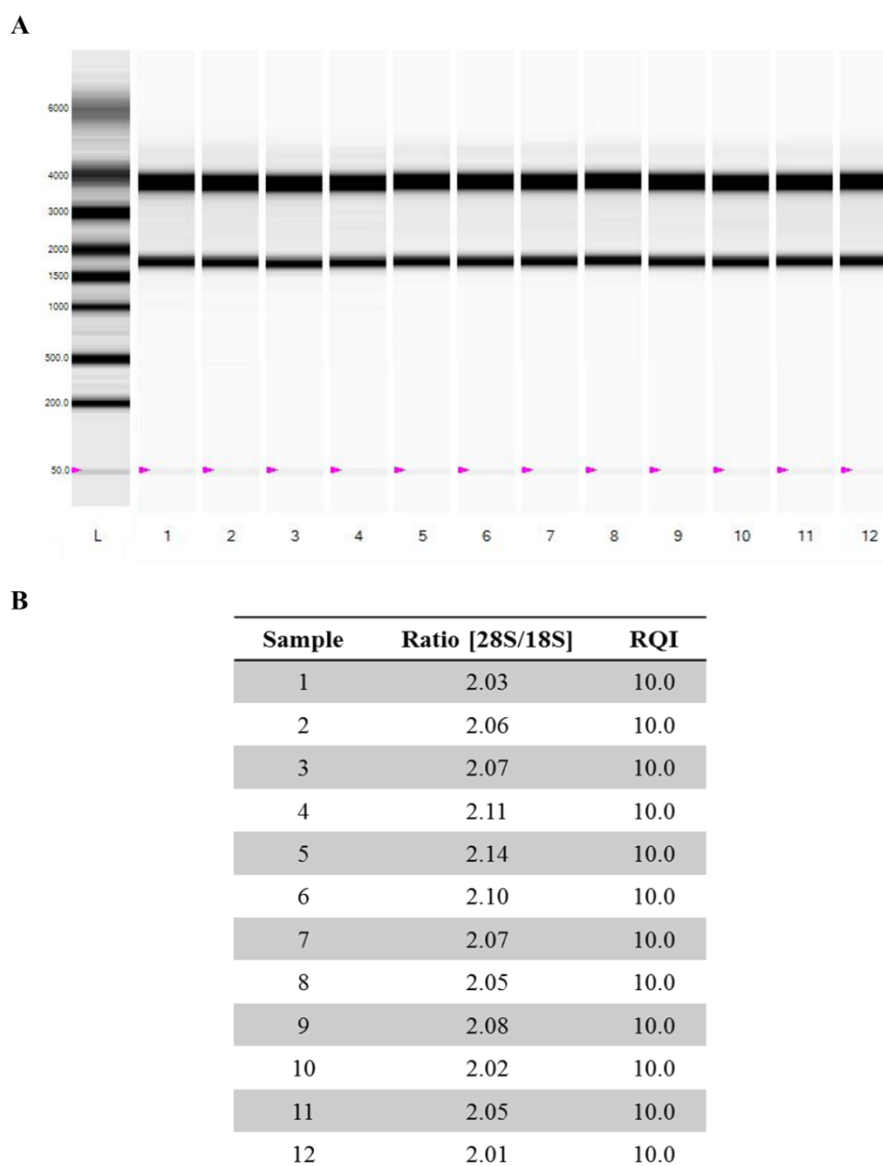


**Figure A.1 | Quality of RNA samples as measured by the Experion™ automated electrophoresis station.** (A) Virtual RNA gel image and (B) RNA quality indicators obtained from the Experion™ software. Ratio [28S/18S], ratio between the intensity of the 28S rRNA band and that of the 18S rRNA; RQI, RNA quality indicator.

## A.2. Evaluation of the specificity of RT-qPCR reactions

To verify whether the RT-qPCR reactions had yielded a single specific product, an electrophoresis with a representative sample of each amplicon was run as described in section 2.16. As can be appreciated in Figure A.2, the electrophoresis showed that a single product was obtained in each reaction, thus confirming that the reactions were specific. Moreover, the products had the expected amplicon size (Table 2.5).

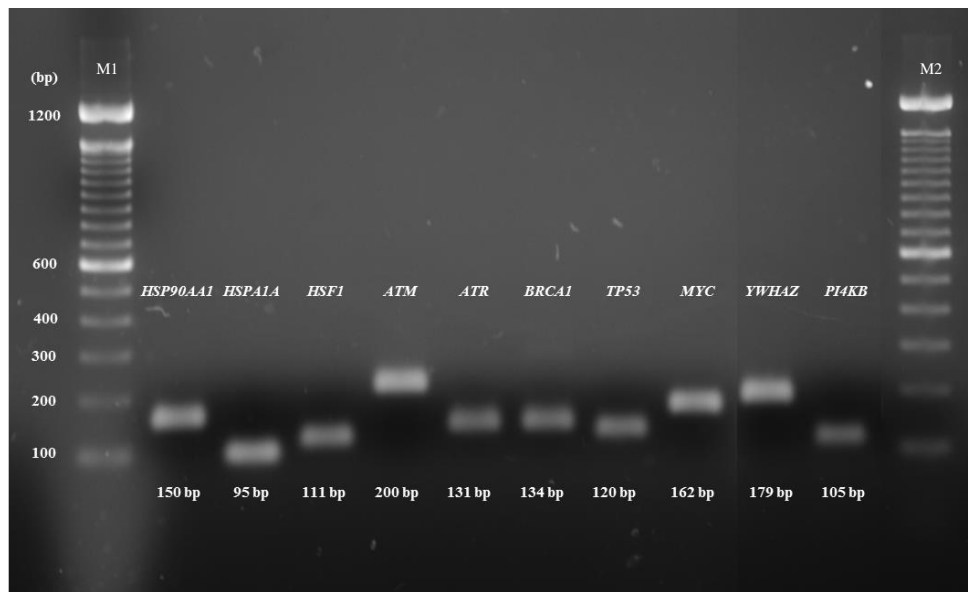


**Figure A.2 | Agarose gel electrophoresis with a representative sample from each amplicon obtained in the RT-qPCR reactions.** The electrophoresis was run as described in section 2.16. bp, base pairs; M1, TrackIt™ 100 bp DNA Ladder; M2, Ready-Load™ 100 bp DNA Ladder; *ATM*, ataxia telangiectasia mutated; *ATR*, ataxia telangiectasia and Rad3-related protein; *BRCA1*, breast cancer 1 susceptibility protein; *HSF1*, heat shock factor 1; *HSP90AA1*, heat shock 90 kDa protein 1 alpha; *HSPA1A*, heat shock 72 kDa protein; *MYC*, v-Myc avian myelocytomatosis viral oncogene homolog; *PI4KB*, phosphatidylinositol 4-kinase, catalytic, beta; *TP53*, tumor protein p53; *YWHAZ*, tyrosine 3-monooxygenase/tryptophan 5-monooxygenase activation protein, zeta.